(2)

FINAL TECHNICAL REPORT

OPTIMUM AEROELASTIC CHARACTERISTICS FOR COMPOSITE SUPERMANEUVERABLE AIRCRAFT

(AFOSR Grant - 89-0055)

December 28, 1991

Principal Investigator: Prof. G. A. Oyibo

Polytechnic University
Long Island Campus
Farmingdale, NY 11735

POLY AE Report 91-10

SECURITY CLASSIFICATION OF THIS PAGE (U)

REPORT DOCUMENTATION PAGE

Form Approved OMB No. 0704-0188

1a. REPORT SECURITY CLASSIFICATION: Unclassified	1b. RESTRICTIVE MARKINGS: N/A
2a. SECURITY CLASSIFICATION AUTHORITY: A	3. DISTRIBUTION/AVAILABILITY OF REPORT: Approved for public release; distribution unlimited
2b. DECLASSIFICATION/DOWNGRADING SCHEDULE: N/A	
4. PERFORMING ORGANIZATION REPORT NUMBER(S): POLY AE ? 91-10	5. MONITORING ORGANIZATION REPORT NUMBER(S)
6a. NAME OF PERFORMING ORGANIZATION: Polytechnic University; 6b. OFFICE SYMBOL (If applicable)	7a. NAME OF MONITORING ORGANIZATION: Air Force Office of Scientific Res. Directorate of Aerospace Sciences
6c. ADDRESS (City, State, and ZIP Code): Route 110, Farmingdale, NY 11735	7b. ADDRESS (City, State, and ZIP Code): Same as 8c
8a. NAME OF FUNDING/SPONSORING ORGANIZATION: USAF Air Force Office of Scientific Research; 8b. OFFICE SYMBOL (If applicable): AFOSR NA	9. PROCUREMENT INSTRUMENT IDENTIFICATION NUMBER: AFOSR-89-0055
8c. ADDRESS (City, State, and ZIP Code): Bolling Air Force Base, DC 20332-6448	10. SOURCE OF FUNDING NUMBERS: PROGRAM ELEMENT NO. 61102F; PROJECT NO. 2302; TASK NO B1; WORK UNIT ACCESSION NO.

11. TITLE (Include Security Classification): OPTIMUM AEROELASTIC CHARACTERISTICS FOR COMPOSITE SUPERMANEUVERABLE AIRCRAFT (U)

12. PERSONAL AUTHOR(S): Prof. Gabriel A. Oyibo, Prof. James Bentson and Prof. T. A. Weisshaar

13a. TYPE OF REPORT	13b. TIME COVERED	14. DATE OF REPORT (Year, Month, Day)	15. PAGE COUNT
Technical Report	FROM 89/9 TO 91/10	91/12/28	

16. SUPPLEMENTARY NOTATION

17. COSATI CODES			18. SUBJECT TERMS (Continue on reverse if necessary and identify by block number)
FIELD	GROUP	SUB-GROUP	Aeroelastic optimization, aeroelasticity, aeroelastic tailoring, unsteady aerodynamics, composite materials, transonic flow, composite structures, structural dynamics, composite wi

19. ABSTRACT (Continue on reverse if necessary and identify by block number)

The investigation of an aeroelastically induced constrained warping phenomenon for a composite, supermaneuverable type aircraft wing has continued in this second phase of the study. The first phase investigation was concentrated mainly on the static phenomena and the search for closed form solutions for free vibration of aircraft wings having constrained warping in the presence of elastic coupling. The wing is analytically modelled as a straight flat laminated plate. Various forms of highly simplified aerodynamic loads are employed in the analysis. The free vibrations and stability aspects of this phenomenon are examined to obtain some physical insights and to determine its importance and/or design implications. Analytical tools employed include an affine transformation concept which was formulated previously (by the present principal investigator) as well as a non-dimensionalization scheme. With the help of these tools, an evolution of effective warping parameters with which to study this phenomenon was carried out. The virtual work theorem and variational principles were used to derive the equations of motion based on the assumed wing displacements. The existence of closed-form free vibrations solutions for composite wings with elastic coupling and constraint of

20. DISTRIBUTION/AVAILABILITY OF ABSTRACT	21. ABSTRACT SECURITY CLASSIFICATION
☐ UNCLASSIFIED/UNLIMITED ☒ SAME AS RPT ☐ DTIC USERS	Unclassified (cont'd on back)
22a. NAME OF RESPONSIBLE INDIVIDUAL: Dr. Spencer Wu	22b. TELEPHONE (Include Area Code): 202-767-4937; 22c. OFFICE SYMBOL: NA

DD Form 1473, JUN 86 Previous editions are obsolete SECURITY CLASSIFICATION OF THIS PAGE

(U)

warping was established. A revelation from these closed-form solutions is that, elastic coupling lowers the first coupled frequencies (in fact a significant amount of coupling could reduce the first frequency to almost zero. The discovery of the closed-form solutions for the free vibration which seems to mark the first time such solutions were ever obtained, not only led to answers to a number of previously unanswered questions but also raised new unanswered questions such as "Does the aeroelastic divergence or flutter problem of such wings have any closed-form solutions".

During the second year of the first phase investigation was concerned with essentially how to find the answer to the above mentioned question. Accordingly in the first quarter,

continued next page

efforts were concentrated on determining the possibility of finding closed-form solutions to the divergence problem. The investigation led to two possible methods of obtaining such solutions. These methods are (a) the "elimination" approach (which was used for the free vibration) and (b) the method of Laplace transformation. Although it's already known that (a) works, (b) was implemented in formulating the analytical expressions for the closed-form solution of the divergence problem due to an anticipated relative ease. In the beginning of the 2nd phase, the closed form divergence and vibrations results which have and are still being extracted are being studied very carefully to establish physical trends in the constraint of warping phenomena. In particular, the computed results are being studied in order to evolve the basic mechanism by which the constrained warping model may be used to explain the concept of aeroelastic tailoring. Preliminary results that are being evolved seem to indicate that in free vibration, if the elastic coupling is varied, there are some circumstances when the first two coupled modes may diverge from one another and other circumstances when they may approach coalescence. The big question therefore is "would such coalescence result in instability" even in absence of air (or at low air speeds)? Another question whose answer is being searched also is "what is the role of such coalescence or diverging potential in aeroelastic tailoring"? The answers to these questions seem to be evolving gradually as the investigation continues. For example, it is seen as shown in this report that coalescence of modes may not result in stabilities (even at very low flight velocities).

In the most recent investigations, efforts have been concentrated on the unsteady aerodynamics. This was considered necessary especially since this research program plans to eventually look at the aeroelastic behavior of wings in transonic flow - a non-linear, very complicated flow regime. It is recognized that problematic phenomena at low subsonic speeds can potentially be disastrous at transonic speeds. Hence a new discovery by the

principal investigator in non-linear fluid dynamics is employed to establish some closed form solutions for 2-D unsteady non-linear flow applicable to transonic regime which are expected to be eventually used for aeroelastic analysis. Some of the results have been compiled and published in the AIAA Journal. In the process of studying the unsteady 2-D nonlinear transonic flows, what seems to be a major breakthrough was discovered: this breakthrough is the discovery that the 3-D steady non-linear transonic flow equations can be transformed into a linear hodograph equivalent. This discovery essentially reverses a hundred years state of thinking and belief in the scientific and mathematical community that the hodograph method was limited to the 2-D flows. The results of this discovery have been written up and published in the AIAA Journal.

In addition another paper AIAA 92-257 which presents practical shock free 3-D wing for transonic flight is to be presented in June, 1992 at the AIAA applied Aerodynamics Conference in Palo Alto, California. This research program seems to be seeing the beginning of what seems to be another breakthrough, perhaps even more significant than what we have seen thus far. This is what seem to be a discovery that transformations methods can even be used to effectively study the ultimate set of equations in continuum gas dynamics known as the Navier Stokes set of equations. This new finding could be the key to effectively unlocking the secret of gas dynamics and aeroelastic phenomena for real gases with viscosity, which have been blurry at best thus far. This finding has resulted in a preliminary paper accepted to be presented at an international conference to be held in Colorado in August of 1992. It is being proposed that the investigation of these new findings be pursued in a proposed next phase of research. This is because if the findings are correct this could be the start of a new era of fluid or gas dynamics analysis.

1.0 ABSTRACT

The investigation of an aeroelastically induced constrained warping phenomenon for a composite, supermaneuverable type aircraft wing has continued in this second phase of the study. The first phase investigation was concentrated mainly on the static phenomena and the search for closed form solutions for free vibration of aircraft wings having constrained warping in the presence of elastic coupling. The wing is analytically modelled as a straight flat laminated plate. Various forms of highly simplified aerodynamic loads are employed in the analysis. The free vibrations and stability aspects of this phenomenon are examined to obtain some physical insights and to determine its importance and/or design implications. Analytical tools employed include an affine transformation concept which was formulated previously (by the present principal investigator) as well as a non-dimensionalization scheme. With the help of these tools, an evolution of effective warping parameters with which to study this phenomenon was carried out. The virtual work theorem and variational principles were used to derive the equations of motion based on the assumed wing displacements. The existence of closed-form free vibrations solutions for composite wings with elastic coupling and constraint of warping was established. A revelation from these closed-form solutions is that, elastic coupling lowers the first coupled frequencies (in fact a significant amount of coupling could reduce the first frequency to almost zero. The discovery of the closed-form solutions for the free vibration which seems to mark the first time such solutions were every obtained, not only led to answers to a number of previously unanswered questions but also raised new unanswered questions such as "Does the aeroelastic divergence or flutter problem of such wings have any closed-form solutions."

During the second year of the first phase, investigation was concerned with essentially how to find the answer to the above mentioned question. Accordingly in the first quarter,

efforts were concentrated on determining the possibility of finding closed-form solutions to the divergence problem. The investigation led to two possible methods of obtaining such solutions. These methods are (a) the "elimination" approach (which was used for the free vibration) and (b) the method of Laplace transformation. Although it's already known that (a) works, (b) was implemented in formulating the analytical expressions for the closed-form solution of the divergence problem due to an anticipated relative ease. In the beginning of the 2nd phase, the closed form divergence and vibrations results which have and are still being extracted are being studied very carefully to establish physical trends in the constraint of warping phenomena. In particular, the computed results are being studied in order to evolve the basic mechanism by which the constrained warping model may be used to explain the concept of aeroelastic tailoring. Preliminary results that are being evolved seem to indicate that in free vibration, if the elastic coupling is varied, there are some circumstances when the first two coupled modes may diverge from one another and other circumstances when they may approach coalescence. The big question therefore is "would such coalescence result in instability" even in absence of air (or at low air speeds)? Another question whose answer is being searched also is "what is the role of such coalescence or diverging potential in aeroelastic tailoring"? The answers to these questions seem to be evolving gradually as the investigation continues. For example, it is seen as shown in this report that coalescence of modes may not result in stabilities (even at very low flight velocities).

In the most recent investigations, efforts have been concentrated on the unsteady aerodynamics. This was considered necessary especially since this research program plans to eventually look at the aeroelastic behavior of wings in transonic flow - a non-linear, very complicated flow regime. It is recognized that problematic phenomena at low subsonic speeds can potentially be disastrous at transonic speeds. Hence a new discovery by the

principal investigator in non-linear fluid dynamics is employed to establish some closed form solutions for 2-D unsteady non-linear flow applicable to transonic regime which are expected to be eventually used for aeroelastic analysis. Some of the results have been compiled and published in the AIAA Journal. In the process of studying the unsteady 2-D nonlinear transonic flows, what seems to be a major breakthrough was discovered: this breakthrough is the discovery that the 3-D steady non-linear transonic flow equations can be transformed into a linear hodograph equivalent. This discovery essentially reverses a hundred years state of thinking and belief in the scientific and mathematical community that the hodograph method was limited to the 2-D flows. The results of this discovery have been written up and published in the AIAA Journal.

In addition another paper AIAA 92-257 which presents practical shock free 3-D wing for transonic flight is to be presented in June, 1992 at the AIAA applied Aerodynamics Conference in Palo Alto, California. This research program seems to be seeing the beginning of what seems to be another breakthrough, perhaps even more significant than what we have seen thus far. This is what seem to be a discovery that transformations methods can even be used to effectively study the ultimate set of equations in continuum gas dynamics known as the Navier Stokes set of equations. This new finding could be the key to effectively unlocking the secret of gas dynamics and aeroelastic phenomena for real gases with viscosity, which have been blurry at best thus far. This finding has resulted in a preliminary paper accepted to be presented at an international conference to be held in Colorado in August of 1992. It is being proposed that the investigation of these new findings be pursued in a proposed next phase of research. This is because if the findings are correct this could be the start of a new era of fluid or gas dynamics analysis.

2.0 NOMENCLATURE

a_i	= chordwise integrals
c'_o, c_o	= affine space half-chord and chord, respectively
D_{ij}	= elastic constants
e	= parameter that measures the location of the reference axis relative to mid-chord
EI, GJ	= bending and torsional stiffness, respectively
$\bar{h}$	= wing box depth
(h_o, α_o)	= affine space bending and torsional displacement, respectively
K,So	= elastic coupling and warping stiffness, respectively
k_{ij}	= elemental stiffness parameter
k_o	= Strouhal number
L_o, M_o	= affine space running aerodynamic lift and moments, respectively
ℓ_o	= affine space half-span for the wing
m_o	= affine space mass per unit span
$(\Delta p, \Delta p_o)$	= differential aerodynamic pressure distributions in physical and affine space, respectively
t	= time
U, U_o	= virtual work expressions in physical and affine space, respectively
U_f	= flutter speed
(x,y,z), $(x_o, y_o, z_o$	= physical and affine space coordinates, respectively
$\gamma_i, \delta_i, \beta_i$	= displacement shape functions
r, L_1, L_2, D^*, D^*_o,	= generic nondimensionalized stiffness parameters

μ_o	= affine mass ratio parameter
μ_{ij}, e	= Poisson ratios and generalized Poisson's ratio, respectively
λ_o	= divergence parameter
ρ, ρ_∞	= affine space material and air density, respectively
θ	= twisting displacements
w	= displacement
ω	= vibration frequency

3.0 INTRODUCTION

In the late 1960's designers began to investigate the possibility of exploiting the directional properties of composite materials to improve aeroelastic characteristics of lifting surfaces. For example, superfighter designers may aeroelastically tailor a wing so that it deforms to the optimum camber under maneuvering loads.

For instance, a wing can be tailed so that its leading edge will twist downward under the stress of a tight turn, thereby decreasing the wing's angle of attack and hence reduce drag.

Exploitation of the directional properties of composite materials to solve aeroelastic instability problems (known as aeroelastic tailoring) may enhance the performance of future high performance military aircraft, particularly the super-maneuverable concepts. This stems from the need for future military weapon systems to exhibit high performance and minimum vulnerability (e.g.: minimum radar cross-sectional area). These requirements may lead to unorthodox aircraft configurations which in turn result in unorthodox aeroelastic instability problems (e.g., the X-29 primary mode of instability, called the 'body freedom' flutter).

Perhaps the aeroelastic tailing concept would have been discovered much earlier if the physics of anisotropic aeroelasticity were more apparent. This inherent physical intractability is largely due to the existence of numerous variables, e.g.,; flight parameters, several composite directional properties, fiber orientation angles, etc., which are not even truly independent, in the anisotropic system. This state of affairs is therefore analogous to that which existed in the basic rigid body aerodynamics before the advent of the similarity rule theory. This theory clearly revealed that, the utilization of non-dimensionalized groups of variables, e.g.: Reynolds, Mach, Strouhal, Froude numbers etc., provide significantly superior physical insight to the problem than the individual physical variables. The new methodology that is being used as the basic tool in this research program is basically the aeroelastic

equivalent of the aerodynamic similarity rule. The expected superiority of this new approach over the state-of-the-art (SOA) counterpart, which utilizes individual physical variables, especially in terms of physical insights, has been demonstrated in references 1-10. For example, a high-aspect-ratio composite wing could behave aeroelastically like a low aspect ratio wing and vice-versa. Similarity parameters can expose conditions for which this might happen. This is significant, (for instance) in the light of the important role played by the wing aspect ratio in the aerodynamics approximations for an aeroelastic analysis. This result may therefore be suggesting some new form of coupling between the elastic and aerodynamic equations in composite wing aeroelasticity. A fundamental aspect of this new methodology has been used in studies at Purdue University [11] and MIT[12].

In this research, an investigation of a wing's spanwise sectional distortion (warping) resulting from aerodynamic forces and its influence on the wing's free vibrations, as well as (aeroelastic) stability, is being carried out. In particular, St. Venant's torsional/twisting theory, which is currently widely used for estimating the wing's twisting displacements has been examined with the help of the new methodology, to determine its limitations, when applied to wings fabricated of composite materials. The relevance and significance of this study for the newly emerging supermaneuverable type aircraft may be seen in the light of the fact that (a) supermaneuverability is characterized by high angle of attack which implies high twisting aerodynamic forces, and (b) most aircraft designers believe future aircraft will be fabricated of 40-70% composite materials.

When the St. Venant's torsional theory is used to estimate a wing's twisting displacement and/or forces, the fact that the wing's root section's distortion is relatively small compared to that of other sections is ignored. However, previous investigators have determined that such an unrealistic assumption may lead to only little errors if the aspect ratio of the wing is

very high.

The research has shown during the first phase that the conclusions reached by previous investigators are basically true for wings fabricated of metals or isotropic materials. A set of new theories is therefore being postulated in this research effort for accurately estimating the twisting displacements, vibrational frequencies and instability boundaries for wings fabricated of composite materials.

In the second phase, the mechanism of instability is defined as the main target of more detailed investigation. This is partially because some new findings during this research program seem to indicate that composite wings undergoing free aeroelastic oscillations exhibit some unique phenomena not known to occur in metal wings. One of this phenomena is what we have referred to as a "damping like behavior" (in absence of actual damping) brought about by the presence of asymmetric coupling. This among other things presents opportunity for a merging of two modes during a free vibration. The natural question is therefore "would such a phenomenon lead to instabilities" as has been well documented for other aeroelastic systems? Of primary interest to an aeroelastician is "how does this phenomenon connected to aeroelastic tailoring? These are some of the questions that we are searching for answers to in this second phase of this research. It is beginning to be apparently evident that modal coalescence is possible. Furthermore it is also evident that this modal coalescence may lead to some form of instability at low flight velocities which we are still trying to discern properly and carefully.

In preparation for more sophisticated flutter or divergence analysis, a new discovery by the principal investigator in nonlinear unsteady fluid dynamics is being refined to enhance and help expose the physical nature of aeroelastic instability of composite wings with elastic coupling and warping restraint. Some of the preliminary results have just been published in the AIAA

Journal. A copy of this publication is included in this writeup. Furthermore, the study of the unsteady transonic fluid dynamics has led us to some new findings. In the process of studying the unsteady 2-D nonlinear transonic flows, what seems to be a major breakthrough was discovered: this breakthrough is the discovery that the 3-D steady non-linear transonic flow equations can be transformed into a linear hodograph equivalent. This discovery essentially reverses a hundred years state of thinking and belief in the scientific and mathematical community that the hodograph method was limited to the 2-D flows. The results of this discovery have been written up and published in the AIAA Journal.

In addition another paper AIAA 92-257 which presents practical shock free 3-D wing for transonic flight is to be presented in June, 1992 at the AIAA applied Aerodynamics Conference in Palo Alto, California. This research program seems to be seeing the beginning of what seems to be another breakthrough, perhaps even more significant than what we have seen thus far. This is what seem to be a discovery that transformations methods can even be used to effectively study the ultimate set of equations in continuum gas dynamics known as the Navier Stokes set of equations. This new finding could be the key to effectively unlocking the secret of gas dynamics and aeroelastic phenomena for real gases with viscosity, which have been blurry at best thus far. This finding has resulted in a preliminary paper accepted to be presented at an international conference to be held in Colorado in August of 1992. It is being proposed that the investigation of these new findings be pursued in a proposed next phase of research. This is because if the findings are correct this could be the start of a new era of fluid or gas dynamics analysis.

REFERENCES

1. Oyibo, G.A., "A Unified Flutter Analysis for Composite Aircraft Wings", AIAA paper No. 84-0906, 25th AIAA SDM Conference, Palm Springs, CA, May 1984.

2. Oyibo, G.A., "Reply by the Author to P.A.A. Laura", AIAA Journal, Vol. 22, April 1984.

3. Oyibo, G.A., "A Unified Flutter Theory for Composite Aircraft Wings" Invited Lecture, 26th Israel Annual Conference on Aviation and Astronautics, Technion, Haifa, Israel, February 1984.

4. Oyibo, G.A., and Brunelle, E.J., "Vibrations of Circular Orthotropic Plates in Affine Space", AIAA Journal, Vol. 22, October 1984.

5. Oyibo, G.A., "Generic Approach to Determine Optimum Aeroelastic Characteristics for Composite Forwardswept Wing Aircraft", AIAA Journal, Vol. 22, No. 1, January 1984, pp. 117-123.

6. Oyibo, G.A., "Unified Aeroelastic Flutter Theory for Very Low Aspect Ratio Panels", AIAA Journal, Vol. 2l, No. 11, November 1983, pp. 1581-1587.

7. Brunelle, E.J., and Oyibo, G.A., "Generic Buckling Curves for Specially Orthotropic Rectangular Plates", AIAA Journal, Vol. 21, August 1983, pp. 1150-1587.

8. Oyibo, G.A., "Unified Panel Flutter Theory with Viscous Damping Effects", AIAA Journal, Vol. 21, May 1983, pp. 767-773.

9. Oyibo, G.A., "Flutter of Orthotropic Panels in Supersonic Flow Using Affine Transformations", AIAA Journal, Vol. 21, February 1983, pp. 283-289.

10. Oyibo, G.A., "The Unified Panel Flutter Theory and the Damping Effects", AFDC paper No. 82-002, presented at the Aerospace

11. Weisshaar, T.A., and Ryan, R.J., "Control of Aeroelastic Instabilities Through Elastic

Cross-Coupling", AIAA paper, No. 84-0985, May 1984.

12. Jensen, D.W., and Crawley, E.F., "Frequency Determination Techniques for Cantilevered Plates with Bending-Torsion Coupling", AIAA Journal, Vol. 22, No. 3, March 1984.

4.0 RESEARCH OBJECTIVES

The overall goal of this phase of the research program is twofold: first, is to formulate closed-form solutions to the aeroelastic divergence and flutter of aircraft wings with warping constraint and elastic coupling, and use these to study the effects of constrained warping on aeroelastic response; second is to develop new plate-beam finite elements and use in modal analysis of vibration and flutter to provide an independent check on the closed-form solution results.

During a preliminary investigation of the constrained warping under aeroelastic forces, a phenomenon being studied in the current research program sponsored by the AFOSR, the Principal Investigator discovered (for the first time), that there are closed-form solutions to the free vibrational and divergence problem of composite aircraft wings having warping constraints and elastic coupling [2]. In this study these newly discovered techniques are to be extended (and expanded) and used for continuing the formulation of closed-form solutions to the aeroelastic flutter and dynamic response problems of aircraft wings with the constraint of warping and elastic coupling. This process is expected to involve determining the necessary symmetries that exist in the flutter and dynamic response equations (by comparing them to their free vibrations and divergence counterpart) to permit the extraction of their characteristic roots for elastically coupled deformations of the wing under the influence of aerodynamic forces.

Experience from the free vibrational and the ongoing divergence investigations has shown that the computations involved in extracting the eigenvalues from the closed-form eigen expressions derived using the new techniques are very challenging. For example, it is difficult to determine how to eliminate or minimize the numerical errors resulting from the

change in the extraction order for eigenvalues. This newly formulated procedure for the flutter and

of dynamic response problems are to be evolved with the help of the experience gained from the study of the vibrations and divergence. The closed-form solutions thus extracted, are to be thoroughly studied to understand the physics of the constrained warping phenomena. In particular, the computed results used to determine the basic mechanism by which the constrained warping model can be used to explain the concept of aeroelastic tailoring. This is necessary because the basic mechanism of aeroelastic tailoring seems to be still rather elusive. For example, it seems to be generally accepted that tailoring occurs because ply angles are "properly" oriented. From our ongoing research, tailoring seems to be more than just a ply angle orientation. Careful study of the data generated are expected to be carried out to try to unfold this apparent mystery. In other words, by using a figure similar to Fig. (1), how can tailoring (higher flutter speed) be explained?

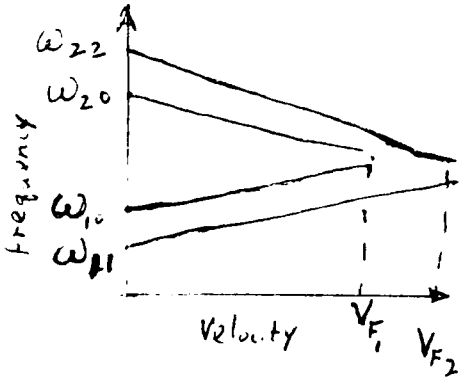

Figure 1

ω_{10}, ω_{20} - is isotropic 1st & 2nd frequency, respectfully.

ω_{11}, ω_{22} - composite 1st & 2nd frequency, respectfully.

V_F; = flutter speed

5.0 STATUS OF RESEARCH EFFORTS

5.1 INTRODUCTION

During the reporting period, the research program progressed according to plan resulting in the accomplishment of the goals defined for the period. These goals, which have been defined in Section 4 of this report, basically are to extend and utilize some of the newly developed important tools in the current ongoing research program which is being sponsored by AFOSR to investigate the constrained warping phenomena of aircraft wings fabricated of composite materials having elastic coupling and subjected to aeroelastic forces. The proposed study is basically comprised of the investigation of (a) the basic mechanism of instability and dynamic response, (b) the mechanism of modal transformation in flutter and dynamic response, and (c) nonlinear and transonic instabilities.

In the first and second reporting period during the preliminary study, Prof. G. A. Oyibo started the investigation of the basic mechanism of aeroelastic instability of composite aircraft wings with restrained warping and elastic coupling. Following a realization that proper understanding of the mechanism of aeroelastic instability particularly the dynamic instabilities, require some sound analytical tools, a review of the important tools developed for the divergence and free vibration for composite wings with warping restraint and elastic coupling during the last phase was started. During this review, a thorough study of the preliminary data generated were carried out. The understanding gained during this review provided the necessary background necessary for properly formulating the instability mechanism problem. Consequently an expansion or extension of these earlier tools started. First, the major scientific revelation to the scientific community made possible (through the help of these tools) by this research program was properly reexamined. The revelation is that a composite wing having a restrained warping

in the presence of an asymmetric elastic coupling (in absence of damping) exhibit a "damping-like" behavior. This new discovery which should be critical to the proper understanding of the mechanism of aeroelastic tailoring is still being thoroughly investigated. The latest results show that modal coalescence is possible. These results are seen to show that such a coalescence could lead to instability (even at low flight speeds). More careful investigations are now being carried out in order to "fine tune" the conclusions of these results and to recommend possible experimental studies to verify them. In addition, a refinement of a new discovery in nonlinear/transonic fluid dynamics by the principal investigator was initiated in anticipation of more realistic or sophisticated flutter/divergence analyses to further the goals of this research. Some of the preliminary results have been compiled and published in the AIAA Journal. In the process of studying the unsteady 2-D nonlinear transonic flows, what seems to be a major breakthrough was discovered: this breakthrough is the discovery that the 3-D steady non-linear transonic flow equations can be transformed into a linear hodograph equivalent. This discovery essentially reverses a hundred years state of thinking and belief in the scientific and mathematical community that the hodograph method was limited to the 2-D flows. The results of this discovery have been written up and published in the AIAA Journal. In addition another paper AIAA 92-257 which presents practical shock free 3-D wing for transonic flight is to be presented in June, 1992 at the AIAA applied Aerodynamics Conference in Palo Alto, California. This research program seems to be seeing the beginning of what seems to be another breakthrough, perhaps even more significant than what we have seen thus far. This is what seem to be a discovery that transformations methods can even be used to effectively study the ultimate set of equations in continuum gas dynamics known as the Navier Stokes set of equations. This new finding could be the key to effectively unlocking the secret of gas dynamics and aeroelastic phenomena for real gases with viscosity,

which have been blurry at best thus far. This finding has resulted in a preliminary paper accepted to be presented at an international conference to be held in Colorado in August of 1992. It is being proposed that the investigation of these new findings be pursued in a proposed next phase of research. This is because if the findings are correct this could be the start of a new era of fluid or gas dynamics analysis.

The investigation of the numerical method for efficiently and accurately extracting the eigenvalues for the vibration and divergence problems continued. New numerical methods for handling some problem regions of these problems are also being examined. Prof. T. A. Weisshaar is also continuing his investigations into how a new beam-plate finite elements may be formulated to capture the constraint of warping effect in order to provide results which may be used to independently check the closed-form solutions which have been, and are being generated.

5.2 ACCURATE DIVERGENCE THEORY FOR COMPOSITE SUPERMANEUVERABLE AIRCRAFT WINGS

5.2.1 INTRODUCTION

Modern supermaneuverable aircraft concepts benefit a great deal from, among other things, significant advances in materials technology and the availability of more accurate aerodynamic prediction capabilities. Supermaneuverability as a design goal invariably calls for an optimization of the design parameters. Optimization may be partially accomplished for example, by using composite materials to minimize weight. Indeed, it has been known that these composite materials can be tailored properly to resolve the dynamic or static instability problems of these types of aircraft. The concept is referred to as aeroelastic tailoring.

While aeroelastic tailoring has tremendous advantages in the design of an aircraft, the analysis which provides the basis for the aeroelastic tailoring itself is generally very involved. This is rather unfortunate since a good fundamental physical insight of the tailoring mechanism is required for accurate and reliable results.

In this investigation an attempt is made to look at some dynamics theories that can be used to understand the aeroelastic tailoring mechanism. Specifically, the accuracy of the St. Venant torsion theory which is relatively simple and frequently used in aeroelastic analysis is examined with particular reference to the effects of the wings aspect ratio as well as other design parameters.

An accurate torsion/twist theory is particularly significant for supermaneuverable aircraft wings since supermaneuverability is basically characterized by high angle of attack.

Although earlier studies (1,2,3) have indicated that the St. Venant's torsion theory is reasonably accurate except for aircraft wings with fairly low aspect ratios, the theory supporting that conclusion was based on the assumption that the wing is constructed of isotropic materials. Basically the St. Venant's torsion theory assumes that the rate of change of the wing's twist angle with respect to the spanwise axis is constant. This assumption is hardly accurate particularly for modern aircraft construction in which different construction materials are employed and the aerodynamic loads vary significantly along the wing's span. However, References 1-3 have shown that (in spite of such an inaccurate assumption) the main parameter that determines the accuracy of the St. Venant's theory is the wing's aspect ratio. Thus, it was determined that the theory is fairly accurate for moderate to high aspect ratio wings constructed of isotropic materials. In recent studies (4,5,6) however, it has been shown that for wings constructed of orthotropic composite materials, the conclusion of References 1-3 need to be modified. Rather than using the geometric aspect ratio of the wing to determine the accuracy of St. Venant's twist theory, it was suggested that a generic stiffness ratio as well as an effective aspect ratio which considers the wing's geometry and the ratio of the principal directional stiffness should be considered in establishing the accuracy of St. Venant's theory.

The present investigation is related to the studies that were initiated in References 5 and 6. In this study the first task was to examine the role of coupling (both mass and elastic coupling) on the accuracy of St. Venant's theory applied to static problems. It was discovered that coupling plays a very significant role on the accuracy of St. Venant's twist theory. The second task was to investigate the torsional vibration for a flat plate model of an aircraft wing fabricated of composite materials in which the constrained warping phenomenon is more realistically represented, with particular emphasis on higher frequencies and to compare results with those from a representation based on St. Venant's theory.

5.2.2 FORMULATION

Consider an aircraft wing fabricated of composite materials and mathematically idealized as a cantilevered plate subjected to an aerodynamic flow over its surfaces. The mathematical statement of the virtual work theorem for such a plate model is well known and documented. It is also known that such mathematical statements of the virtual work theorem for a laminated plate model are characterized with the existence of so many variables (in the statement), reflecting the various directional properties for the laminated plate model, which would tend to interfere with any physical insight that might be desired from a phenomenological analysis employing such a mathematical statement. The newly discovered affine transformation concept (5,6 and 7) was developed principally to resolve such a problem.

This new concept therefore can be used to evolve the mathematical statement of the virtual work theorem in an affine space given by the following equation.

$$\delta \bar{U}_o = 0 = 2\int_0^t \iint_A \left\{ (w,_{x_o x_o})^2 + 2D^* \left[(1-\epsilon)(w,_{x_o y_o})^2 + \epsilon\, w,_{x_o x_o} w,_{y_o y_o} \right] + (w,_{y_o y_o})^2 + L_1 w,_{x_o x_o} w_{x_o y_o} + L_2 w,_{y_o y_o} w,_{x_o y_c} \right\} dx_o dy_o dt \qquad (1)$$

$$- \frac{\delta}{2}\int_0^t \iint_A \rho_o \ddot{w}^2 dx_o dy_o dt + \int_0^t \iint_A \Delta p_o \delta w dx_o dy_o dt$$

where:

$$\bar{U}_o = \frac{\bar{U}}{D_{22}}\left(\frac{D_{22}}{D_{11}}\right)^{1/4} \quad ; \quad D^* = \frac{D_{12} + 2D_{66}}{(D_{11}D_{22})^{1/2}} \quad ; \quad \epsilon D^* = \frac{D_{12}}{(D_{11}D_{22})^{1/2}}$$

$$L_1 = \frac{4D_{16}}{(D_{11})^{3/4}(D_{22})^{1/4}} \; ; \; L_2 = \frac{4D_{26}}{(D_{11})^{1/4}(D_{22})^{3/4}} \qquad (2)$$

$$\Delta p_o = \frac{\Delta p}{D_{22}} \; ; \; \rho_o = \frac{\rho \bar{h}}{D_{22}}$$

D_{ij} are the elastic constants, ρ, is the material density, Δp is the differential pressure distribution, w is the displacement, t is the time, A integrals represent area integrals and $\bar{h}$ is the wing box depth.

Equations (1) and (2) therefore form the basis of the newly developed methodology. The equations of motion of a plate model of an aircraft wing can now be derived by prescribing a realistic wing displacement and using Equation (1).

When Equation (1) is compared to its physical space counterpart, it is seen that Equation (1) has fewer variables. It is also seen that Equation (1) contains only non-dimensionalized stiffness quantities (compared to dimensional stiffness quantities in its physical space counterpart). Another feature of this new methodology which makes it unique is that the non-dimensionalization (a consequence of the affine transformation) is accomplished before assuming the wing deformations. This means that the non-dimensionalization is independent of how the wing deforms. A non-dimensionalization scheme that depends on a particular assumption of the wings deformations could lead the analyst to an incorrect physical interpretation of results, since the wing's deformations assumptions have inherent errors because they are based on the analyst's judgments and experience. This observation may become clearer during the evolution of a warping parameter with which to study the effects of the warping constraint phenomenon on the status and dynamics of a wing fabricated of composite materials later in this study.

If the chordwise curvature is neglected in an initial approximation, the wing's deformation may be assumed as follows:

$$w(t,x_o,y_o) = h_o(t,y_o) + x_o\alpha_o(t,y_o) \tag{3}$$

where h_o and α_o are the bending and twisting displacements, respectively.

It can be shown that when Equation (3) is substituted into Equation (1) and the variational calculus is carried out for arbitrary h_o and α_o, the following equations of motion are obtained:

$$a_1 h_o^{iv} + a_2 \alpha_o^{iv} + a_5 \alpha_o^{iii} + \rho_o a_1 \ddot{h}_o + \rho_o a_2 \ddot{\alpha}_o = L_o$$

$$a_2 h_o^{iv} - a_5 h_o^{iii} + a_3 \alpha_o^{iv} - a_4 \alpha_o'' + \rho_o a_3 \ddot{\alpha}_o + \rho_o a_2 \ddot{h}_o = M_o \tag{4}$$

where:

$$a_1 = \int_{e\bar{c}_0}^{\bar{c}_0} dx_0 \quad ; \quad a_2 = \int_{e\bar{c}_0}^{\bar{c}_0} x_0\, dx_0$$

$$a_3 = \int_{e\bar{c}_0}^{\bar{c}_0} x_0^{\,2} dx_0 \quad ; \quad a_4 = 2\int_{e\bar{c}_0}^{\bar{c}_0} D^*(1-\epsilon)dx_0 \qquad (5)$$

$$L_0 = \int_{e\bar{c}_0}^{\bar{c}_0} \Delta p_0 dx_0 \quad ; \quad a_5 = \int_{e\bar{c}_0}^{\bar{c}_0} L_2 dx_0$$

$$M_0 = \int_{e\bar{c}_0}^{\bar{c}_0} x_0\, \Delta p_0 dx_0$$

$$-\infty < e < 0 \quad ; \quad \bar{c}_0 = \frac{c_0}{1-e}$$

$$(\,)' = \frac{\partial}{\partial y_0}, \; (\dot{}) = \frac{\partial}{\partial t} \qquad (6)$$

5.2.3 EVOLUTION OF WARPING PARAMETERS

The evolution of the warping parameter with which to study the constrained aeroelastic warping phenomenon for wings fabricated of composite materials is a process that depends on the sophistication of the wing's mathematical model; whether coupling effects are included, whether the wing's chordwise curvatures are included and so on. Therefore, any warping parameter is as good as the corresponding wing's displacements assumptions. However, Equation (1) makes it possible for the analyst to determine its effective independent variables even before the displacement assumptions are made.

By non-dimensionalizing the spanwise space variable in Equation (4), depending on whether one is interested in the static, dynamic, coupled or uncoupled displacements, one of the following warping parameters may be useful.

$$\lambda_c = \frac{\ell_o}{c_o}\sqrt{\frac{3}{2}D_o^*} \tag{7}$$

$$\bar{\lambda}_c = \frac{\ell_o}{c_o}\sqrt{\frac{3}{2}(D_o^* - \frac{L_2^2}{8})} \tag{8}$$

$$\bar{\lambda}_c = \frac{\ell_o}{c_o}\sqrt{\frac{3}{2}\frac{D_o^*}{1-3\bar{a}_2^2}} \tag{9}$$

where:

$$D_o^* = D^*(1 - \epsilon) \quad ; \qquad \bar{a}_2 = \frac{a_2}{c_o^2} \tag{10}$$

(ℓ_o/c_o) is defined as the wing's effective aspect ratio and D_o^* and L are the generalized stiffness and coupling ratios, respectively (defined in earlier work such as References 5 and 6).

Equations (7) thru (9) represent the appropriate warping parameter for dynamic deformation, static displacement with elastic cross-coupling, and static deformation with "geometric" coupling ($e \neq 1$), respectively.

It was discovered in this study that evolving the warping parameter in a manner shown in Equations (1) thru (3), should enable one to investigate the effects of warping on the composite wing's dynamics (or the accuracy of St. Venant's theory) effectively. From the lamination theory for composites it is known that while D_o^* and (ℓ_o/c_o) are always positive, L and $\bar{a}_2$ can be positive or negative. However, from Equations (1) and (3), it is clear that whether a composite wing has positive or negative coupling, the warping effect (in terms of λ_c) is unchanged.

Using the Laplace transform method on the divergence form of equations 4 in which strip aerodynamic theory is used, the following Laplace function becomes important in the divergence problem,

$$F_1(s) = 9_{13}\,[s^7 - a_{14}s^5 + a_{15}s^4 + a_{16}s^3 + a_{17}s^2 + a_{18}] \qquad (7)$$

where

$$a_{13} = \bar{a}_1\bar{a}_3,\quad a_{14} = -\frac{(\bar{a}_1\bar{a}_4 - \bar{a}_5^2)}{\bar{a}_1\bar{a}_3},\quad a_{15} = \frac{\bar{F}_2\bar{a}_3}{\bar{a}_1\bar{a}_3}$$

$$a_{16} = \frac{\bar{F}_4 a_5 - \bar{F}_3\bar{a}_1}{\bar{a}_1\bar{a}_3},\quad a_{17} = \frac{\bar{F}_1\bar{a}_5 - \bar{F}_2\bar{a}_4}{\bar{a}_1\bar{a}_3}$$

$$a_{18} = \frac{\bar{F}_1\bar{F}_4}{\bar{a}_1\bar{a}_3}$$

, s is Laplace variable,

$\bar{F}_i$ (i=1,2,3,4) are aerodynamic forces and moments

Let

$$F_1(s) \equiv a_{13}[(s+b)^2+a_1^2]\,[(s+\underline{b}_2)^2+a_2^2]\,[(s+b_3)^2+a_3^2]\,[s+b_4] \qquad (8)$$

$$T_{01}(s) = a_{13}[s^4 + 9_{01}2^2 + a_{02}s + a_{03}] \qquad (9)$$

$$a_{01} = \frac{\bar{a}_5}{\bar{a}_1\bar{a}_5},\quad a_{02} = \frac{\bar{a}_3\bar{F}_2}{\bar{a}_1\bar{a}_3},\quad a_{03} = \frac{\bar{a}_5 F_4}{\bar{a}_1\bar{a}_3}$$

$$F_{014}(s) = [F_1(s)/(s+b_4)]$$

$$p_{014} = \frac{T_{01}(-b_4)}{F_{014}(-b_4)}$$

$$F_{011}(s) = F_1(s)/[(s+b_1)^2+a_1^2]$$

$$P_{0115} + iP_{0116} = \frac{T_{01}(-b_1+ia_1)}{F_{011}(-b_1+ia_1)}$$

$$f_{011} = \frac{P_{0116}}{a_1} \quad , \quad P_{011} = P_{0115} + \left(\frac{b_1}{a_1}\right) P_{0116} \tag{10}$$

$$F_{012}(s) = F_1(s)/[(s+b_2)^2+a_2^2]$$

$$P_{0115}+iP_{0116} = \frac{T_{01}(-b_1+ia_1)}{F_{011}(-b_1+ia_1)}$$

$$f_{011} = \frac{P_{0116}}{a_1} \quad , \quad P_{011} = P_{0115} + \left(\frac{b_1}{a_1}\right) P_{0116}$$

$$F_{012}(s) = F_1(s)/(s+b_2)^2+a_2^2]$$

$$P_{0125} + iP_{0126} = \frac{T_{01}(-b_2+ia_2)}{F_{012}(-b_2+ia_2)} \tag{11}$$

$$f_{012} = \frac{P_{0126}}{a_2} \quad , \quad P_{012} = P_{0125} + \left(\frac{b_2}{a_2}\right) P_{0126}$$

$$F_{013}(s) = F_1(s)/[(s+b_3)^2+a_3^2]$$

$$P_{0135} + iP_{0136} = \frac{T_{01}(-b_3 + ia_3)}{F_{013}(-b_3+ia_3)} \tag{12}$$

$$f_{013} = \frac{P_{0136}}{a_3} \quad , \quad P_{013} = P_{0135} + \left(\frac{b_3}{a_3}\right) P_{0136}$$

$$T_{02}(s) = a_1 a_3 \, [a_{04} s + a_{05}]$$

$$a_{04} = \frac{\bar{a}_1 \bar{F}_4}{\bar{a}_1 \bar{a}_3} \quad , \quad a_{05} = - \frac{\bar{a}_5 \bar{F}_2}{\bar{a}_1 \bar{a}_3} \tag{13}$$

$$P_{024} = T_{02} \, (-b_4) / F_{014} \, (-b_4)$$

$$P_{0215} + iP_{0216} = \frac{T_{02}(-b_1 + ia_1)}{F_{011}(-b_1 + ia_1)} \quad ; \tag{14}$$

$$f_{021} = \frac{P_{0216}}{a_1} \quad ; \; P_{021} = P_{0215} + \left(\frac{b_1}{a_1}\right) P_{0216}$$

$$P_{0225} + iP_{0226} = \frac{T_{02}(-b_2 + ia_2)}{F_{012}(-b_2 + ia_2)} \tag{15}$$

$$f_{022} = \frac{P_{0226}}{a_2} \quad , \quad P_{022} = P_{0225} + \left(\frac{b_2}{a_2}\right) P_{0226}$$

$$P_{0235} + iP_{0236} = \frac{T_{02}(-b_3 + ia_3)}{F_{013}(-b_3 + ia_3)} \tag{16}$$

$$f_{023} = \frac{P_{0236}}{a_3} \quad , \quad P_{023} = P_{0235} + \left(\frac{b_3}{a_3}\right) P_{0236}$$

$$T_{03}(s) = \bar{a}_1 \bar{a}_3 \, [s^3 + a_{06}] \quad , \quad a_{06} = \frac{\bar{a}_3 \bar{F}_2}{\bar{a}_1 \bar{a}_3} \tag{17}$$

$$P_{034} = \frac{T_{03}(-b_4)}{F_{014}(-b_4)}$$

$$P_{0315} + iP_{0316} = \frac{T_{03}(-b_1+ia_1)}{F_{011}(-b_1+ia_1)} \quad ; \quad f_{031} = \frac{P_{0316}}{a_1} \quad ,$$

$$P_{031} = P_{0315} + \left(\frac{b_1}{a_1}\right) P_{0316} \tag{18}$$

$$P_{0325} + iP_{0326} = \frac{T_{03}(-b_2+ia_2)}{F_{012}(-b_2+ia_2)} \quad , \quad f_{032} = \frac{P_{0326}}{a_2} \quad ;$$

$$P_{032} = P_{0325} + \left(\frac{b_2}{a_2}\right) P_{0326} \tag{19}$$

$$P_{0335} + iP_{0336} = \frac{T_{03}(-b_3+ia_3)}{F_{013}(-b_3+ia_3)} \quad ; \quad f_{033} = \frac{P_{0336}}{a_3} \quad ;$$

$$P_{033} = P_{0335} + \left(\frac{b_3}{a_3}\right) P_{0336} \tag{20}$$

$$T_{04} = \bar{a}_1\bar{a}_3 \left[a_{08}s^2 + a_{09}\right] \quad , \quad a_{08} = \frac{\bar{a}_5\bar{a}_1}{\bar{a}_1\bar{a}_3} \quad ; \quad a_{09} = \frac{a_1\bar{F}_4}{\bar{a}_1\bar{a}_3}$$

$$P_{044} = \frac{T_{04}(-b_4)}{F_{04}(-b_4)} \tag{21}$$

$$P_{0415} + iP_{0416} = \frac{T_{04}(-b_1+ia_1)}{F_{011}(-b_1+ia_1)} \quad ; \quad f_{041} = \frac{P_{0416}}{a_1} \quad ,$$

$$P_{041} = P_{0415} + \left(\frac{b_1}{a_1}\right) P_{0416} \tag{22}$$

$$P_{0425} + iP_{0426} = \frac{T_{04}(-b_2+ia_2)}{F_{012}(-b_2+ia_2)} \quad ; \quad f_{042} = \frac{P_{0426}}{a_2} \quad ;$$

$$P_{042} = P_{0425} + \left(\frac{b_2}{a_2}\right) P_{0426} \tag{23}$$

$$P_{0435} + iP_{0436} = \frac{T_{04}(-b_3+ia_3)}{F_{013}(-b_3+ia_3)} \quad , \quad f_{043} = \frac{P_{0436}}{a_3} \quad ;$$

$$P_{043} = P_{0435} + \left(\frac{b_3}{a_3}\right) P_{0436} \tag{24}$$

$$T_{21}(s) = \bar{a}_5 F_1(s) - (\bar{F}_1 + \bar{a}_5 s^3) T_{01}(s)$$

$$T_{210}(s) = s(\bar{a}, s^3 + \bar{F}_2) F_1(s) \tag{25}$$

Let

$$F_{210}(s) \equiv s[(s+\beta_1)^2 + \alpha_1^2]\ [(s+\beta_2)^2+\alpha_2^2]\ [(s+\beta_3)^2+\alpha_3^2]$$

$$[s+\beta_4]\ [s+\beta_5]\ [(s+\beta_6)^2+\alpha_6^2] \tag{26}$$

$$F_{21}(s) = \frac{T_{21}(s)}{F_{210}(s)} \equiv \frac{P_7}{s} + \frac{P_4}{s+\beta_4} + \frac{P_5}{s+\beta_5} + \sum_{n=1,2,3,6} \frac{f_h^+ s + P_h}{(s+\beta_n)^2+\alpha_n^2} \tag{27}$$

or in proper notation

$$F_{21}(s) \equiv \frac{p_{217}}{s} + \frac{p_{214}}{s+\beta_{14}} + \frac{p_{215}}{s+\beta_{15}} + \sum_{n=1,2,3,6} \frac{f_{21n}s + p_{21n}}{(s+\beta_n)^2+\alpha_n^2} \tag{28}$$

or

$$F_{MN}(s) = \frac{p_{MN7}}{s} + \frac{p_{MN4}}{s+\beta_4} + \frac{p_{MN5}}{s+\beta_5} + \sum_{n=1,2,3,6} \frac{f_{MNh}s + p_{MNh}}{(s+\beta_n)^2+\alpha_n^2} \tag{29}$$

$$MN = 21,22,23,24$$

Define

$$F_{21n}(s) = F_{210}(s)/[(s+\beta_n)^2+\alpha_n^2] \quad , \quad n = 1,2,3,6$$

$$F_{21n}(s) = F_{22n}(s) = F_{23n}(s) = F_{24n}(s) \tag{30}$$

$$F_{217}(s) = F_{210}(s)/s \quad , \quad F_{214}(s) = F_{210}(s)/(s+\beta_4)$$

$$F_{215}(s) = F_{210}(s)/(s+\beta_5) \tag{31}$$

$$P_{217} = \frac{T_{21}(0)}{F_{217}(0)} \quad , \quad P_{214} = \frac{T_{21}(-\beta_4)}{F_{214}(-\beta_4)}$$

$$P_{215} = \frac{T_{21}(-\beta_5)}{F_{215}(-\beta_5)} \tag{32}$$

$$P_{2115} + i\, P_{2116} = \frac{T_{21}(-\beta_1+\alpha_1)}{F_{211}(-\beta_1+i\alpha_1)} \tag{33}$$

$$f_{211} = \frac{P_{2116}}{\alpha_1} \quad , \quad P_{211} = P_{2115} + \left(\frac{\beta_1}{\alpha_1}\right) P_{2116}$$

or

$$P_{21n5} + iP_{21n6} = \frac{T_{21}(-\beta_n+i\alpha_n)}{F_{21n}(-\beta_n+i\alpha_n)} \qquad n = 1,2,3,6 \tag{34}$$

$$f_{21n} = \frac{P_{21n6}}{\alpha_n} \quad ; \quad P_{21n} = P_{21n5} + \left(\frac{\beta_n}{\alpha_n}\right) P_{21n6} \tag{35}$$

Similarly

$$T_{22}(s) = (\bar{F}_1+\bar{a}_5 s^3)\ (\bar{a}_1\bar{F}_4 s - \bar{a}_5\bar{F}_2)\ - \bar{a}_1 s F_1(s) \tag{36}$$

$$P_{227} = \frac{T_{22}(0)}{F_{217}(0)} \quad P_{224} = \frac{T_{22}(-\beta_4)}{F_{214}(-\beta_4)}$$

$$P_{225} = \frac{T_{22}(-\beta_5)}{F_{215}(-\beta_5)} \tag{37}$$

$$P_{22n5}+iP_{22n6} = \frac{T_{22}(-\beta_n}{F_{21n}(-\beta_n+i\alpha_n)}$$

$$f_{22n} = \frac{P_{22n6}}{\alpha_n} \quad , \quad P_{22n} = P_{22n5} + \left(\frac{\beta_n}{\alpha_n}\right) P_{22n6} \tag{38}$$

$$T_{23}(s) = \bar{a}_3 \ (\bar{F}_1+\bar{a}55^3) \ (\bar{a}_1 s^3+\bar{F}_2)$$

$$P_{237} = \frac{T_{23}(0)}{F_{217}(0)} \quad , \quad P_{234} = \frac{T_{23}(-\beta_4)}{F_{214}(-\beta_4)} \quad , \quad P_{235} = \frac{T_{23}(-\beta_5)}{F_{215}(-\beta_5)}$$

$$P_{23n5}+ \ iP_{23n6} = \frac{T_{23}(-\beta_n+i\alpha_n)}{F_{21n}(-\beta_n+i\alpha_n)} \tag{39}$$

$$P_{23n} = \frac{P_{23n6}}{\alpha_n} \quad , \ P_{23} = P_{23n5} + \left(\frac{\beta_n}{\alpha_n}\right) P_{23n6} \tag{40}$$

$$T_{24}(s) = \bar{a}_1 F_1(s) - (\bar{F}_1+\bar{a}_5 s^3)(\bar{a}_5 s^2+\bar{F}_4)$$

$$P_{247} = \frac{T_{24}(o)}{F_{217}(o)} \quad , \quad P_{244} = \frac{T_{24}(-\beta_4)}{F_{214}(-\beta_4)} \quad , \quad P_{245} = \frac{T_{24}(-\beta_5)}{F_{215}(-\beta_5)}$$

$$P_{24n5} + iP_{24n6} = \frac{T_{24}(-\beta_n+i\alpha_n)}{F_{21n}(-\beta_n+i\alpha_n)} \quad ; \quad f_{24n} = P_{\frac{24n6}{\alpha}} \quad ; \tag{41}$$

$$P_{24n} = P_{24n5} + \left(\frac{\beta_n}{\alpha_n}\right) P_{24n6}$$

$$F''_{01}(11) = b_4^2\, p_{014} e^{-b_4} - \sum_{n=1,2,3} F_{oin}^{1/2} A_n e^{-b_n} \sin(a_n + g_{oin} + 2\bar{g}_n)$$

$$F_{oin} = f_{oin}^2 + \bar{f}_{oin}^2 \; ; \quad \bar{f}_{oin} = \frac{p_{oin} - f_{oin} b_n}{a_n}$$

$$A_n = a_n^2 + b_n^2 \; , \quad \sin\bar{g}_n = b_n / A_n^{1/2}, \quad \cos\bar{g}_n = \frac{a_n}{A_n^{1/2}} \tag{42}$$

$$\sin g_{oin} = \frac{f_{oin}}{F_{oin}^{1/2}} \; , \quad \cos g_{oin} = \frac{f_{oin}}{F_{oin}^{1/2}}$$

or

$$F''_{om}(1) = b_4^2\, p_{om4} e^{-b_4} - \sum_{n=1,2,3} F_{omn}^{1/2}\, A_n e^{-b_n} \sin(a_n + g_{omn} + 2\bar{g}_n)$$

$\boxed{m = 1,2,3,4}$

(43)

$$F_{omn} = f_{omn}^2 + \bar{f}_{omn}^2 \; ; \quad \bar{f}_{omn} = \frac{p_{omn} - f_{omn} b_n}{a_n}$$

$$A_n = a_n^2 + b_n^2 \; , \quad \sin\bar{g}_n = b_n / A_n^{1/2} \; , \quad \cos\bar{g}_n = \frac{a_n}{A_n^{1/2}}$$

$$\sin g_{omn} = \frac{f_{omn}}{F_{omn}^{1/2}} \; ; \quad \cos g_{omn} = \frac{\bar{f}_{omn}}{F_{omn}^{1/2}}$$

$$F'_{om}(1) = -b_4 p_{om4} e^{-b_4} + \sum_{n=1,2,3} F_{om}^{1/2}\, A_n^{1/2} e^{-b_n} \cos(a_n + g_{omn} + \bar{g}_n) \tag{44}$$

$m = 1,2,3,4$

$$F'''_{om}(1) = b_4^3 p_{om4} e^{-b_4} - \sum_{n=1,2,3} F_{om}^{1/2} A_n^{3/2} e^{-b_n} \cos(a_n + g_{omn} + 3\bar{g}_n) \qquad (45)$$

$m = 1,2,3,4$

$$F''_{MN}(1) = \sum_{m=4,5} \beta_m^2 p_{MNm} e^{-\beta_n} - \sum_{n-1,2,3,6} \bar{F}_{MNn}^{1/2} \bar{A}_n e^{-\beta_n} \sin(2_n + G_{MNn} + 2\bar{G}_n) \qquad (46)$$

$\boxed{MN = 21,22,23,24}$

$$\bar{F}_{MNn} = f_{MNn}^2 + \bar{f}_{MNn}^2 \;,\quad \bar{A}_n = \alpha_n^2 + \beta_n^2 \;,\quad \bar{f}_{MNn} = \frac{p_{MNn} - f_{MNn}\beta_n}{\alpha_n} \qquad (47)$$

$$\mathrm{Sin}G_{MNn} = \frac{f_{MNn}}{\bar{F}_{MNn}^{1/2}} \;;\quad \cos G_{MNn} = \frac{\bar{f}_{MNn}}{\bar{F}_{MNn}^{1/2}} \;;\quad \sin\bar{G}_n = \frac{\beta_n}{\bar{A}_n^{1/2}} \;,$$

$$\cos\bar{G}_n = \frac{\alpha_n}{\bar{A}_n^{1/2}}$$

$$F'''_{MN}(1) = -\sum_{m=4,5} \beta_m^3 p_{MNm} e^{-\beta_m} - \sum_{n=1,2,3,6} \bar{F}_{MNn}^{1/2} \bar{A}_n^{3/2} e^{-\beta_n} \cos(\alpha_n + G_{MNn} + 3G_r \qquad (48)$$

$n = 1,2,3,6$

$$\bar{F}_{11} = F_{21}'''(1) \; ; \; \bar{F}_{12} = F_{22}'''(1) \; ; \; \bar{F}_{13} = F_{23}'''(1) \; ; \; \bar{F}_{14} = F_{24}'''(1)$$

$$\bar{F}_{21} = -F_{01}''(1) \; ; \; \bar{F}_{22} = F_{02}''(1) \; ; \; \bar{F}_{23} = F_{03}''(1) \; ; \; \bar{F}_{24} = -F_{04}''(1)$$

$$\bar{F}_{31} = \bar{a}_1 F_{21}''(1) + \bar{a}_5 F_{01}'(1) \; ; \; \bar{F}_{32} = \bar{a}_1 F_{22}''(1) - \bar{a}_5 F_{02}'(1) \; ;$$

$$\bar{F}_{33} = \bar{a}_1 F_{23}''(1) - \bar{a}_5 F_{03}'(1) \qquad (49)$$

$$\bar{F}_{34} = \bar{a}_1 F_{24}''(1) + \bar{a}_5 F_{04}'(1)$$

$$\bar{F}_{41} = (\bar{a}_4 - \frac{a_5^{-2}}{\bar{a}_1}) F_{01}'(1) - \bar{a}_3 F_{01}'''(1) \; ; \; \bar{F}_{42} = \bar{a}_3 F_{02}'''(1) - (\bar{a}_4 - \frac{a_5^{-2}}{\bar{a}_1}) F_{02}'(1)$$

$$\bar{F}_{43} = \bar{a}_3 F_{03}'''(1) - (\bar{a}_4 - \frac{\bar{a}_5^{\,2}}{\bar{a}_1}) F_{03}'(1) \; ; \; \bar{F}_{44} = (\bar{a}_4 - \frac{\bar{a}_5^{\,2}}{\bar{a}_1}) F_{04}'(1) - \bar{a}_3 F_{04}'''(1)$$

Determine eigenvalues that makes the following determinant zero

$$\begin{vmatrix} \bar{F}_{11} & \bar{F}_{12} & \bar{F}_{13} & \bar{F}_{14} \\ \bar{F}_{21} & \bar{F}_{22} & \bar{F}_{23} & \bar{F}_{24} \\ \bar{F}_{31} & \bar{F}_{32} & \bar{F}_{33} & \bar{F}_{34} \\ \bar{F}_{41} & \bar{F}_{42} & \bar{F}_{43} & \bar{F}_{44} \end{vmatrix} = 0 \qquad (50)$$

Equation 50 is therefore expected to represent the closed-form expression for the divergence eigenvalues. Numerical methods are now being used to extract these eigenvalues in order to obtain the divergence speeds.

RESULTS

The results obtained so far seem to verify existing results and establish new trends. Due to the fact that the evolution of these new trends are yet to be fully completed, only a summary of these results are presented below.

The results obtained by solving equation 50 were carefully to evolve the physical insight into the mechanism of divergence instability in the presence of warping restraint and elastic coupling. This study revealed the following, as can be seen from figures 1-7.

First, it is seen that the view held by many analysts that elastic coupling plays a significant role in aeroelastic divergence tailoring is verified.

Second, it is seen that another view that, higher aeroelastic divergence stability boundaries are feasible with negative elastic coupling (than positive elastic coupling), is basically true, but up to a point. It is further seen that there seems to be a limit to how negative the elastic coupling can be made to obtain better stability boundaries - after such a limit, a further negative increment of elastic coupling would seem to lower the stability boundaries.

Third, it is found that the effective aspect ratio defined in the first phase of this research program (λ_c), for simpler models can still be used in this relatively more complex model, to measure

the effect of warping restraint on the phenomenon of divergence instability. The results show that ignoring the warping restraint would lead to conservative estimates for the divergence instability boundaries. It is also seen that the restraint of warping effects are more significant for small effective aspect ratio (λ_c) and/or large elastic coupling.

REFERENCES

1. Reissner, E. and Stein, M., "Torsion and Transverse Bending of Cantilevered Plates", NACA TN 2369, June 1951.
2. Bisplinghoff, R.L., Ashley, H. and Halfman, R.L., "Aeroelasticity", Addison Wesley, 1955.
3. Petre, A., Stanescu C., and Librescu, L., "Aeroelastic Divergence of Multicell Wings (Taking their Fixing Restraints into Account)", Aeromecanique, 1962, pp. 689-698.
4. E. F. Crawley and J. Dugundji, "Frequency Determination and Non-dimensionalization for Composite Cantilever Plates", Journal of Sound and Vibration, Vol. 72, No. 1, pp. 1-10, 1980.
5. Oyibo, G.A. and Berman, J.H., "Influence of Warpage on Composite Aeroelastic Theories", AIAA Paper No. 85-0710, April 1985.
6. Oyibo, G.A. and Berman, J.H., "Anisotropic Wing Aeroelastic Theories with Warping Effects", DGLR Paper No. 85-57, Second International Symposium on Aeroelasticity and Structural Dynamics, Technical University of Aachen, West Germany, April 1985.

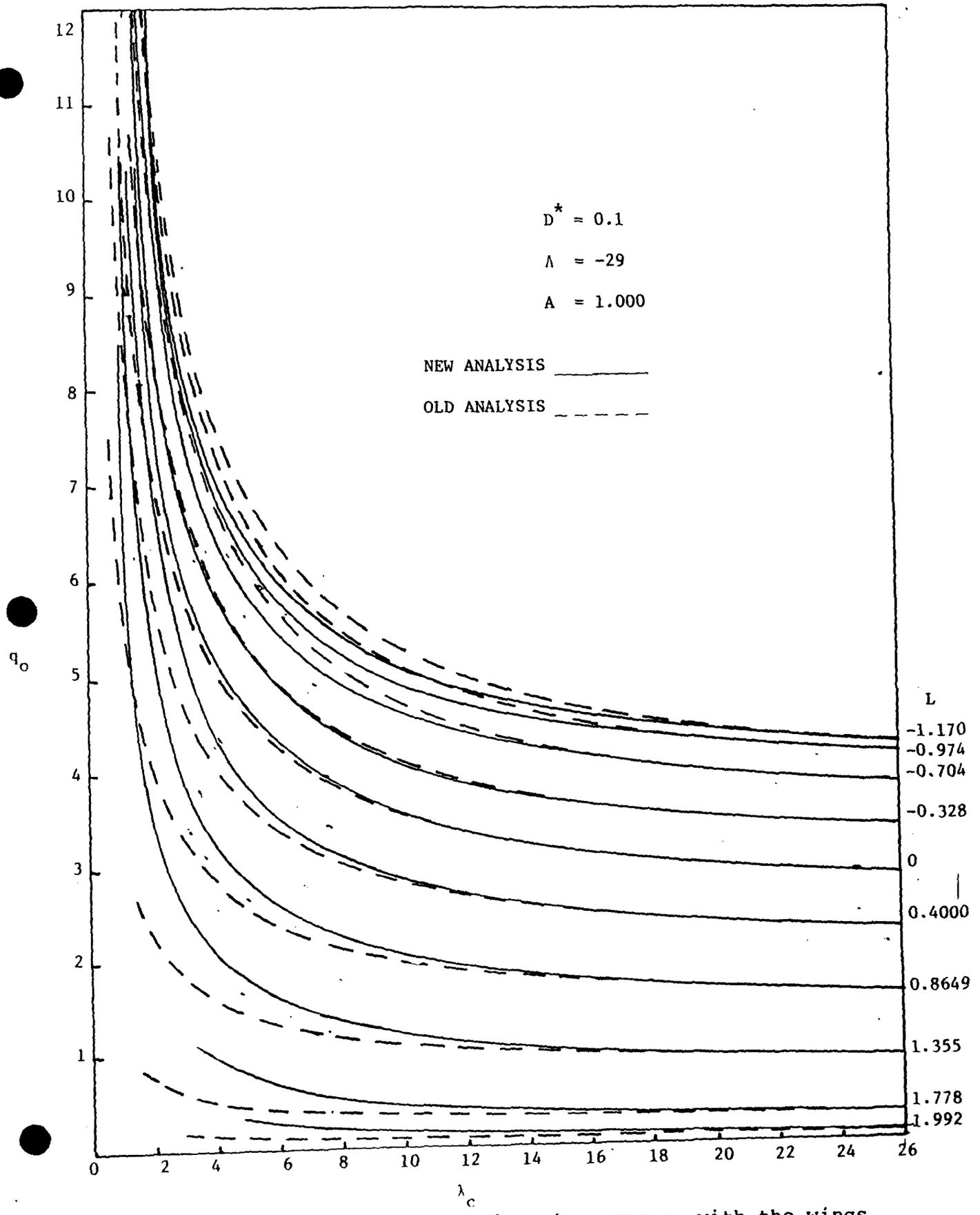

Figure 1 Variation of Divergence dynamic pressure with the wings Effective Aspect ratio

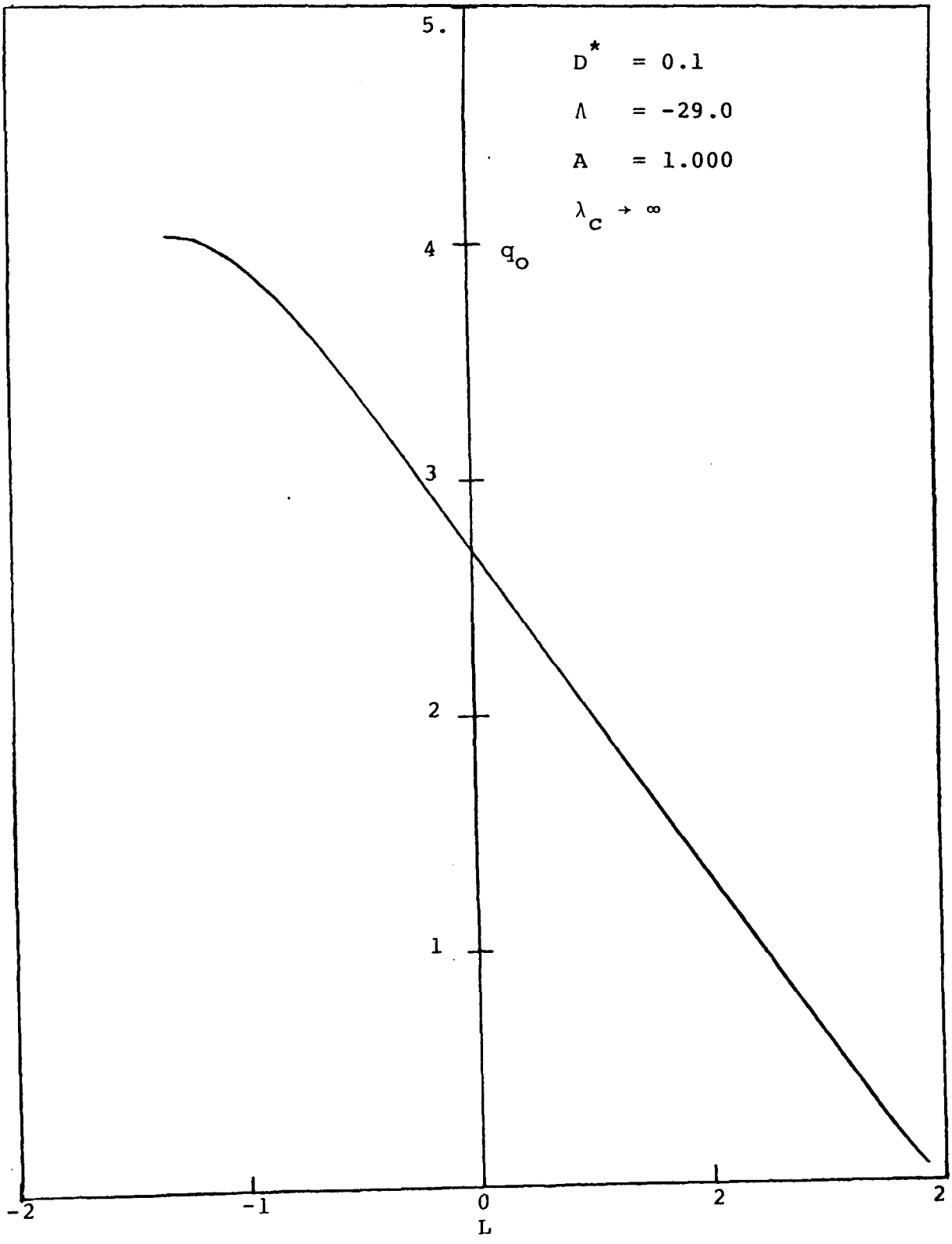

Figure 2 Variation of divergence dynamic pressure with coupling for large effective wing aspect ratio

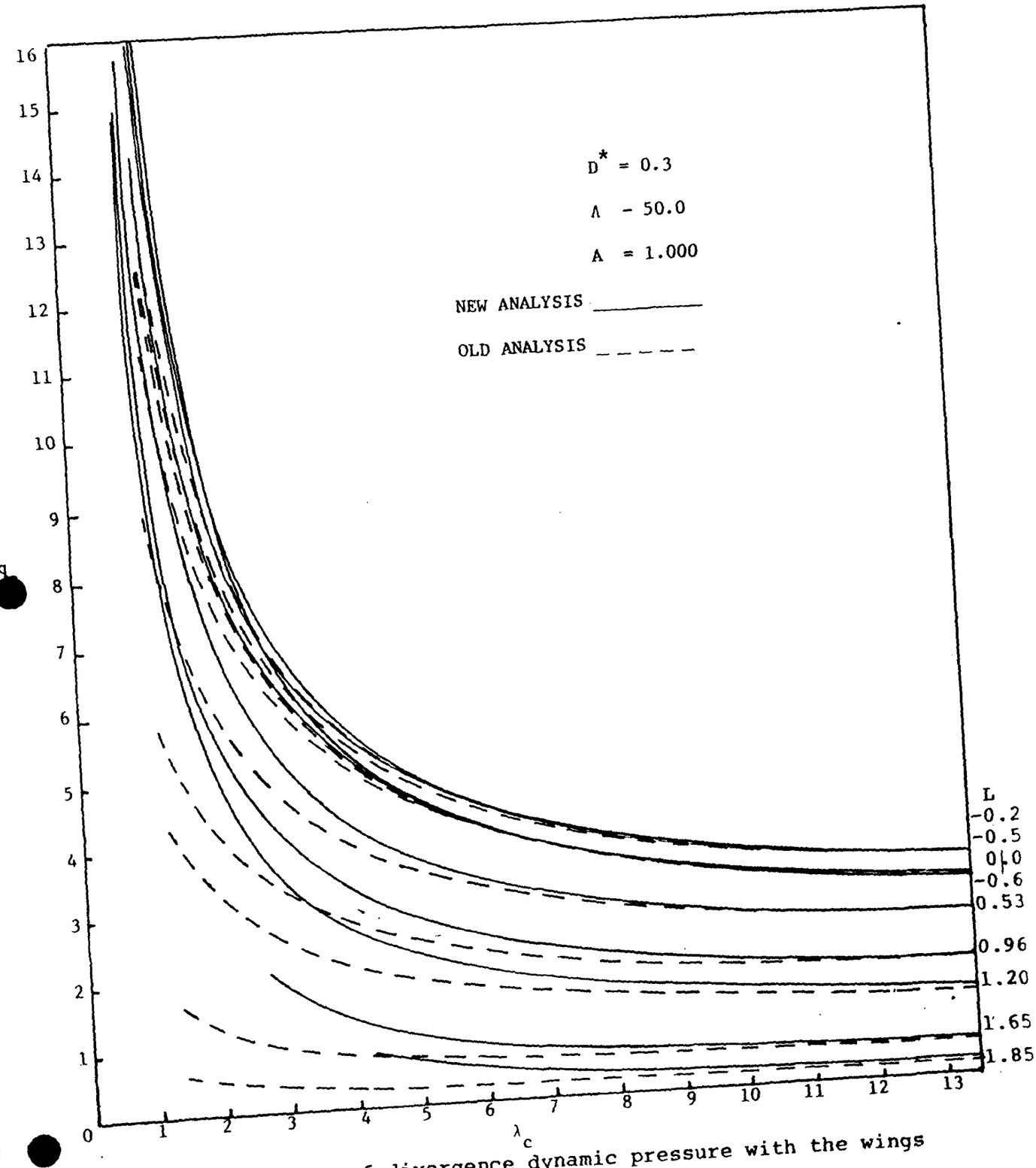

Figure 3 Variation of divergence dynamic pressure with the wings effective aspect ratio

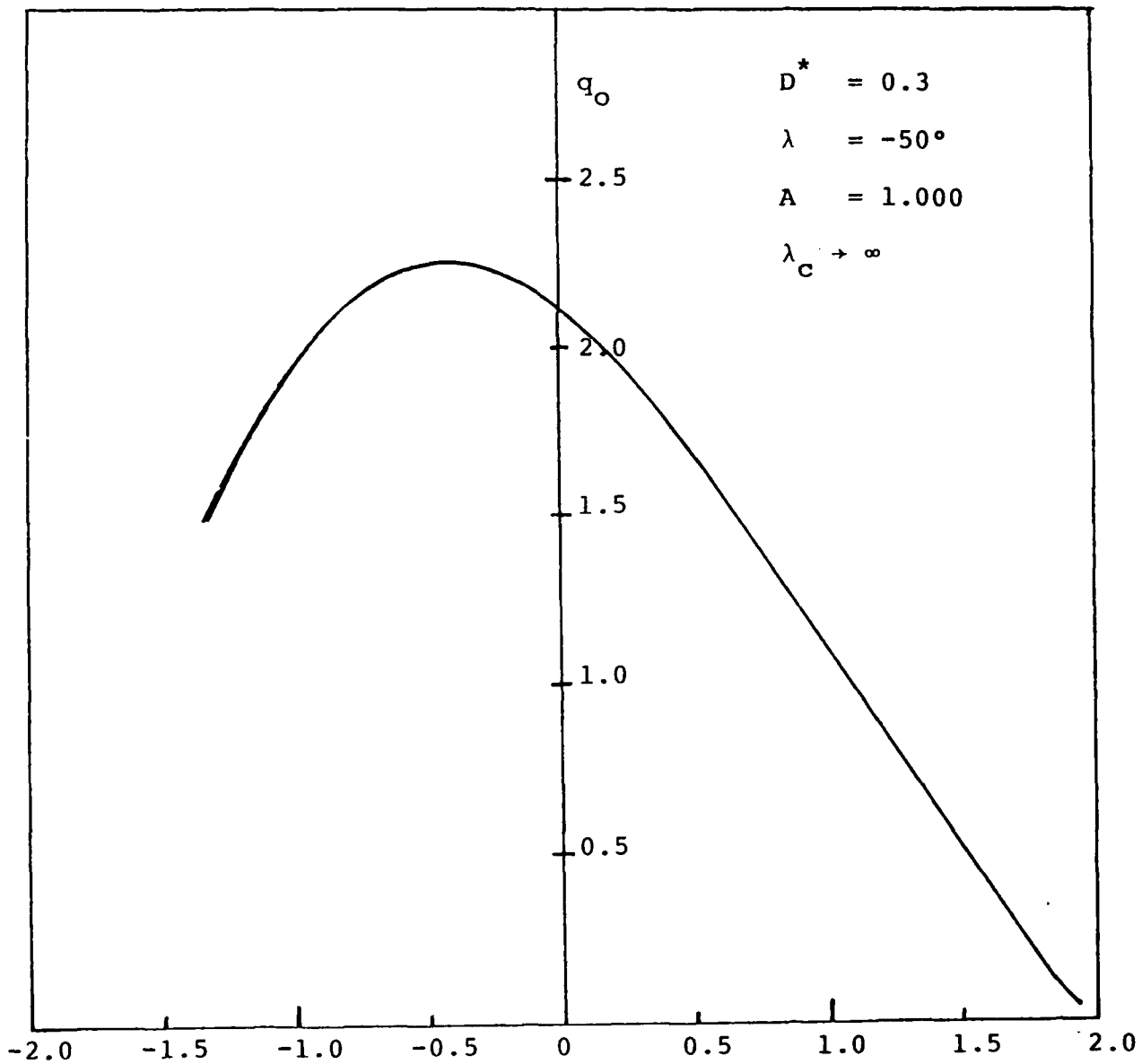

Figure 4 Variation of divergence dynamic pressure with coupling for large effective wing aspect ratio

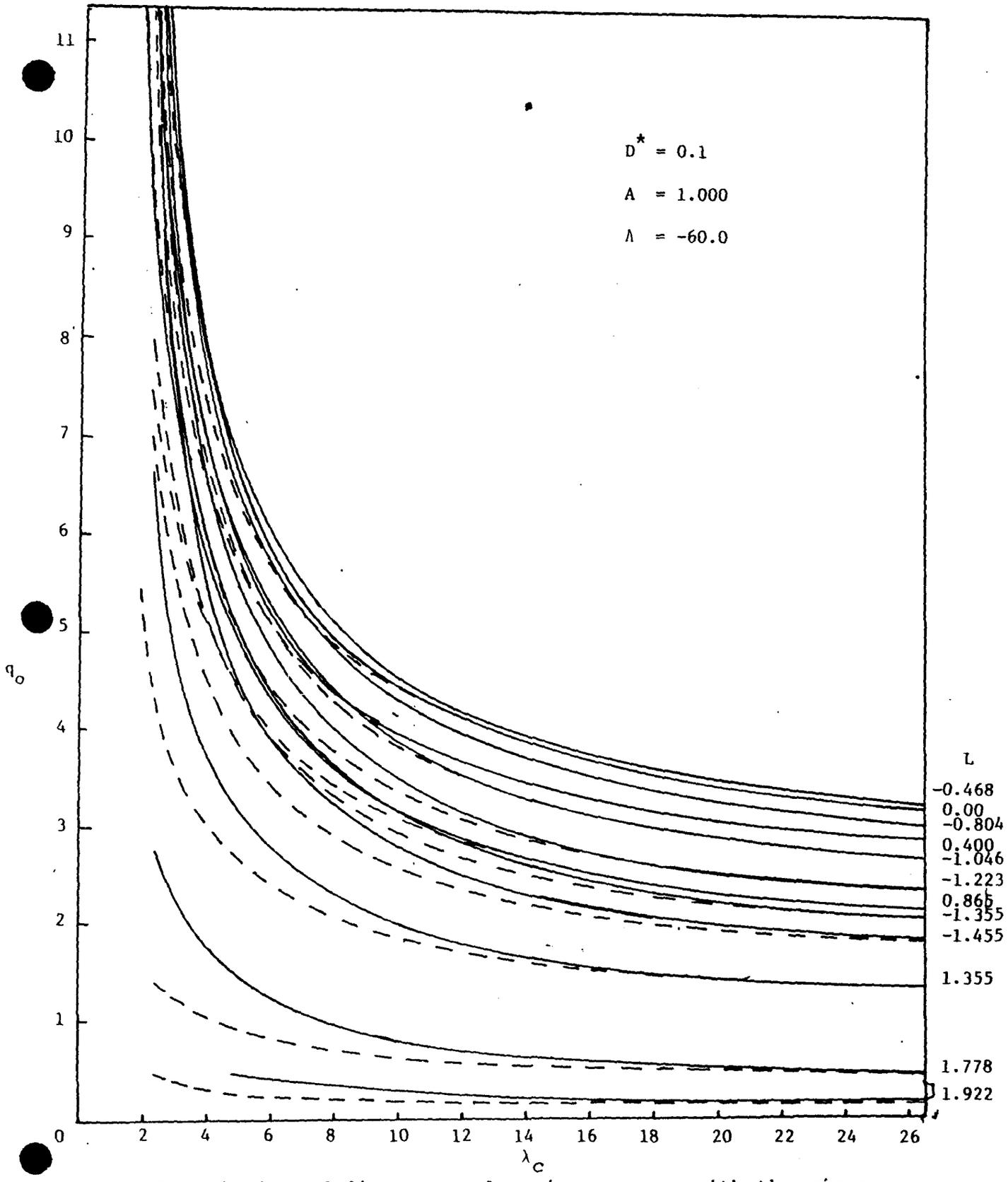

Figure 5 Variation of divergence dynamic pressure with the wings effective aspect ratio

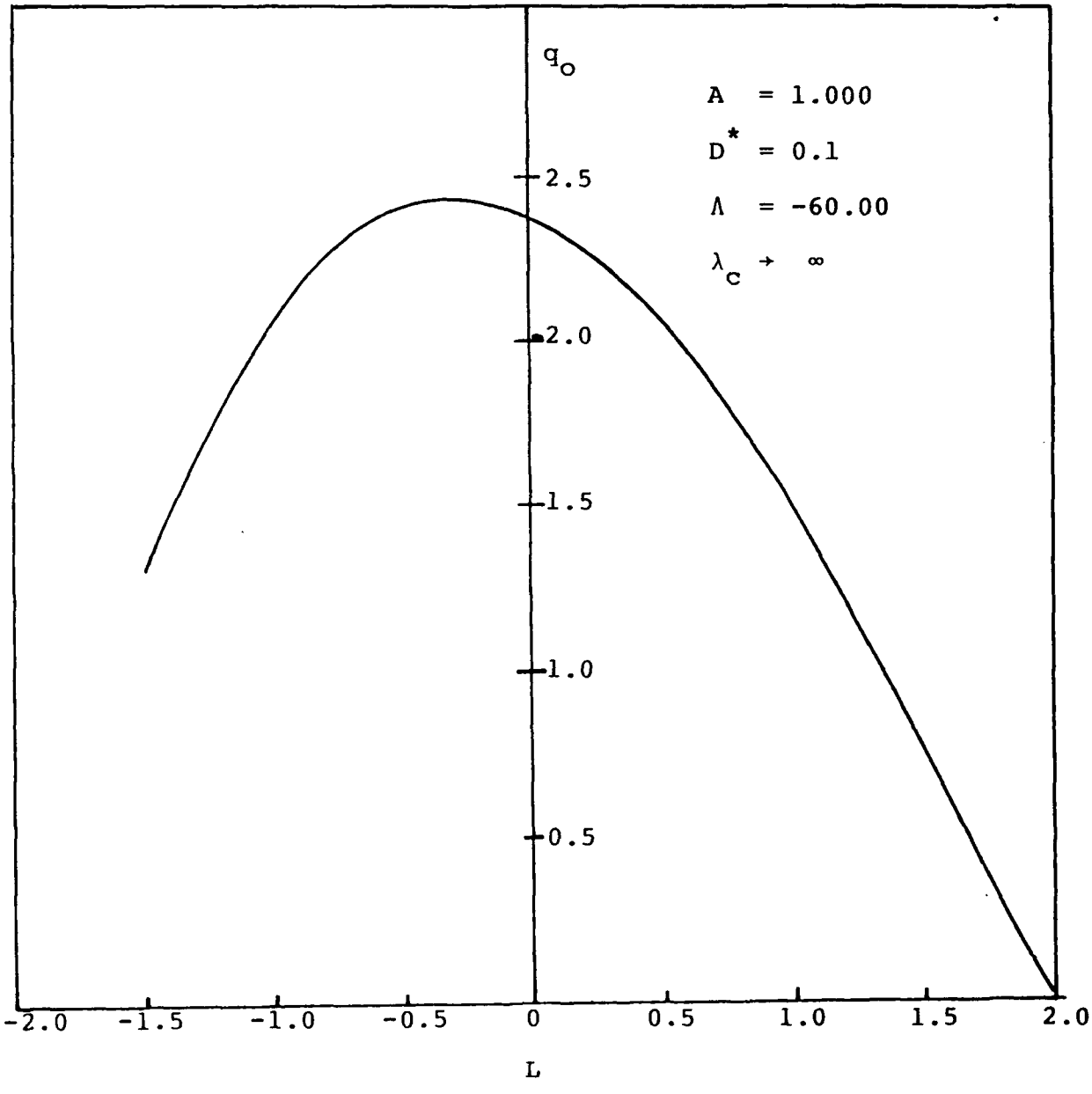

Figure 6 Variation of divergence dynamic pressure with coupling for large effective wing aspect ratio

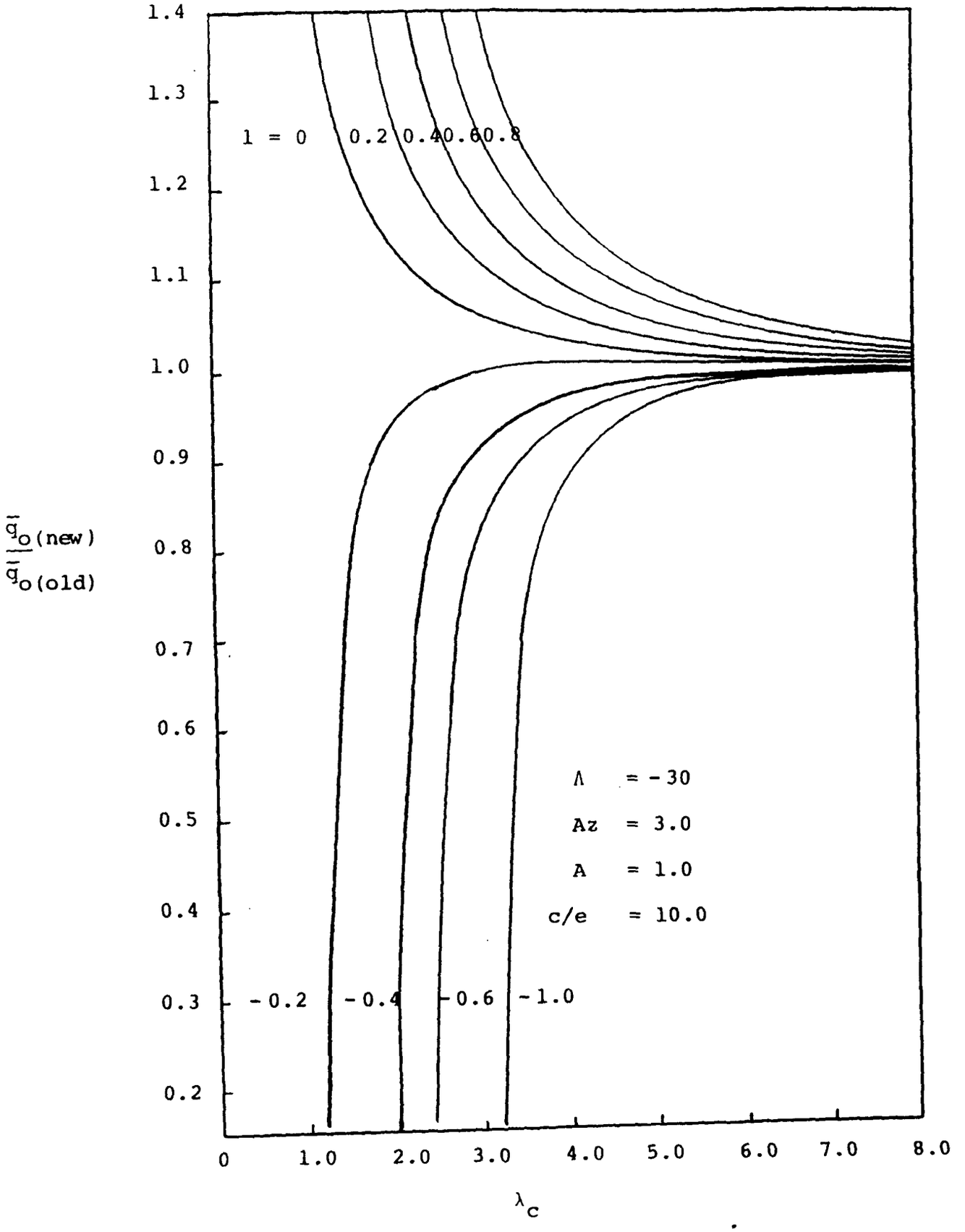

Figure 7: Variation of the nondimensionalized dynamic pressure with wings effective aspect ratio

5.3

Exact Solutions to Aeroelastic Oscillations of Composite Aircraft Wings with Warping Constraint and Elastic Coupling[†]

Gabriel A. Oyibo[*] and James Bentson[*]
Polytechnic University
Farmingdale, New York

Abstract

Exact solutions within the framework of standard aeroelastic bending and twisting assumptions are found to the free oscillations of composite aircraft wings having warping constraint and elastic coupling. The problem is treated as a regular boundary value problem consisting of two fourth order partial differential equations coupled by the presence of elastic coupling. This system, which is linear, therefore is equivalent to an eighth order ordinary differential equation . Classical linear "operator" method is therefore used to extract fundamental solutions which are superimposed appropriately to obtain an exact functional form for the mode shapes. These mode shapes are therefore made to satisfy the necessary boundary conditions, a process that leads to the formulation of the required eigenvalue problem. The eigenvalues are extracted numerically by using appropriate ordering of the eight roots of the operator equation. The bending-torsion frequencies obtained as a result of this analysis are compared favorably with existing results. New insights made possible by these results which are preliminary, ap-

[†]Research sponsored by the Air Force Office of Scientific Research (AFOSR), under Contracts F49620-85-C-0090 and F49620-87-C-0046.

[*]Associate Professor Dept. of Aerospace Engineering

pear to be that (a) the first coupled frequency decreases with increasing coupling and (b) the phenomenon of modal transformations found by earlier investigators is explainable in terms of some conservative inter-modal energy transfer.

5.3.1 NOMENCLATURE

a_i	= chordwise integrals
c_o', c_o	= affine space half-chord and chord, respectively
D_{ij}	= elastic constants
e	= parameter that measures the location of the reference axis relative to mid-chord
EI, GJ	= bending and torsional stiffness, respectively
$\bar{h}$	= wing box depth
(h_o, α_o)	= affine space bending and torsional displacement, respectively
K,So	= elastic coupling and warping stiffness, respectively
k_{ij}	= elemental stiffness parameter
k_o	= Strouhal number
L_o, M_o	= affine space running aerodynamic lift and moments, respectively
ℓ_o	= affine space half-span for the wing
m_o	= affine space mass per unit span
$(\Delta p, \Delta p_o)$	= differential aerodynamic pressure distributions in physical and affine space, respectively
t	= time
U, U_o	= virtual work expressions in physical and affine space, respectively
U_f	= flutter speed
$(x,y,z,), (x_o, y_o, z_o)$	= physical and affine space coordinates, respectively
$\gamma_i, \delta_i, \beta_i$	= displacement shape functions
$r, L_1, L_2, D^*, D^*_o,$	= generic nondimensionalized stiffness parameters
μ_o	= affine mass ratio parameter
μ_{ij}, ε	= Poisson ratios and generalized Poisson's ratio, respectively
λ_o	= divergence parameter

ρ, ρ_∞ = affine space material and air density, respectively

θ = twisting displacements

w = displacement

ω = vibration frequency

5.3.2
Introduction

Perhaps one of the more elusive aspects of supermaneuverability as a design concept is its aeroelastic implications. One generally accepted definition of supermaneuverable aircraft is that it is designed to operate at high angles of attack. Strictly speaking high angle of attack problems are nonlinear. However due to the high degree of complexities involved in dealing with nonlinear aeroelastic problems, an average aeroelastician would prefer to deal with a linearized version of the problem (at least as a first approximation). If linear aeroelastic equations are used under such conditions, at least it should be assumed that the high angle of attack would introduce large twisting displacements which would imply that terms containing twisting displacement should be retained. Even under low angle of attack assumptions, the early works of Reissner and Stein[1] and later works of Libescu et al[2] have shown that for metal wings there are conditions under which the so called St. Venant's torsion principle is inapplicable. This is when the restraint of warping effect is important and a more accurate analysis would need to include a higher order term involving the twisting displacement. Although the retention of such a term implies solving fourth order (instead of second order) differential equations for the twisting and bending displacements, the equations can be easily decoupled for metal wings. However for composite wings, the decoupling of these equations is neither easy practically nor is it even desirable from aeroelastic tailoring standpoint.[3-7] These studies have also shown that the restraint of warping is very important

in composite wings. Therefore it would seem that an aeroelastic analysis of a supermaneuverable (high angle of attack) aircraft wing fabricated of composite materials would need to consider the effects of restraint of warping as well as elastic coupling.

Previous investigation of this latter problem (free vibration) at MIT[3,4] used analytical methods to solve the decoupled problem, while numerical methods were utilized to solve the coupled problems. Consequently general results were presented for the decoupled problem while representative results were presented for the coupled problem.

In this paper the coupled free vibration is treated analytically as a pair of coupled fourth order (differential equations) boundary value problem to which exact closed form eigen-solutions are sought. The enforcement of the necessary boundary conditions resulted in a fairly complicated transcendental function to be used to determine the required eingenvalues from which the natural frequencies are to be obtained. This transcendental function was complex in contrast to its decoupled counterpart (which is real). That should be indicating the presence of the phase angle that exists between the twisting and bending displacements. A comparison with a damped (decoupled) system in which complex determinant signifies phase angles between damping and other forces, led us to the formulation of an explanation for the "modal transformation" phenomenon which was reported in studies at MIT[3,4] and Purdue[8] (which seemed to have lacked explanation until this study). The explanation is that the modal transformation may be viewed as a form of steady state conservative (energy stays in this system

since there is no damping) inter-

modal energy transfer between the vibration modes. In fact work currently in progress at Purdue[8] seem to support and confirm this explanation. The results which favorably compared with those obtained at MIT,[3,4] also revealed that coupling has a tendency to lower the first coupled natural frequency of a composite aircraft wing. In fact it is seen that a substantial amount of coupling could reduce the first coupled frequency to almost zero (hence a possibility of coupling with rigid body modes).

5.3.3

Problem Statement

For a composite aircraft wing cantilevered at the root as shown in Figure 1, the virtual work theorem in the physical space is given by

$$\delta\bar{U} = 0 = \frac{\delta}{2}\int_0^t\int_A\int\Big[D_{11}(w_{,xx})^2 + 2D_{12}\,w_{,xx}\,w_{,yy} + D_{22}(w_{,yy})^2\Big] + 4D_{16}\,w_{,xx}\,w_{,xy} + 4D_{26}\,w_{,yy} + 4D_{66}\,(w_{,xy})^2\;dxdydt - \frac{\delta}{2}\int_0^t\int_A\int\rho\,\bar{h}\,\dot{w}^2 dxdydt + \int_0^t\int_A\int\Delta p\delta w\,dxdydt \qquad (1)$$

where:

D_{ij} are the elastic constants, ρ, is the material density, Δp is the differential pressure distribution, w is the displacement, t is the time, A integrals represent area integrals and h is the wing box depth.

Using the following affine transformation of variables;

$$x = \left(\frac{D_{11}}{D_{22}}\right)^{1/4} x_o \quad ; \quad y = y_o \quad ; \quad z = z_o \qquad (2a)$$

then in affine space the virtual work theorem becomes:

$$\delta\bar{U}_o = 0 = 2\int_0^t\iint_A \Big\{ (w,_{x_o x_o})^2 + 2D^* \Big[(1-\varepsilon)(w,_{x_o y_o})^2 + \varepsilon w,_{x_o x_o} w,_{y_o y_o}\Big] + (w,_{y_o y_o})^2 + L_1 w,_{x_o x_o} w_{x_o y_o} + L_2 w,_{y_o y_o} w,_{x_o y_o}\Big\} dx_o dy_o dt$$
$$- \frac{\delta}{2}\int_0^t\iint_A \rho_o \dot{w}^2 dx_o dy_o dt + \int_0^t\iint_A \Delta p_o \delta w dx_o dy_o dt \qquad (2b)$$

where

$$\bar{U}_o = \frac{\bar{U}}{D_{22}}\left(\frac{D_{22}}{D_{11}}\right)^{1/4} \quad ; \quad D^* = \frac{D_{12} + 2D_{66}}{(D_{11}D_{22})^{1/2}}$$
$$; \ \varepsilon D^* = \frac{D_{12}}{(D_{11}D_{22})^{1/2}} \quad ; \quad L_1 = \frac{4D_{16}}{(D_{11})^{3/4}(D_{22})^{1/4}} \quad ;$$
$$L_2 = \frac{4D_{26}}{(D_{11})^{1/4}(D_{22})^{3/4}} \quad ; \ \Delta p_o = \frac{\Delta p}{D_{22}} \quad ; \quad \rho_o = \frac{\rho\bar{h}}{D_{22}} \qquad (3)$$

If the affine space equivalent of the standard aeroelastic displacement assumptions is made, i.e.,

$$w(x_o, y_o, t) = h_o(y_o, t) + x_o \alpha_o(y_o, t) \ .. \qquad (4)$$

where h_o and α_o are the bending and twisting displacements respectively, then it can be shown through the use of the calculus of variations that a coupled set of aeroelastic equations of motion for the composite aircraft wing, in which the restraint of warping and elastic coupling effects are accounted for is given by

$$a_1 h_o^{iv} + a_2 \alpha_o^{iv} - a_5 \alpha_o^{iii} + \rho_o a_1 \ddot{h}_o + \rho_o a_2 \ddot{\alpha}_o = L_o$$

$$a_2 h_o^{iv} + a_5 h_o^{iii} + a_3 \alpha_o^{iv} - a_4 \alpha_o'' + \rho_o a_3 \ddot{\alpha}_o + \rho_o a_2 \ddot{h}_o = M_o \qquad (5)$$

$$\text{at } y_o = 0$$

with boundary conditions

$$h_o = 0,\ h_o' = 0,\ \alpha_o = 0,\ \alpha_o' = 0 \qquad (6)$$

$$\text{at } y_o = \ell_o$$

$$a_3 \alpha_o'' + a_2 h_o'' - L_2 a_2 \alpha_o' = 0,\ a_1 h_o'' - a_5 \alpha_o' + a_2 \alpha_o'' = 0$$

$$a_2 \alpha_o''' + a_1 h_o''' - a_5 \alpha_o'' = 0$$

$$a_2 h_o''' + a_3 \alpha_o''' + a_5 h_o'' - a_4 \alpha_o' = 0$$

where:

$$a_1 = \int_{e\bar{c}_o}^{\bar{c}_o} dx_o \quad ; \quad a_2 = \int_{e\bar{c}_o}^{\bar{c}_o} x_o\, dx_o$$

$$a_3 = \int_{e\bar{c}_o}^{\bar{c}_o} x_o^2 dx_o \quad ; \quad a_4 = 2\int_{e\bar{c}_o}^{\bar{c}_o} D^*(1-\epsilon)dx_o$$

$$L_o = \int_{e\bar{c}_o}^{\bar{c}_o} \Delta p_o dx_o \quad ; \quad a_5 = \int_{e\bar{c}_o}^{\bar{c}_o} L_2 dx_o \qquad (7)$$

$$M_o = \int_{e\bar{c}_o}^{\bar{c}_o} x_o \Delta p_o dx_o$$

$$-\infty < e < 0 \quad ; \quad \bar{c}_o = \frac{c_o}{1-e}$$

$$(\,)' = \frac{\partial}{\partial y_o} ; \quad (\dot{}) = \frac{\partial}{\partial t}$$

For free vibrations, if a_2 (through the geometric construction of the wing) is made to be zero, equations 5 reduce to

$$a_1 h_o^{iv} - a_5 \alpha_o''' + \rho_o a_1 \ddot{h}_o = L_o$$

$$a_3 \alpha_o^{iv} + a_5 h_o''' - a_4 \alpha'' + \rho_o a_3 \ddot{\alpha}_o = M_o \qquad (8a)$$

with boundary conditions

at $y = 0$,

$$h_o = 0,\ h_o' = 0,\ \alpha_o = 0,\ \alpha' = 0$$

at $y_o = \ell_o$

$$a_1 h_o''' = a_5 \alpha_o''' = 0,\ a_1 h_o'' - a_5 \alpha_o' = 0 \qquad (8b)$$

$$a_3 \alpha_o''' + a_5 h_o''' - a_4 \alpha_o' = 0$$

It may be stated here that the restraint of warping effect is represented by the product of α^{IV} and a_3 while the elastic coupling effect is represented by the a_5 terms.

5.3.4

Methods of Solution

Two methods for solving equations 8 are examined in this paper. These are (a) an "exact closed form" approach and (b) a "semi-exact closed form" approach. The exact closed form approach is defined here as one in which explicit expressions are derived for the eight roots of the eighth order operator equations representing equations 8a, and through the superimposition of fundamental solutions corresponding to each of the eight operator roots, the boundary conditions 8b are satisfied. The semi-exact closed form approach is the same as (a) except that the roots of the operator equation are determined numerically through the usage of some standard root extraction subroutines.

In either case, to solve for the operator roots of equation 8a, it may be rewritten in operator form as follows,

$$\beta_n = \bar{x}_n^{1/2} \qquad n = 1,2,3,4 \tag{13}$$

and $\bar{x}_n$ can be obtained either from the numerical solution of equation 11 or according to the method described in Abramowitz and Stegun,[10] as follows

Define

$$\lambda_c = (\ell_o/c_o)\sqrt{\tfrac{3}{2}D_o^*} \qquad \bar{\lambda}_c = (\ell_o/c_o)\sqrt{\tfrac{3}{2}(D_o^* - \tfrac{L_2^2}{2})} \tag{14}$$

$$P_1 = 4(\bar{\lambda}_c^4 + \lambda_c^4) - 8/3\bar{\lambda}_c^2\lambda_c^2 + \frac{\bar{k}^2}{27}$$

$$P_2 = \frac{1}{6}(32\bar{\lambda}_c^2\lambda_c^2 + \frac{\bar{k}^2}{3}) \tag{15}$$

$$S_1 = 2\bar{k}\left[\bar{k}P_1 + (\bar{k}^2P_1^2 - 8P_2^3)^{\frac{1}{2}}\right]^{\frac{1}{3}}$$

$$S_2 = 2\bar{k}\left[\bar{k}P_1 - (\bar{k}^2P_1^2 - 8P_2^3)^{1/2}\right]^{1/3} \tag{16}$$

$$u_1 = S_1 + S_2 - \frac{\bar{k}^2}{3}$$

$$u_2 = -\frac{1}{2}(S_1+S_2) - \frac{\bar{k}^2}{3} + i\sqrt{\tfrac{3}{2}}(S_1-S_2) \tag{17}$$

$$u_3 = -\frac{1}{2}(S_1+S_2) - \frac{\bar{k}^2}{3} - i\sqrt{\tfrac{3}{2}}(S_1-S_2)$$

$$f_{3,4} = -8\bar{\lambda}_c^2 \mp \left[64\bar{\lambda}_c^4 + u_i + \bar{k}^2 \right]^{\frac{1}{2}}$$

$$f_{5,6} = \frac{u_i}{2} \pm \left[\left(\frac{u_i}{2}\right)^2 - \frac{\bar{k}^4}{4} \right]^{\frac{1}{2}} \qquad (18)$$

$$\bar{x}_{1,2} = \frac{-f_3 \pm \sqrt{f_3^2 - 4f_5}}{2}$$

$$\bar{x}_{3,4} + \frac{-f_4 \pm \sqrt{f_4^2 - 4f_6}}{2} \qquad (19)$$

where u_i $(i = 1,2,3)$ is the root that makes $f_{3,4,5,6}$ all real.

5.3.5
Consistency Conditions

From equations 12(a) and 12(b) it is seen that there are sixteen arbitrary integration constants as opposed to the expected eight constants. The additional eight constants have been introduced superfluously as a result of the differential operation which was done in order to eliminate one of the dependent variables in the two coupled differential equations (equations 9). In order to get rid of these superfluous solutions it is necessary to enforce some consistency conditions. This may be accomplished by

substituting equations 12(a) and 12(b) into one of the equations 9 and requiring the equation to be satisfied identically. This procedure shall establish a set of explicit relationships between the constants A_n and B_n in which A_n can be determined in terms of B_n or vice-versa.

When the superfluous solutions are eliminated, equations 12 can now be used to satisfy the boundary conditions for this problem (equations 8b). Consequently the condition for nontrivial solutions is enforced to obtain the transcendental functional expression for determining the eigenvalues of this problem.

5.3.6

Eigenvalues

The following steps and definitions are carried out in order to obtain the transcendental functional expression for determining the necessary eigenvalue (for this eighth order boundary value problem) from which the coupled natural frequencies may be obtained

Define

$$h_n = \beta_n^4 - \frac{\bar{k}2}{2} \quad ; \quad t_n = \beta_n^2 - \frac{1}{\beta_n^2} h_n$$

$$\bar{h}_n = \frac{h_n}{\beta_n^3} \qquad h_n' = \frac{h_n}{\beta_n} \tag{20}$$

$$\bar{t}_n = 16(\lambda_c^2 - \bar{\lambda}_c^2)\ \beta_n^2 + (-1)^{n+1} \frac{h_n}{\beta_n^2} [\beta_n^2 + (-1)^n 16\lambda_c^2] \tag{21}$$

$$a_{15} = \frac{\bar{h}_3+\bar{h}_2}{\bar{h}_1+\bar{h}_2} \qquad a_{17} = \frac{\bar{h}_4-\bar{h}_2}{\bar{h}_1+\bar{h}_2} \qquad a_{35} = \frac{\bar{h}_3-\bar{h}_1}{\bar{h}_1+\bar{h}_2}$$

$$a_{37} = \frac{\bar{h}_1+\bar{h}_4}{\bar{h}_1+\bar{h}_2} \qquad a_{26} = \frac{\bar{h}_3-\bar{h}_2}{\bar{h}_2-\bar{h}_1} \qquad a_{28} = \frac{\bar{h}_4-\bar{h}_2}{\bar{h}_2-\bar{h}_1} \qquad (22)$$

$$a_{46} = \frac{\bar{h}_1-\bar{h}_3}{\bar{h}_2-\bar{h}_1} \qquad a_{48} = \frac{\bar{h}_1-\bar{h}_4}{\bar{h}_2-\bar{h}_1}$$

$$F_{51} = -\beta_1{}^3 a_{15}\sinh\beta_1+\beta_2{}^3 a_{35}\sin\beta_2+\beta_3{}^3\sinh\beta_3$$

$$F_{61} = \beta_1{}^3 a_{26}\cosh\beta_1-\beta_2{}^3 a_{46}\cos\beta_2+\beta_3{}^3\cosh\beta_3$$

$$F_{71} = \beta_1{}^3 a_{17}\sinh\beta_1-\beta_2{}^3 a_{37}\sin\beta_2+\beta_4{}^3\sin\beta_4 \qquad (23)$$

$$F_{81} = \beta_1{}^3 a_{28}\cosh\beta_1-\beta_2{}^3 a_{48}\cos\beta_2-\beta_4{}^3\cos\beta_4$$

$$F_{52} = h_1' a_{15}\sinh\beta_1-h_2' a_{35}\sin\beta_2-h_3'\sinh\beta_3$$

$$F_{62} = -h_1' a_{26}\cosh\beta_1+h_2' a_{46}\cos\beta_2-h_3'\cosh\beta_3$$

$$F_{72} = -h_1' a_{17} \sinh\beta_1 + h_2' a_{37} \sin\beta_2 - h_4' \sin\beta_4$$

$$F_{82} = -h_1' a_{28} \cosh\beta_1 + h_2' a_{48} \cos\beta_2 + h_4' \cos\beta_4$$

$$F_{53} = -t_1 a_{15} \cosh\beta_1 - t_2 a_{35} \cos\beta_2 + t_3 \cosh\beta_3$$

$$F_{63} = t_1 a_{26} \sinh\beta_1 - t_2 a_{46} \sin\beta_2 + t_3 \sinh\beta_3$$

$$F_{73} = t_1 a_{17} \cosh\beta_1 + t_2 a_{37} \cos\beta_2 - t_4 \cos\beta_4 \qquad (24)$$

$$F_{83} = t_1 a_{28} \sinh\beta_1 - t_2 a_{48} \sin\beta_2 - t_4 \sin\beta_4$$

$$F_{54} = \bar{t}_1 a_{15} \cosh\beta_1 + \bar{t}_2 a_{35} \cos\beta_2 - \bar{t}_3 \cosh\beta_3$$

$$F_{64} = -\bar{t}_1 a_{26} \sinh\beta_1 + \bar{t}_2 a_{46} \sin\beta_2 - t_3 \sinh\beta_3$$

$$F_{74} = -\bar{t}_1 a_{17} \cos\beta_1 - \bar{t}_2 a_{37} \cos\beta_2 + \bar{t}_4 \cos\beta_4$$

$$F_{84} = -\bar{t}_1 a_{28} \sinh\beta_1 + \bar{t}_2 a_{46} \sin\beta_2 + \bar{t}_4 \sin\beta_4$$

$$a_{57} = \frac{F_{61}F_{72}-F_{62}F_{71}}{F_{51}F_{62}-F_{52}F_{61}} \qquad a_{58} = \frac{F_{61}F_{82}-F_{62}F_{81}}{F_{51}F_{62}-F_{52}F_{61}}$$

$$a_{67} = \frac{F_{52}F_{71}-F_{51}F_{72}}{F_{51}F_{62}-F_{52}F_{61}} \qquad a_{68} = \frac{F_{52}F_{81}-F_{51}F_{82}}{F_{51}F_{62}-F_{52}F_{61}} \tag{25}$$

Then, $\bar{k}_n$ are given by the roots of

$$\bar{F} = (F_{53}a_{57}+F_{63}a_{67}+F_{73})(F_{54}a_{58}+F_{64}a_{68}+F_{84})-$$

$$(F_{54}a_{57}+F_{64}a_{67}+F_{74})\ (F_{53}a_{58}+F_{63}a_{68}+F_{83})=0 \tag{26}$$

Equation 26 is therefore the exact closed form transcendental functional expression from which the eigenvalues $\bar{k}_n$ may be extracted. The coupled natural frequencies are related to these eigenvalues by the following expression,

$$\omega_n = \left(\frac{D_{22}}{\rho}\right)^{1/2} \frac{\bar{k}_n}{\ell_o^2}\ (\lambda_c,\ \bar{\lambda}_c/\lambda_c)\ \ldots \tag{27}$$

5.3.7

Computations

The extraction of the eigenvalues from the exact-closed form transcendental expression in equation 26 proved to be a very challenging computational exercise due mainly to its complex nature, the existence of branch points, the necessity to order the operator roots appropriately and the existence of numerical noise.

The characteristic roots for the equations of motion, $\bar{x}_n$, were extracted in two different ways in order to assure accuracy: one method was by using a Jenkins-Traub computational method from the IMSL library. The second method was by using an exact-closed form approach outlined in Abramowitz and Stegun.[10] When these roots are being extracted numerically, they do not necessarily come out in a continuous manner. Therefore a subroutine that reorders them so that they become continuous with respect to the eigenvalue $\bar{k}_n$ is also employed. Once this reordering of these roots is completed, the parameters needed for computing the transcendental function, $\bar{F}$, in equation 26 are computed. Finally, the transcendental expression itself is computed and the roots, $\bar{k}_n$, are found numerically.

One interesting result is that the values of $\bar{F}$ are complex here. It is known, however, that each of the two uncoupled problems (bending or torsion) when treated separately has a real transcendental expression for extracting the eigenvalues. This behavior of the transcendental expression for extracting the coupled eigenvalues (i.e., being complex as opposed to being real) was the first hint that led the first author to examine any possible mathematical similarity between the problem at hand (a coupled non-damped oscillations problem) and simple damped oscillations problem in which the expression for determining the eigenvalues is in general complex due to the need to determine the oscillation frequency and the amount of damping in the mode, etc. In the coupled problem the complex nature of this transcendental expression for extracting the eigenvalues seems to be basically a reflection of

the phase that normally should exist between the bending and torsional modes. Realizing that in the damped case, there is a nonconservative energy transfer between the oscillating system and its environment as well as intermodal energy transfer, it became clear to the first author that in the undamped coupled system there may be a conservative energy transfer in the oscillating system. At the time of this thought it seemed to the first author that if it made sense, the idea should provide an explanation for the modal changes which were noticed during the studies at Purdue and MIT[3,4] as coupling in the system was changed. This prediction which turns out to be useful and confirmed by other recent studies from Purdue University[8] shall be discussed in more detail below.

The most convenient way to obtain the eigenvalues, $\bar{k}_n$, was found to be by graphical means. Thus the values of the real and imaginary parts of the complex transcendental function $\bar{F}$ are plotted against the values of $\bar{k}_1$ on the same curve as shown in Figure 2. The values of $\bar{k}_n$ at which the real and imaginary parts of the transcendental function are simultaneously equal to zero corresponds to the desired eigenvalues for this coupled problem.

One of the problems with the computational model described above is that, when the coupling parameter, L_2, becomes identically zero, the coupled system of equations becomes computationally ill conditioned and unsolvable. To circumvent this the results for the uncoupled case ($\bar{\lambda}_c/\lambda_c = 1$) are obtained from a series of calculations using successively smaller values for the coupling parameter, L_2. This led us to accept the values of eigenvalues

for zero coupling as the value corresponding to the limit as the coupling approaches zero. Although this continuity assumption seems to make sense, it is not backed by a rigorous mathematical proof. Luckily it was possible to check these results with results generated for an isotropic/metal aluminum/wing by MIT,[3,4] and the agreement was found to be good for the cases checked.

5.3.8
Results and Discussions

The natural frequencies ω_n for the coupled bending-torsion oscillations for a composite aircraft wing in the presence of elastic coupling and warping restraint is found (as shown by equation 27) to be a function of the ratio $(D_{22}/\rho)^{1/2}$, the length ℓ_o and the nondimensionalized frequency parameter $\bar{k}_n$ for the wing. In this problem, $\bar{k}_n$, is a function of only two parameters, i.e., λ_c which may be considered as an effective nondimensionalized aspect ratio and $\bar{\lambda}_c/\lambda_c$, which in a way, measures the amount of elastic coupling in the wing ($\bar{\lambda}_c/\lambda_c = 1$ for zero coupling). It is therefore seen from equation 27 that in order to increase ω_n one needs to make ℓ_o as small as possible and/or make (D_{22}/ρ) and $\bar{k}_n$ as large as possible. Such an exercise may be necessary when a tailoring of the frequency is needed to avoid instabilities (e.g., very low structural frequencies may provide an atmosphere for a coupling between the flexible modes and rigid body motions, which in turn has a potential to result in instability). This kind of tailoring is made convenient through the use of equation 27 in which, for a particular wing configuration and composite material, every variable in the equation shall be known ex-

cept $\bar{k}_n$ and D_{22}. Obviously if we want high ω_n, as we said earlier, D_{22} should be made to be as high as possible (and of course ρ as low as possible). Once this is done the only other parameter to be tailored is $\bar{k}_n$.

The plot of $\bar{k}_1$ as a function of λ_c and $\bar{\lambda}_c$ is shown in Figure 3 for all configurations having low camber to twisting coupling, and all values of bending to twisting coupling. The results computed at MIT,[3,4] which were used to verify the present results, are shown in Figure 3 as well. The important trend made visible is this investigation as shown in Figure 3, is that $\bar{k}_1$ (and hence ω_1) decreases with increasing nondimensionalized coupling L_2, which perhaps may be a more effective way to actually measure and compare elastic couplings, D_{16} and D_{26}. For example, the results from MIT[3,4] which were computed for some representative configurations, in dimensionalized form seem to represent systems with a fairly significant variation in coupling D_{26} or D_{16} (depending on the coordinate system). However when nondimensionalized, the results as shown in Figure 3 seem to show little variation in coupling. In fact they appear to be so close to the zero coupling case ($\bar{\lambda}_c/\lambda_c = 1$) or isotropic (or metal) case, that $\bar{k}_1$ for a metal or isotropic wing should be a good approximation (if it was necessary to make an approximation). The low value for the effective coupling was also evident in the nondimensionalized results from MIT[3,4] where the bending frequency hardly varied with material changes. The question that could be asked is therefore "Do all possible composite wing configurations result in very low effective nondimensionalized coupling, ($\bar{\lambda}_c/\lambda_c \approx 1$)?" If the answer is "yes",

then it may be proposed that for $\lambda_c > .5$, $\bar{k}_1\ (\lambda_c, \bar{\lambda}_c/\lambda_c)$ may be approximated as $\bar{k}_1(\lambda_c, 1)$, which is also the isotropic or metal value. For this case it is seen that the computation of the natural frequencies of composite aircraft wing having aeroelastic oscillations, merely requires the computation of (D_{22}/ρ) for a given wing half span ℓ_o, since $\bar{k}_n\ (\lambda_c, \bar{\lambda}_c/\lambda_c)$ is approximately equal to $\bar{k}_n\ (\lambda_c, 1)$ which is approximately equal to a constant (3.5) for n = 1. This result should make frequency computations for the bending mode significantly easier.

The problem with an affirmative answer which may likely be a "practical" answer, to the question posed above, is that there doesn't seem to be a theoretical or rigorous analytical reason (to the best of the authors' knowledge) why $\bar{\lambda}_c/\lambda_c$ must always be approximately 1. Therefore, if on the other hand, the answer to our question is negative, then the following observations may be made: (a) significant variation in $\bar{k}_1$ is possible with variations in effective nondimensionalized coupling $(\bar{\lambda}_c/\lambda_c)$. In fact it can be seen from Figure 3 that if $\bar{\lambda}_c/\lambda_c$ approaches zero, k_1 (and hence ω_1) approaches zero. (b) The values of $\bar{k}_1$ vary significantly with λ_c for low λ_c but approach asymptotic values for large λ_c. (c) The highest values of $\bar{k}_1$ is for isotropic (metals) or quasi-isotropic configurations. (d) For large values of λ_c, there appears to be a simple approximate (hopefully linear relationship) between $\bar{k}_1$ and $\bar{\lambda}_c/\lambda_c$ (or a measure of coupling). (e) For very large coupling $(\bar{\lambda}_c/\lambda_c \to 0)$, $\bar{k}_1$ approaches zero, which may provide the ingredient necessary for coupling between the elastic and rigid motions.

Perhaps a number of implications of some of these observations should be examined: Observation (c) seems to imply that the highest first frequency would correspond to isotropic or quasi-isotropic configurations if (D_{22}/ρ) and ℓ_o are the same. It is known however the metals have lower values of (D_{22}/ρ) than composites. It therefore means that quasi-isotropic or orthotropic configurations are desirable for such a design goal. Observation (e) would seem to imply that if a designer, interested in tailoring the wing frequencies, arbitrarily introduces large effective nondimensionalized coupling $(\bar{\lambda}_c/\lambda_c \to 0)$, then $\bar{k}_1$ (and hence ω_1) would approach zero. This may result in coupling between flexible and rigid motions which may or may not lead to instabilities. Could this have happened in the case of the X-29 Forward Swept Composite Wing Aircraft for which one of the primary modes of instability results from the coupling between flexible and rigid body motions? In other words was "too much" coupling (effective) <u>inadvertently</u> built into the wing during the design process? If that is the case, is there an alternative, equivalent design without any penalties (weight or otherwise) that could have been explored? Although the answers to these questions can, strictly speaking, only be possible after carrying the necessary aeroelastic analysis in which unsteady aerodynamic forces are considered, it appears from Figure 3 that a rough idea of the final picture may be obtained from the natural frequency analysis. Afterall, it is a common belief that the phenomena that actually lead to aeroelastic instabilities are linked to damping and coupling.

Earlier in this paper it was mentioned that previous studies by other investigators have found what appeared to be some kind of modal transformations as ply orientation was changed in a design process for a composite wing. While variation in ply orientation may change several directional stiffness parameters for the wing, the coupling stiffness parameter, L_2, may be singled out as a significant design parameter, because it may vary considerably (orthotropic configurations have zero values while it may be fairly significant in other configurations). Furthermore it should be remembered that the main reason for ply orientation variation is for 'tailoring', which is believed to be primarily tied to couplings (D_{16} and D_{26}). The absence (or the presence) of these couplings is basically what differentiates orthotropic configurations from anisotropic configurations. From these observations, and the fact that the entity that ties the bending and torsional equations is the coupling, it became clear that the role of coupling in modal transformations should be significant.

In order to see the role of coupling therefore in this study, the modal assumptions for the coupled problem were made similar to those normally made for the uncoupled problem (e.g., the frequency was assumed to be real) so as to provide an opportunity to compare, contrast and discern the final results easily. When this was done and the eigen-problem was formulated resulting in a complex transcendental expression from which the eigenvalue are to be extracted, a careful examination began.

A significant difference between the coupled and uncoupled

problems was that (as shown in Figure 2) the transcendental expression from which the eigenvalues are extracted is complex for the coupled problem while it is real for uncoupled problems. The complex nature of this transcendental expression basically reflects the fact that the bending and twisting oscillations are generally out of phase. Therefore the resultant coupled frequency that represents both the bending and twisting oscillation may be viewed as some kind of vector representation of the individual contributions. In order to formulate some explanations for the phenomenon of modal transformation in coupled (conservative) system, it may be necessary to compare and contrast coupled systems with damped systems. Damped systems, by definition are nonconservative, i.e., the system experiences a net loss or gain in energy. It is well known that in a damped system the transcendental expression for extracting the eigenvalues is complex, again, due to the phase angle that exists between the damping force and the conservative forces in the system. It is also known that some damping (desirable types) would tend to reduce the oscillation of the system (the non-desirable type tend to make the oscillations diverge). Therefore since damping is linked to some energy transfer which in turn tend to lead to a change in the oscillation frequencies, it was thought that the complex nature which is common to the coupled and damped system determinants (transcendental functions) from which the eigenvalues are extracted may be a similarity that may provide some explanations to the modal transformations in coupled systems. Using the similarity argument, the coupled system which for the present problem, is conservative, may

be viewed as having some conservative inter-modal energy transfer within the system when the coupling is changed, resulting in steady state changes or transformations of the modal energy content of a coupled mode compared to the uncoupled case. It may be worthwhile to point out that some results recently obtained at Purdue University[8] and communicated to the authors seem to strongly support this hypothesis.

5.3.10
Empirical Relations

A careful study of Figure 3 has led the authors to propose the following closed form asymptotic relationship that may be useful for some preliminary design consideration:

$$\bar{k}_1 = 3.5\ (\bar{\lambda}_c/\lambda_c) \quad , \quad \lambda_c > 3{\cdot}0 \tag{28}$$

Equation 28 was derived from Figure 4. Equation 28 as well as equation 27 show that the first coupled frequency decreases with increasing coupling, a trend that seems to be supported by new results from Purdue University[8] and the data from MIT.[3] In reference 3 for example, the first nondimensionalized frequency computed by Raleigh-Ritz (in which coupling is zero) had a value of 3.52, which is consistently higher than those computed by finite element method in which coupling is finite (not equal to zero). Equations 27 and 29 which are closed form (generally rare for anistropic systems) should be easy to use.

Before this discussion is concluded, it is probably necessary to explain why only the results of the first mode are shown in this paper. First of all it should be pointed out that some second mode data have been generated but are still being studied very critically to understand the general trends. It may also be pointed out that the extraction of the eigenvalues is a little challenging since some care is needed in ordering the roots of the operator equations.

5.3.11

Concluding Remarks

This paper has attempted to present exact closed form solutions to the coupled bending-torison vibration problem for a simplified model of composite aircraft wings with war ping constraint. Increasing the coupling was found to decrease the first coupled frequency. A comparison between the coupled problem and a sample damped problem led the authors to propose some explanation to the "modal transformation" phenomenon found by earlier investigators. Some simplified closed form expressions are provided for the first coupled frequencies which may be useful for fast applications.

5.3.12

Acknowledgement

The authors acknowledge valuable discussions with Drs. A. Amos, and A. Nachman who are monitors for the AFOSR Contracts F49620-85-C-0090/F49620-87-C-0046 under which this study was conducted. We also appreciate Professor T. A. Weisshaar's efforts in providing the data for validating the results presented here. Finally we acknowledge the programming efforts of Mr. John Calle-

ja, a graduate student in the department and we thank Mrs. B. Hein for patiently typing the manuscript.

5.3.13

REFERENCES

1. Reissner, E. and Stein, M., "Torsion and Transverse Bending of Cantilevered Plates," NACA TN 2369, June 1951.
2. Petre, A., Stanescu, C., and Librescu, L., "Aeroelastic Divergence of Multicell Wings (Taking their Fixing Restraints into Account,)" Aeromecanique, 1962, pp. 689-698.
3. E. F. Crafley and J. Dugundji, "Frequency Determination and Nondimensionalization for Composite Cantilever Plates," Journal of Sound and Vibration, Vol. 72, No. 1, pp. 1-10, 1980.
4. Jensen, D.W. and Crawley, E.F., "Frequency Determination Techniques for Cantilevered Plates with Bending-Torsion Coupling," AIAA Journal, Vol. 22, No. 3, March 1984, pp. 415-420.
5. Oyibo, G.A. and Berman, J.H., "Influence of Warpage on Composite Aeroelastic Theories," AIAA Paper No. 85-0710, April 1985.
6. Oyibo, G.A. and Berman, J.H., "Anisotropic Wing Aeroelastic Theories with Warping Effects," DGLR Paper No. 85-57, Second International Symposium on Aeroelasticity and Structural Dynamics, Technical University of Aachen, West Germany, April 1985.
7. Oyibo, G.A., and Weisshaar, T.A., "Optimum Aeroelastic Characteristics for Composite Supermaneuverable Aircraft," Final Technical Report, AFOSR Contract F49620-85-C-0090, Report No. AE002V7407, July 31, 1986.
8. Weisshaar, T.A., "Vibration Tailoring", AFOSR Contract F49620-87-0046 Second Quarterly Technical Report, POLY AE Report 88-2, December, 1987.
9. Hildebrand, F.B., "Advanced Calculus for Applications," Prentice-Hall, Inc., Englewood Cliffs, New Jersey, 1976.
10. Abramowitz, M., and Stegun, I. A., "Handbook of Mathematical Functions" National Bureau of Standards, US Printing Office, 1965.

THIS
PAGE
IS
MISSING
IN
ORIGINAL
DOCUMENT

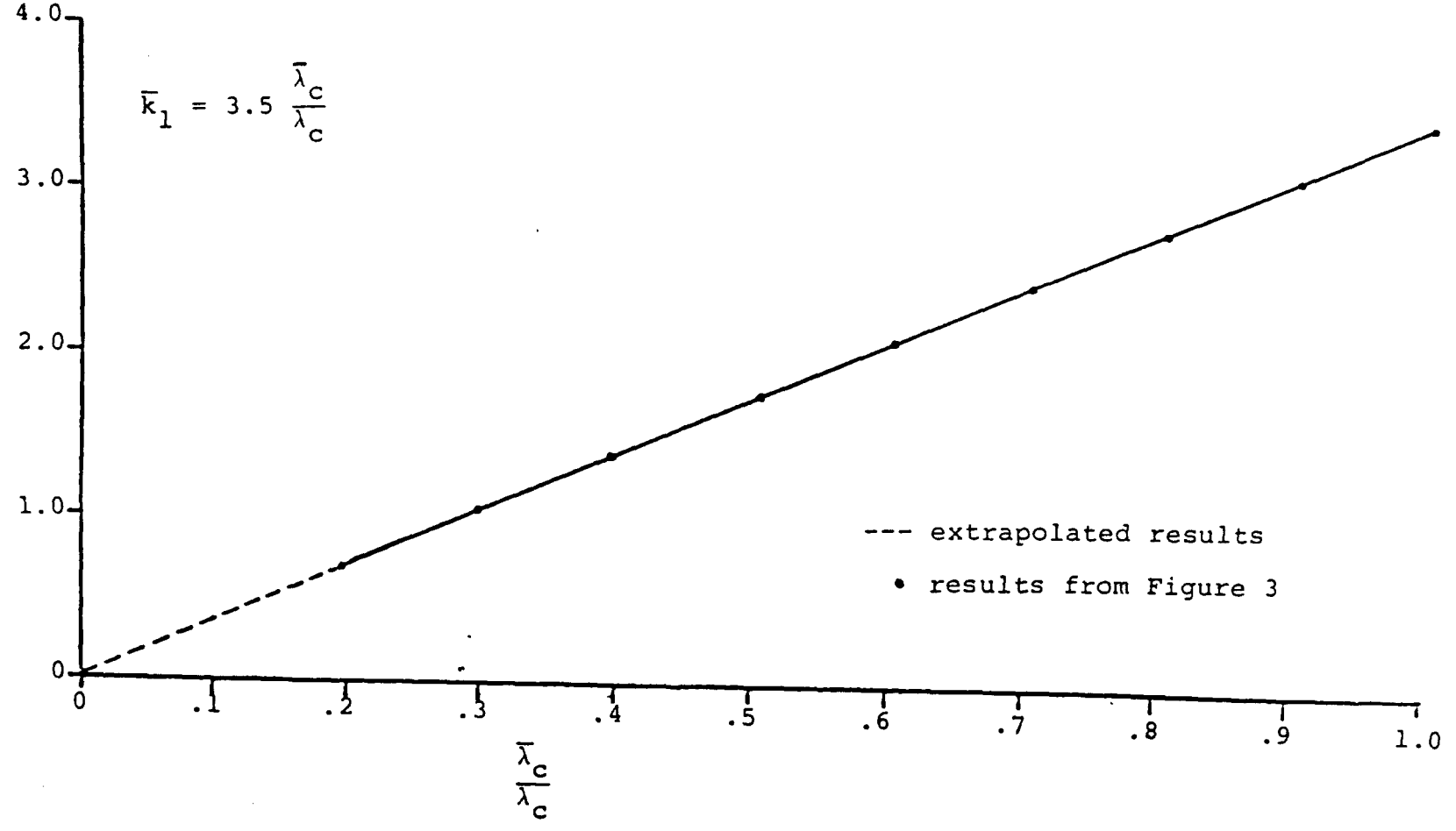

Figure 4 Empirical (asymptotic) relationship between the first modal eigenvalue and effective coupling ($\lambda_c \to \infty$)

5.4 INVESTIGATION OF THE BASIC MECHANISM OF AEROELASTIC INSTABILITY FOR COMPOSITE AIRCRAFT WINGS

It is well known in aeroelasticity that the mechanism of instability is governed by the interaction of aerodynamic forcing functions and the vibrational modes of the structure. The aerodynamic forces generally provides ingredients such as damping and coupling to such an interaction. As a result, the structural modes may loose damping and/or stiffness which may result in some form of coalescence of two or more modes leading eventually to instability which may or may not be catastrophic. Physically therefore it is sensible to say that some of the main ingredients of aeroelastic instability are damping and coupling.

Crisp[1] has shown that the necessary condition for instability may be studied by investigating the matrix form of the aeroelastic equations of motion. Thus

$$[A]\{\ddot{q}_i\} + [B]\{\dot{q}_i\} + [C]\{q_i\} = 0 \qquad (1)$$

where q_i are the mode shapes and A,B,C, are the mass, damping and stiffness matrices, respectively. He considered

$$\tau = 1/2 \quad [\dot{q}_i] \quad [A] \quad \{\dot{q}_i\}$$

$$F = 1/2 \quad [\dot{q}_i] \quad [B] \quad \{\dot{q}_i\} \qquad (2)$$

$$U = 1/2 \quad [q_i] \quad [C] \quad \{q_i\}$$

where τ and U are some generalized kinetic and potential energies, respectively. F is basically the Rayleigh's dissipation function[2].

[A], [B] and [C] are symmetrical for elementary metal mechanical systems but the addition of the aerodynamic and dampings spoils this symmetry for metal or isotropic systems for the last two. In the case of composite anisotropic system, aerodynamics is not even needed for asymmetric [C], since such asymmetry can be provided by elastic couplings. Crisp has further shown in the case with non-symmetric [B] and [C] they may be decomposed into symmetric and skew-symmetric portions or

$$[B] = [B_1] + [B_2] \tag{3}$$

$$[C] = [C_1] + [C_2]$$

where $[B_1]$, $[C_1]$ are the symmetric portions and $[B_2]$, $[C_2]$ are the skew-symmetric portions. By considering the total energy for the system $\tau + U = E$, Crisp obtained the following expression for work done on this system,

$$\frac{dE}{dt} = - [\dot{q}_i] \ [B_1] \ \{\dot{q}_i\} - [\dot{q}_i] \ [C_2] \ \{q_i\} \tag{4}$$

It is then seen that without damping ([B] = 0), a composite wing can exhibit a "damping-like" behavior as was shown in section 5.4 probably for the first time in aeroelasticity. This investigation is being continued in order to search for the explanation for aeroelastic tailoring. A preliminary plot of the second mode is presented in Figure 1. Figure 2 also shows that modal coalescence

is also a reality. Further studies have also shown that such a coalescence could lead to instability. We are currently examining the necessary physical ingredients for such an instability and its implications. Figure 3 shows a typical flutter instability evolution process. Figures 2 and 3 therefore display some interesting resemblance. We are in the process of discerning the striking resemblance.

REFERENCES

1. Crisp, J.D.C., "The Equation of Energy Balance for Fluttering Systems with Some Applications in the Sumpersonic Regime," J. Aero/Space Sciences, Vol. 26, No. 11, November 1959, pp. 703-716, 738.
2. Strutt, J.W. (Baron Rayleigh), The Theory of Sound, Vol. 1, 2nd ed., Dover Publications, New York, 1945.

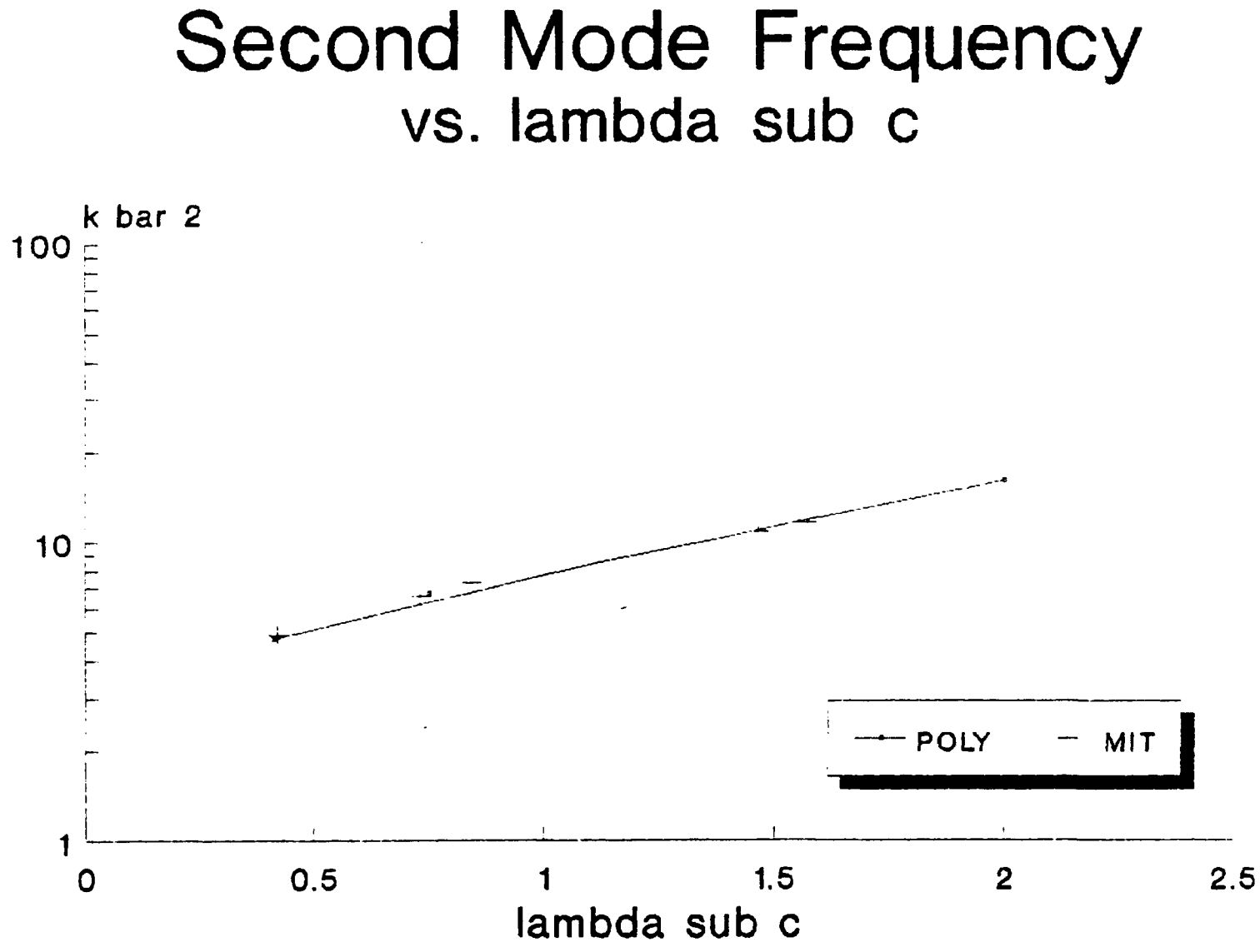

FIGURE 1. Vibration

5.5 Some Implications of Warping Restraint on the Behavior of Composite Anisotropic Beams*

Dr. Gabriel A. Oyibo**

Polytechnic University

Farmingdale, New York

5.5.1 Nomenclature

$(x,y,z,)$, (x_o,y_o,z_o) = physical and affine space coordinates, respectively

a_i = chordwise integrals

$(\Delta p, \Delta p_o)$ = differential aerodynamic pressure distributions in physical and affine space respectively

r, L_1, L_2, D^*, D_o^*, = generic nondimensionalized stiffness parameters

r_o, M_o = affine space running aerodynamic lift and moment, respectively

$\bar{U}, \bar{U}_o$ = virtual work expressions in physical and affine space, respectively

D_{ij} = elastic constants

ρ, ρ_∞ = affine space material and air density, respectively

* Research sponsored by the Air Force Office of Scientific Research (AFSC), under Contract F49620-85-C-0090 and F49620-87-C-0046. The United States Government is authorized to reproduce and distribute reprints for governmental purposes notwithstanding any copyright notation hereon.

** Associate Professor, Aerospace Engineering Dept., member AIAA

w = displacement

$\bar{h}$ = wing box depth

(h_o, α_o) = affine space bending and torsional displacement, respectively

c_o', c_o = affine space half-chord and chord, respectively

ℓ_o = affine space half-span for the wing

e = parameter that measures the location of the elastic axis relative to mid-chord

m_o = affine space mass per unit span

ω = vibration frequency

5.5.2 Introduction

The performance of modern supermaneuverable aircraft can be made to benefit a great deal from, significant advances in materials technology and the availability of more accurate aerodynamic prediction capabilities. Supermaneuverability as a design goal invariably calls for an optimization of the design parameters. Optimization may be partially accomplished for example, by using composite materials to minimize weight. Indeed, it has been known that these composite materials can be tailored to resolve the dynamic or static instability problems of these types of aircraft. The concept is referred to as aeroelastic tailoring.

While aeroelastic tailoring has tremendous advantages in the design of an aircraft, the analysis which provides the basis for the aeroelastic tailoring itself is generally very involved. This is rather unfortunate since a good fundamental physical insight of the tailoring mechanism is required for accurate and reliable results.

In this paper an attempt is made to look at some dynamic theories that can be used to understand the aeroelastic tailoring mechanism. Specifically, the accuracy of the St. Venant torsion theory which is relatively simple and frequently used in aeroelastic analysis is examined with particular reference to the effects of the wing's aspect ratio as well as other design parameters.

Although earlier studies[1,2,3] have indicated that the St. Venant's torsion theory is reasonably accurate except for aircraft wings with fairly low aspect ratios, the theory supporting that conclusion was based on the assumption that the wing is constructed of isotropic materials. Basically, the St. Venant's torsion theory assumes that the rate of change of the wing's twist angle with respect to the spanwise axis is constant (for constant stiffness and torque). This assumption is hardly accurate particularly for modern aircraft construction in which different construction materials are employed and the aerodynamic loads vary significantly along the wing's span. However, References 1-3 have shown that (in spite of such an inaccurate assumption) the main parameter that determines the accuracy of the St. Venant's theory is the wing's aspect ratio. Thus, it was determined that the theory is fairly accurate for moderate to high aspect ratio wings constructed of isotropic materials. In recent studies[4,5] however, it has been shown that for wings constructed of orthotropic composite materials, the conclusions of References 1-3 need to be modified. Rather than using the geometric aspect ratio of the wing to determine the accuracy of St. Venant's twist theory, it was suggested that a generic stiffness ratio, as well as an effective aspect ratio which considers the wing's geometry and the ratio of the

principal directional stiffness, should be considered in establishing the accuracy of St. Venant's theory.

The present paper is basically an extension of the studies that were begun in References 4 and 5. In thi. study the task was to examine the role of coupling (elastic coupling) on the accuracy of St. Venant's theory applied to static problems. It was discovered that coupling plays a very significant role on the accuracy of St. Venant's twist theory.

5.5.3

Formulation

Consider an aircraft wing fabricated of composite materials and mathematically idealized as a canti-levered plate subjected to forces and moments. It can be shown that the equations of motion for such a model can be described as follows.

$$a_1 h_o^{iv} + a_2 \alpha_o^{iv} + a_5 \alpha_o^{iii} + \rho_o a_1 \ddot{h}_o +$$

$$\rho_o a_2 \ddot{\alpha}_o = L_o \qquad (1)$$

$$a_2 h_o^{iv} - a_5 h_o^{iii} + a_3 \alpha_o^{iv} - a_4 \alpha_o^{ii} + \rho_o a_3 \ddot{\alpha}_o +$$

$$\rho_o a_2 \ddot{h}_o = M_o$$

where

$$a_1 = \int_{e\bar{c}o}^{\bar{c}_o} dx_o \quad ; \quad a_2 = \int_{e\bar{c}_o}^{\bar{c}_o} x_o \, dx_o \quad ; \quad a_3 = \int_{e\bar{c}_o}^{\bar{c}_o} x_o^2 dx_o \quad ;$$

$$a_4 = 2 \int_{e\bar{c}_o}^{\bar{c}_o} D^*(1-\varepsilon) dx_o \qquad (2)$$

$$L_o = \int_{e\bar{c}_o}^{\bar{c}_o} \Delta p_o dx_o \quad ; \quad a_5 = \int_{e\bar{c}_o}^{\bar{c}_o} L_2 dx_o$$

$$M_o = \int_{e\bar{c}_o}^{\bar{c}_o} x_o \Delta p_o dx_o$$

and

$$-\infty<e<0 \quad ; \quad \bar{c}_o = \frac{c_o}{1-3}$$

$$(\,)' = \frac{\partial}{\partial y_o} \quad ; \quad (\dot{}) = \frac{\partial}{\partial t} \tag{3}$$

$$\bar{U}_o = \frac{U}{D_{22}}\left(\frac{D_{22}}{D_{11}}\right)^{1/4} \quad ; \quad D^* = \frac{D_{12} + 2D_{66}}{(D_{11}D_{22})^{1/2}}$$

$$\epsilon D^* = \frac{D_{12}}{(D_{11}D_{22})^{1/2}} \tag{4}$$

$$L_1 = \frac{4D_{16}}{(D_{11}{}^{3/4}(D_{22})^{1/4}} \quad ; \quad L_2 = \frac{4D_{26}}{(D_{11})^{1/4}(D_{22})^{3/4}}$$

$$\Delta p_o = \frac{\Delta p}{D_{22}} \quad ; \quad \rho_o = \frac{\rho \bar{h}}{D_{22}}$$

D_{ij} are the elastic constants, ρ, is the material density, Δp is the differential pressure distribution, w is the displacement, t is the time, and $\bar{h}$ is the wing box depth.

5.5.4

Evolution of Warping Parameters

The evolution of the warping parameter with which to study the aeroelastic warping constraint phenomenon for wings fabricated of composite materials is a process that depends on the sophistication of the wing's mathematical model; whether coupling effects are included, whether the wing's chordwise curvatures are included and so on. Therefore, any warping parameter is as good as the corresponding wing's displacements assumptions. However, the virtual work equation makes it possible for the analyst to determine its effective independent variables even before the dis-

placement assumptions are made. By non-dimensionalizing the spanwise space variable in Equation (1), depending on whether one is interested in the static, dynamic, coupled or uncoupled displacements, one of the following warping parameters may be useful.

$$\lambda_c = \frac{\ell_o}{c_o} \sqrt{\frac{3}{2} D_o^*} \tag{5}$$

$$\bar{\lambda}_c = \frac{\ell_o}{c_o} \sqrt{\frac{3}{2} \left(D_o^* - \frac{L^2}{8}\right)} \tag{6}$$

where

$$D_o^* = D^*(1-\varepsilon) \tag{7}$$

(ℓ_o/c_o) is defined as the wing's effective aspect ratio and D_o^* and L are the generalized stiffness and coupling ratios respectively (defined in earlier work such as References 5 and 6).

Equations (5) and (6) represent the appropriate warping parameter for dynamic deformation, static displacement with elastic cross-coupling.

It was discovered in this study that evolving the warping parameter in a manner shown in Equation (1) thru (3), should enable one to effectively investigate the effects of warping on the composite wing's dynamics (or the accuracy of St. Venant's theory.) From the lamination theory for composites it is known that while D_o^* and (ℓ_o/c_o) are always positive, L can be positive or negative. However, from Equations (1) and (3), it is clear that whether a composite wing has positive or negative coupling, the warping effect (in terms of $\bar{\lambda}_c$) is unchanged.

5.5.5

Computations

By using the evolved warping parameters defined in Equations 7 and 8 and appropriate boundary conditions, the boundary value problems associated with Equation (4) are solved in a closed-form manner to determine the wing's static twist.

The wing loading conditions considered in this analysis are as follows: (a) steady state distributed twist loads and (b) steady state concentrated twist oads.

5.5.6

a. Steady distributed twist loads

For a wing with a constant uniformly distributed spanwise twisting moment, f_o resulting from a steady state coupled bending-torsion displacements, the exact closed form solutions for the mode shape α_o, satisfying the appropriate boundary conditions is given by

$$\alpha_o(y_o) = \frac{6f_o\ell_o^2}{c_o^3(4\bar{\lambda})^2}\left[y_o - \frac{\bar{y}_o^2}{2} - \frac{\sinh 4\bar{\lambda}_c y_o}{4\bar{\lambda}_c}\right. \tag{8}$$

$$\left. \frac{1}{4\bar{\lambda}_c}\left(\tanh 4\bar{\lambda}_c + \frac{1}{4\bar{\lambda}_c \cosh 4\bar{\lambda}_c}\right)\left(\cosh 4\bar{\lambda}_c \bar{y}_o - 1\right)\right]$$

Equation 8 is therefore a closed form coupled twist distribution for a composite wing with the warping effects accounted for.

where

$$\bar{y}_o = y_o/\ell_o \tag{9}$$

When equation 8 is evaluated at the wing tip and compared to an equivalent expression predicted by St. Venant's theory, the following expression is obtained.

$$\frac{\alpha_o(1)}{\alpha_o(1)_{St.V}} = 1 - \frac{\tanh 4\bar{\lambda}_c}{2\bar{\lambda}_c} - \frac{1}{9\bar{\lambda}_c^2}\left(\frac{1}{\cosh 4\bar{\lambda}_c} - 1\right) \tag{10}$$

where α_o (1) is the wing tip twist given by equation 15 while α_o (1) is the wing tip twist given by the St. Venant torsion theory. A plot of equation 10 is shown in Figure 1.

5.5.7

b. Steady state concentrated tip twist loads

If the wing is under the influence of a concentrated twisting moment, F_o at the tip as a result of a steady state coupled bending torsion displacement, the exact closed form twist distribution that satisfies these equations of motion and their associated boundary conditions is given by

$$\alpha_o(\bar{y}_o) = \frac{6F_o\ell_o}{c^3{}_o(4\bar{\lambda}_c)^2}\left[\bar{y}_o - \frac{\sinh 4\bar{\lambda}_c y_o}{4\bar{\lambda}_c} + \frac{\tanh 4\bar{\lambda}_c}{4\bar{\lambda}_c}(\cosh\bar{\lambda}_c\bar{y}_o - 1)\right] \tag{11}$$

When the twist distribution given by equation 11 is evaluated at the wing tip and compared to its counterpart predicted by the St. Venant's torsion theory the following expression is obtained.

$$\frac{\alpha_o(1)}{\alpha_o(1)_{St.V}} = 1 - \frac{\tanh 4\bar{\lambda}_c}{4\bar{\lambda}_c} \tag{12}$$

It should be noted that the ratio given by equation 12 was plotted for the real values of $\bar{\lambda}_c$ in references 5 and 6 and was shown to represent conditions where any errors resulting from using St. Venant's torsion theory are conservative (over-design rather than under-design). In this analysis equation 12 is examined when $\bar{\lambda}_c$ is imaginary, which is possible if L_2 is very large. Under such circumstances, equation 12 becomes

$$\frac{\alpha_o(1)}{\alpha(1)_{St.V}} = 1 - \frac{\tan 4\bar{\lambda}_c}{4\bar{\lambda}_c} \tag{13}$$

Figure 2 depicts the conditions given by equation 13. It is therefore seen from the figure that there are certain ranges of $\bar{\lambda}_c$ for which nonconservative errors are possible by using the St. Venant's twist theory.

5.5.8

Results and Conclusions

The results are shown in Figures 1 and 2. Figure 1 shows a comparison of the static wing tip twist obtained in the present study and that obtained via St. Venant's twist theory in the presence of statically distributed forces and low to moderate coupling. Figures 2 shows the trend for concentrated forces and substantial coupling. In Figure 1 it is seen that the presence of coupling makes the errors of St. Venant's theory worse. This seems to suggest that the more sophisticated theory is more important for wings with coupling (e.g., wings aeroelastically-tailored using elastic cross-coupling).

Figure 2 also shows that nonconservative errors ($\left|\frac{\alpha_o(1)}{\alpha_{o_{St.V}}(1)}\right|>1$) are are possible.

Using Figures 1 and 2, the following conclusions can be summarized: (i) ignoring warping arbitrarily using St. Venant's theory could result in very significant errors (as high as over 80% errors) in analytical results for composite aircraft wings, (ii) warping is more important (St. Venant's theory is less accurate) for wings with coupling, (iii) St. Venant's theory (which has always been shown to be conservative[1,2]), can be non-conservative or St. Venant's approximation can lead to an unsafe design error (under design rather than over design from a stability point of view).

REFERENCES

1. Reissner, E. and Stein, M., "Torsion and Transverse Bending of Cantilevered Plates," NACA TN 2369, June 1951.

2. Bisplinghoff, R.L., Ashley, H. and Halfman, R.L., "Aeroelasticity," Addison Wesley, 1955.

3. Petre, A., Stanescu, C., and Librescu, L., "Aeroelastic Divergence of Multicell Wings (Taking their Fixing Restraints into Account,)" Revue de Mechanique Appliquee, Vol. 12, No. 6, 1961, pp 689-698.

4. E.F. Crawley and J. Dugundji, "Frequency Determination and Nondimensionalization for Composite Cantilever Plates," Journal of Sound and Vibration, Vol. 72, No. 1, pp. 1-10, 1980.

5. Oyibo, G.A. and Berman, J.H., "Influence of Warpage on Composite Aeroelastic Theories," AIAA Paper. No. 85-0710, April 1985.

6. Oyibo, G.A. and Berman, J.H., "Anisotropic Wing Aeroelastic Theories with Warping Effects," DGLR Paper No. 85-57, Second International Symposium on Aeroelasticity and Structural Dynamics, Technical University of Aachen, West Germany, April 1985.

5.5.10

Acknowledgements

The author is grateful to the AFOSR for sponsoring this research. He is particularly thankful to Dr. A. K. Amos, and Dr. A. Nachman, the Program Managers who monitor the research program, for their constructive criticism. He also appreciates various comments from Dr. Sinclair Scala and Mr. Julian Berman, both of Fairchild Republic Company, and Professor Terrence Weisshaar of Purdue University.

Figures

Figure 1: Wing Tip Twist Ratios for Simple and More Involved Theory (distributed load and low to moderate coupling)

Figure 2: Wing Tip Twist Ratios Comparing Simple and More Involved Theory (with substantial coupling)

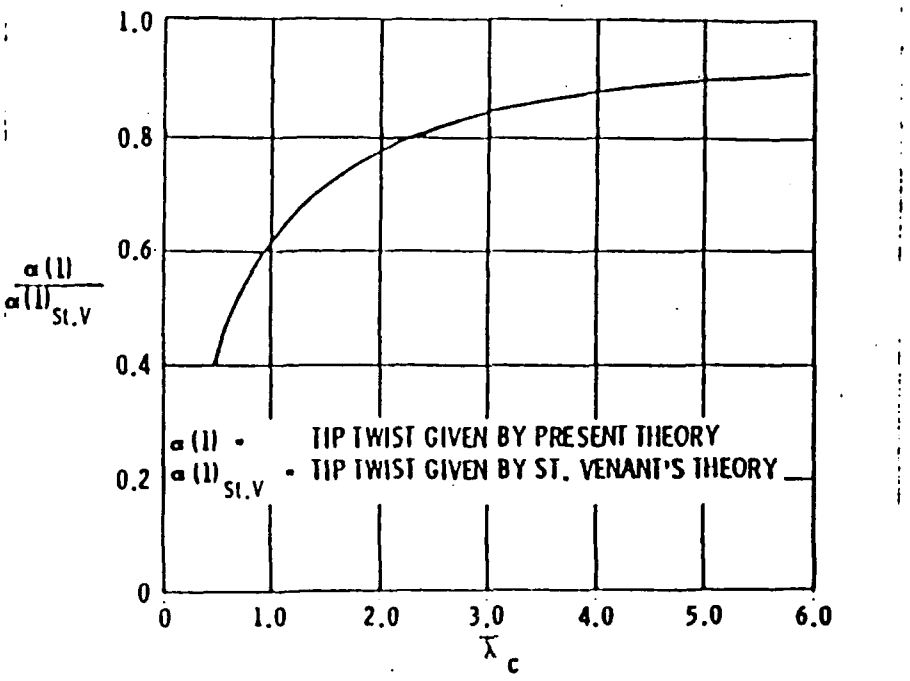
1.0
0.8
0.6
0.4
0.2
0
$\frac{\alpha(1)}{\alpha(1)_{St.V}}$
$\alpha(1)$ - TIP TWIST GIVEN BY PRESENT THEORY
$\alpha(1)_{St.V}$ - TIP TWIST GIVEN BY ST. VENANT'S THEORY
0
1.0
2.0
3.0
4.0
5.0
6.0
$\bar{\lambda}_c$

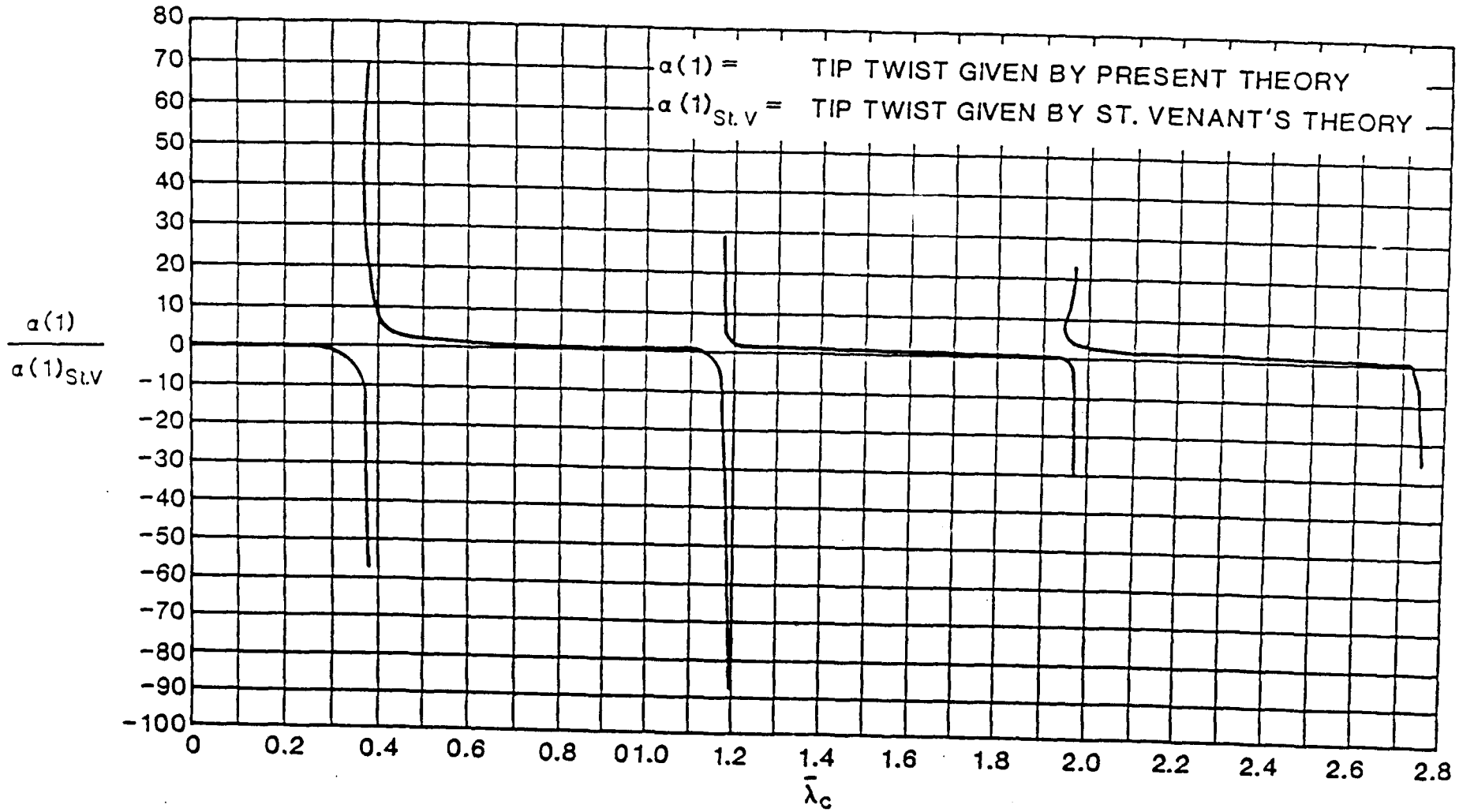
α(1) = TIP TWIST GIVEN BY PRESENT THEORY
α(1)St. V = TIP TWIST GIVEN BY ST. VENANT'S THEORY
α(1) / α(1)St.V
80
70
60
50
40
30
20
10
0
-10
-20
-30
-40
-50
-60
-70
-80
-90
-100
0
0.2
0.4
0.6
0.8
01.0
1.2
1.4
1.6
1.8
2.0
2.2
2.4
2.6
2.8
λ̄c

Closed-Form Solutions for Nonlinear Quasi-Unsteady Transonic Aerodynamics

Gabriel A. Oyibo*
Polytechnic University, Farmingdale, New York

The existence of exact closed-form solutions for nonlinear unsteady aerodynamics is established. The full nonlinear unsteady velocity potential equations for an airfoil are considered. Evidence indicating why the traditional hodograph approach is ineffective for solving these equations is provided. Therefore, a suitable mapping scheme is employed in transforming these full nonlinear equations into the hodograph plane. A close examination of the resulting hodograph equations reveals closed-form solutions can be obtained for the nonlinear unsteady aerodynamic characteristics of an airfoil in potential flow. The shockless transonic results presented in this inviscid analysis show trends that are in agreement with the results of previous investigators and available experimental data. "Dips" were observed in the pressure distributions as the freestream Mach number is varied. It appears that there are finite optimum reduced frequencies for the pressure distributions. This result might suggest a solution to the "transonic dip" problem. Perhaps an important practical consequence of this study is the possibility of employing this approach to solve an inverse problem of designing an airfoil section with given or desired aerodynamic characteristics. Desirable candidates for such a design procedure would include supercritical oscillating shock-free or "transonic dipless" airfoil sections. Such airfoils, therefore, could be designed to meet both the performance and stability criteria simultaneously.

Nomenclature

b,c	= airfoil chord length and velocity of sound, respectively
(x,z); (u,w)	= Cartesian and hodograph coordinates, respectively
C_p,C_L	= pressure and lift coefficients, respectively
k,M	= reduced frequency and Mach number, respectively
q,P	= resultant flow velocity and pressure, respectively
J	= Jacobian of the hodograph transformation
F_m,B_m	= hypergeometric function and arbitrary constant, respectively
$Q,\bar{Q}$	= velocity potential and stream-function quantity, respectively
m,i	= integer and square root of minus one, respectively
ρ,ω	= air density and oscillation frequency, respectively
t,γ	= time and ratio of gas specific heats, respectively
ϕ,∇	= velocity potential and vector differential operator, respectively
$\chi,\bar{\psi}$	= transformed velocity potential and stream function, respectively
$()_0$	= affine space or nondimensionalized quantities
$()_\infty$	= quantities at infinity
θ	= angle inclined by velocity vector and positive x axis
$\bar{T}$	= dimensionless velocity variable

Introduction

THE hodograph transformation has been established as a very vital tool with which to analyze two-dimensional nonlinear steady transonic flow problems comprehensively. The significance of the hodograph representation results from the fact that whereas the linearized equations in the physical plane fail to explain certain observed transonic flow phenomena, the nonlinear equations, which more accurately describe the flow, do not seem to have simple closed-form solutions in the physical plane. With the help of suitable mapping functions, these nonlinear equations could be transformed into the hodograph plane,[1-14] where they become linear, resulting in a possibility of obtaining closed-form solutions for them. Although the hodograph approach could introduce difficulties associated with involved boundary conditions resulting from some practical problems, many investigators believe that its advantages, particularly in terms of physical insights, far outweigh its disadvantages.

Outstanding contributions from various investigators have been responsible for the development of the hodograph method for solving nonlinear potential flow problems. The early work of Molenbrock[1] and Chaplygin[2] was complemented by the later efforts of investigators like Lighthill[3] and Guderleg.[4] Consequently, researchers like Nieuwland,[5] Bauer, Garabedian, and Korn,[6] and Boersteel[7] were able to establish the hodograph approach as an effective design tool for efficient airfoils like the supercritical shockless sections. The basic idea here is to suppress the boundary-layer separation by "pushing" the shock waves on the wing toward its trailing edge and eventually diluting (or weakening) them as much as possible. Sobieczky[8,9] and his collaborators have also presented interesting results more recently.

The hodograph transformation has been known and used for over a century. Curiously, however, evidence from a literature search seems to indicate that its use has largely been restricted to the analysis of the nonlinear, steady, two-dimensional flow problems like steady transonic flow.

The reasons for this restriction or why there has not been an extension of this approach to unsteady two-dimensional or three-dimensional flow problems also appear to be absent in the literature as well. The implication, therefore, seems to be that such an approach can only be used to solve steady-state

Received April 20, 1987; revision received March 19, 1988.

*Associate Professor, Aerospace Engineering Department. Member AIAA.

airfoil problems like performance and not dynamic instability problems (which require the unsteady flow solutions).

In transonic aeroelasticity, phenomena like the "transonic dip" require nonlinear unsteady aerodynamics for their understanding. The need to operate modern aircraft in the transonic region, among other things, has been responsible for the recent tremendous interest in transonic flow problems. Aeroelasticians and computational fluid dynamicists have been investigating these problems with a good degree of success; Refs. 15–24 are just a few examples. As a result, numerous computer codes are now available for computing transonic aerodynamics, many of them using various approximations of the full nonlinear potential equations. In spite of this progress, however, recent publications and presentations, like Ref. 24, seem to indicate that a great deal still remains to be done to thoroughly understand aeroelastic phenomena like the transonic dip. The author, inspired by a recent experience,[25] shares the view held by some investigators that a more fundamental approach could provide some of the necessary physical insights for improving our understanding of these phenomena. Such insights may not be readily extractable from an analysis in which big computer codes are used.

This paper presents the results of a preliminary investigation of the unsteady transonic aerodynamics in which the full nonlinear unsteady two-dimensional velocity potential flow equations are employed. Evidence indicating why the traditional hodograph approach is not effective for solving these equations is presented. With the help of a certain mapping scheme, the nonlinear equations are transformed into the hodograph plane. A close examination of the transformed equations reveals that if J, the Jacobian of the transformation, is prescribed, ab initio, the hodograph velocity potential satisfies a linear second-order partial differential equation. The significance of this result includes the fact that the following results appear to be possible for the first time:

1) Exact closed-form solutions for the nonlinear unsteady velocity potential can be obtained.

2) The solution of an inverse problem of designing an airfoil section with given or desired unsteady aerodynamic characteristics can be attempted.

These results, therefore, imply that it is possible to design an airfoil that can meet both the performance and dynamic stability criteria simultaneously.

The results shown in this paper are obtained by piecing the fundamental solutions in a manner similar to Nieuwland's approach.[5] From these results it appears that there are "dips" in the pressure distributions as the freestream Mach number is varied in the transonic region, a phenomenon that also has been established (Ref. 24, for example) for the aeroelastic stability characteristics. It also is observed that there appear to be finite optimum reduced frequencies for the pressure distributions. This, therefore, appears to agree with the trends established by Marble[26] for a quasi-one-dimensional flow.

Equations of Motion

By considering the concept of "control volume" for a fluid flow, it can be proved from the first principles that the physical principle of continuity of mass demands that the following equation be satisfied for any arbitrary volume:

$$\left(\frac{\partial}{\partial t}+\boldsymbol{q}\cdot\nabla\right)\rho+\rho(\nabla\cdot\boldsymbol{q})=0 \tag{1}$$

where $\boldsymbol{q}$ is the fluid-flow velocity vector, ρ is the fluid density, and ∇ is a differential vector operator.

Using a similar approach, the physical principle of the conservation of momentum can be represented by the following equation:

$$\left[\frac{\partial}{\partial t}+(\boldsymbol{q}\cdot\nabla)\right]\rho\boldsymbol{q}+\rho\boldsymbol{q}(\nabla\cdot\boldsymbol{q})=-\nabla P \tag{2}$$

By using Leibnitz's rule and Kelvin's theorem for an irrotational flow as well as the assumption that a velocity potential ϕ exists, such that

$$\boldsymbol{q}=\nabla\phi \tag{3}$$

in light of Eq. (1), Eq. (2) can be integrated to obtain the following:

$$\frac{\partial\phi}{\partial t}+\frac{\nabla\phi\cdot\nabla\phi}{2}+\int_{P_\infty}^{P}\frac{dP}{\rho}=\frac{q_\infty^2}{2} \tag{4}$$

where $(\,)_\infty$ is a reference point quantity (e.g., infinity). Equation (4) is basically the Bernoulli–Kelvin equation.

By considering isentropic flow with the following relationship between the pressure P and density

$$p\rho^{-\gamma}=\text{const} \tag{5}$$

and defining the quantity c given by

$$c^2=\frac{dP}{d\rho} \tag{6}$$

called the speed of sound, the Leibnitz rule can be employed to derive the following velocity potential equation from Eqs. (1) and (4):

$$a^2\nabla^2\phi-\left[\frac{\partial}{\partial t}(\nabla\phi\cdot\nabla\phi)+\frac{\partial^2\phi}{\partial t^2}+\nabla\phi-\nabla(\nabla\phi\cdot\nabla\phi)\right]=0 \tag{7}$$

When Eq. (7) is expanded and the vector calculus is carried out, the following nonlinear velocity potential equation in the physical Cartesian coordinates is obtained:

$$(c^2-u^2)\frac{\partial^2\phi}{\partial x^2}-2uw\frac{\partial^2\phi}{\partial x\,\partial z}+(c^2-w^2)\frac{\partial^2\phi}{\partial z^2}-2u\frac{\partial^2\phi}{\partial x\,\partial t}-2w\frac{\partial^2\phi}{\partial z\,\partial t}-\frac{\partial^2\phi}{\partial t^2}=0 \tag{8}$$

where

$$u=\frac{\partial\phi}{\partial x},\qquad w=\frac{\partial\phi}{\partial z} \tag{9}$$

Once Eq. (8) is solved for ϕ, the Bernoulli–Kelvin equation (4), along with Eqs. (5) and (6), can be used to determine the pressure P as a function of the velocity potential ϕ. Therefore, in terms of ϕ, the pressure coefficient C_p, defined by

$$C_p=\frac{P-P_\infty}{\gamma P_\infty M^2} \tag{10}$$

can be expressed as

$$C_p=\frac{2}{\gamma M_\infty^2}\left[\left(1+\frac{\gamma-1}{2}M_\infty^2\left\{1-\frac{[\nabla\phi\cdot\nabla\phi+2(\partial\phi/\partial t)]}{q_\infty^2}\right\}\right)^{\gamma/\gamma-1}-1\right] \tag{11}$$

where M_∞, the reference Mach number, is given by

$$M_\infty=\frac{q_\infty^2}{c_\infty^2} \tag{12}$$

Traditional Hodograph Methods and Exact Solutions

Early investigators like Molenbrock[1] and Chaplygin[2] were able to show that if the steady approximation of Eq. (8) were mapped onto the hodograph plane using the Legendre transformation, it is possible to determine the exact fundamental

solutions (to this nonlinear equation). Of course, this was a breakthrough in the study of transonic flow. However, nothing seemed to have been said about the applicability of this type of transformation for solving the unsteady problem. In an effort to determine if the three-dimensional form of Legendre's transformation can be used for solving Eq. (8), the following results were obtained.

Consider the transformation

$$\phi = x\zeta + z\eta + t\tau - \chi \tag{13}$$

which is the Legendre transformation in three variables, where

$$\zeta = \frac{\partial \phi}{\partial x}, \qquad \eta = \frac{\partial \phi}{\partial z}, \qquad \tau = \frac{\partial \phi}{\partial t}$$

$$x = \frac{\partial \chi}{\partial \zeta}, \qquad z = \frac{\partial \chi}{\partial \eta}, \qquad t = \frac{\partial \chi}{\partial \tau} \tag{14}$$

Equation (13) transforms Eq. (8) into its counterpart in the hodograph space given by

$$(c^2 - \zeta^2)[\chi_{\eta\eta}\chi_{\tau\tau} - \chi_{\eta\tau}^2] + 2\zeta\eta[\chi_{\eta\zeta}\chi_{\tau\tau} - \chi_{\zeta\tau}\chi_{\eta\tau}] + (c^2 - \eta^2)[\chi_{\zeta\zeta}\chi_{\tau\tau} - \chi_{\zeta\tau}^2] - 2\zeta[\chi_{\eta\zeta}\chi_{\tau\eta} - \chi_{\eta\eta}\chi_{\tau\zeta}] - 2\eta[\chi_{\zeta\zeta}\chi_{\eta\tau} - \chi_{\zeta\eta}\chi_{\zeta\eta}] - \chi_{\zeta\zeta}\chi_{\eta\eta} + \chi_{\zeta\eta}^2 = 0 \tag{15}$$

Obviously, by comparing Eqs. (8) and (15) it can be seen that Eq. (15) does not look easier than Eq. (8). This type of comparison, therefore, explains why the traditional approach is not effective for solving Eq. (8).

New Hodograph Mapping Scheme

Before formulating the new mapping scheme that can transform Eq. (8) into its relatively easier counterpart in the hodograph plane, a nondimensionalization scheme, which uses the following set of affine transformations, is considered.

Affine Transformations

$$\phi = q_\infty b\phi_0, \qquad x = bx_0, \qquad z = bz_0, \qquad t = \frac{bt_0}{q_\infty} \tag{16}$$

Equation (16) transforms Eq. (8) into its nondimensionalized counterpart in the affine space, given by

$$(c_0^2 - u_0^2)\frac{\partial^2 \phi_0}{\partial x_0^2} - 2u_0 w_0 \frac{\partial^2 \phi_0}{\partial x_0 \partial z_0} + (c_0^2 - w_0^2)\frac{\partial^2 \phi_0}{\partial z_0^2} - 2u_0 \frac{\partial^2 \phi_0}{\partial x_0 \partial t_0} - 2w_0 \frac{\partial^2 \phi_0}{\partial z_0 \partial t_0} - \frac{\partial^2 \phi_0}{\partial t_0^2} = 0 \tag{17}$$

Although b in Eqs. (16) can be any arbitrary length quantity, it is convenient, at least for computational purposes, to choose b as the chord length of a wing section.

Equation (17) is, therefore, the nonlinear velocity potential equation in the affine space, where

$$u_0 = \frac{\partial \phi_0}{\partial x_0}, \qquad w_0 = \frac{\partial \phi_0}{\partial z_0}, \qquad c_0 = \frac{c}{q_\infty} \tag{18a}$$

or

$$u_0 = \frac{u}{q_\infty}, \qquad w_0 = \frac{w}{q_\infty}, \qquad c_0 = \frac{c}{q_\infty} \tag{18b}$$

Hodograph Transformations

Consider ϕ_0 to be a harmonic function of the form given by

$$\phi_0(x_0, z_0, t_0) = \Phi_0(x_0, z_0)e^{ikt_0}, \quad n\pi - \epsilon \le kt_0 \le n\pi - \epsilon$$
$$= \Phi_0(x_0, z_0), \quad n\pi + \epsilon \le kt_0 \le (n+1)\pi - \epsilon \tag{19}$$

where $\epsilon \to 0$, $n = 0,1,2,3,\ldots$. This is essentially a quasi-unsteady assumption. Therefore, it can be argued that this analysis is not really unsteady. Clearly a response to that argument is that the analysis is probably the first one in almost one century to show that transonic (nonlinear) flows other than two-dimensional or unsteady one-dimensional flows can be studied in the hodograph space. It thus provides an aspect of transonic flow that has never been seen before. If this assumption seems crazy to some readers, it should be noted that it is not without precedent. For example, this assumption is not likely to be crazier than the famous von Kármán–Tsien assumptions that led to the definition of a gas known as "Kármán–Tsien" gas. This gas has the ratio of the specific heats to be equal to -1, i.e., $\gamma = -1$. However, the Kármán–Tsien's approximation did provide good benchmark results that compared favorably even with experimental results. The analysis received the blessing of such important scientists as Sir M. J. Lighthill—particularly pp. 367–373 of Ref. 28.

A second example is the fact that the so-called small-disturbance theory approximation has been known to give good results. Therefore, it would seem that the primary (most important) thing in any transonic flow analysis is the *preservation* of the flow's *nonlinear character*. Every other thing seems to be secondary.

Furthermore, it should be pointed out that as a consequence of the assumptions in Eq. (19), if the steady-state solution $\phi_0(x_0, z_0)$ has shocks, such shocks would be retained in the quasi-unsteady solutions as well.

Finally, perhaps it also should be remembered that all of the transonic flow equations (and, indeed, all mathematical physics equations), including the Navier Stokes equations, are all approximations.

The nondimensionalized frequency (or Strouhal number) k is, as a result of Eqs. (16), given by

$$k = \frac{\omega b}{q_\infty} \tag{20}$$

where ω is the circular frequency of oscillations. If Eqs. (19) and (20) are substituted into Eqs. (17), the following equation is obtained:

$$(c_0^2 - u_0^2)\frac{\partial^2 \phi_0}{\partial x_0^2} - 2u_0 w_0 \frac{\partial^2 \phi_0}{\partial x_0 \partial z_0} + (c_0^2 - w_0^2)\frac{\partial^2 \phi_0}{\partial z_0^2} + k^2\phi_0 = 2ik(u_0^2 + w_0^2) \tag{21}$$

Equation (21) also can be written in the following manner:

$$(c_0^2 - u_0^2)\frac{\partial^2 \phi_0}{\partial x_0^2} - 2u_0 w_0 \frac{\partial^2 \phi_0}{\partial x_0 \partial z_0} + (c_0^2 - w_0^2)\frac{\partial^2 \phi_0}{\partial z_0^2} + k^2\phi_0 = 2ikq_0^2 \tag{22}$$

where q_0, the resultant velocity, is given by

$$q_0^2 = u_0^2 + w_0^2 \tag{23}$$

Now consider the following transformation:

$$\chi_0 = u_0 x_0 + w_0 z_0 - \phi_0 \tag{24}$$

where

$$x_0 = \frac{\partial \chi_0}{\partial u_0}, \qquad z_0 = \frac{\partial \chi_0}{\partial w_0} \tag{25}$$

$$\chi_0 = \tilde{\chi} e^{ikt_0} \tag{26}$$

When Eqs. (24–26) are substituted into Eq. (22), the following equation in the hodograph plane must be solved to

obtain the transformed velocity potential:

$$(\bar{c}^2-\bar{u}^2)\frac{\partial^2\bar{\chi}}{\partial\bar{w}^2}+2\bar{u}\bar{w}\frac{\partial^2\bar{\chi}}{\partial\bar{u}\,\partial\bar{w}}+(\bar{c}^2-\bar{w}^2)\frac{\partial^2\bar{\chi}}{\partial\bar{u}^2}+k^2J\left[\bar{u}\frac{\partial\bar{\chi}}{\partial\bar{u}}+\bar{w}\frac{\partial\bar{\chi}}{\partial\bar{w}}-\bar{\chi}\right]=0 \tag{27}$$

where

$$\bar{u}=\frac{\partial\Phi}{\partial x_0},\qquad \bar{w}=\frac{\partial\Phi}{\partial z_0} \tag{28}$$

and $\bar{c}$ and J are the nondimensionalized steady-state velocity of sound and Jacobian of the transformation, represented by Eqs. (24–26), respectively.

From Eq. (27), it is seen that if the Jacobian J is prescribed, ab initio, the resulting *linear* equation can be solved closed-form to determine the exact fundamental solutions for the transformed potential χ and, hence, ϕ. Consequently, these solutions can be pieced together to determine the shape of an airfoil. Notice that the familiar steady hodograph equation can be recovered from Eq. (27) if k is set equal to zero. It also should be noted that the presence of the Jacobian in Eq. (27) should not necessarily be considered as an added problem in comparison to the steady hodograph equation in which the Jacobian does not appear explicitly, since its behavior must be studied in both cases in order to ensure unique solutions.

Solution Methods

Although Morawetz[25] has shown that continuous solutions for Eq. (27) (steady-state approximation was used to arrive at this conclusion) for a closed body in the transonic regime do not exist, investigators like Nieuwland[5] have shown that fundamental closed-form solutions of the steady approximation of Eq. (27) can be pieced together employing the appropriate boundary conditions to obtain interesting transonic flows over airfoils. In this paper an effort is made to obtain closed-form fundamental solutions of Eq. 27, which are consequently pieced together after the appropriate boundary conditions are enforced to study some steady and unsteady transonic flows.

Polar Coordinates

In an attempt to obtain fundamental solutions of Eq. (27), it is helpful to transform this hodograph equation of motion into a polar coordinate system.

Consider the following transformations:

$$\bar{u}=\bar{q}\cos\theta,\qquad \bar{w}=\bar{q}\sin\theta \tag{29}$$

Equations (29) transform Eq. (27) into the following polar coordinate counterpart:

$$\bar{c}^2\bar{\chi}_{\bar{q}\bar{q}}+\left[\left(\frac{\bar{c}}{\bar{q}}\right)^2-1\right]\bar{\chi}_{\theta\theta}+\bar{q}\left[\left(\frac{\bar{c}}{\bar{q}}\right)^2-1+\left(k\frac{2J}{\bar{q}}\right)\right]\bar{\chi}_{\bar{q}}+\left(k\frac{2J}{\bar{q}}\right)\bar{\chi}=0 \tag{30}$$

where J is now the Jacobian of the transformation into the polar coordinates whose relationship to J can be seen as follows:

$$J=\frac{\partial(x_0,z_0)}{\partial(\bar{u},\bar{w})} \tag{31a}$$

$$J=\frac{\partial(x_0,z_0)}{\partial(\bar{q},0)} \tag{31b}$$

$$\frac{\partial(x,z)}{\partial(\bar{u},\bar{w})}=\frac{\partial(x_0,z_0)}{\partial(\bar{q},0)}\cdot\frac{\partial(\bar{q},0)}{\partial(\bar{u},\bar{w})} \tag{32}$$

or

$$J=J\frac{\partial(\bar{q},0)}{\partial(\bar{u},\bar{w})}=\frac{J}{\bar{q}} \tag{33}$$

To study the fundamental solution of Eq. (30), consider a flow in which

$$J=J(\bar{q}) \tag{34}$$

Therefore, a general solution of the form

$$\bar{\chi}=Q(\bar{q})\cos(m\theta+\epsilon) \tag{35}$$

can be assumed for Eq. (30) in order to obtain the following equation for $Q(\bar{q})$.

$$\bar{c}^2Q_{\bar{q}\bar{q}}+\bar{q}\left[\left(\frac{\bar{c}}{\bar{q}}\right)^2-1+\left(k^2\frac{J}{\bar{q}}\right)\right]Q_{\bar{q}}-\left\{\left[\left(\frac{\bar{c}}{\bar{q}}\right)^2-1\right]m^2+\left(k^2\frac{J}{\bar{q}}\right)\right\}Q=0 \tag{36}$$

Equation (36) can be rewritten in a slightly different manner if the following definition is employed:

$$M=\frac{\bar{q}}{\bar{c}} \tag{37}$$

where M is the local Mach number.

Equation (36), in light of Eq. (37), becomes

$$\bar{q}^2Q_{\bar{q}\bar{q}}+\bar{q}\left[1-M^2+M^2\left(k^2\frac{J}{\bar{q}}\right)\right]Q_{\bar{q}}-\left[(1-M^2)m^2+M^2\left(k^2\frac{J}{\bar{q}}\right)\right]Q=0 \tag{38}$$

Equation (38) must be solved to obtain the transformed velocity potential $\bar{\chi}$ and, hence, the physical space velocity potential ϕ. A similar approach can be used to show that the following equation must be solved to obtain the transformed stream function given by

$$\psi=-\bar{Q}(\bar{q})\cos(m\theta+\bar{\epsilon}) \tag{39}$$

i.e.,

$$\bar{q}^2\bar{Q}_{\bar{q}\bar{q}}+\bar{q}\left[1+M^2+M^2\left(k^2\frac{J}{\bar{q}}\right)\right]\bar{Q}_{\bar{q}}-\left[(1-M^2)m^2+M^2\left(k^2\frac{J}{\bar{q}}\right)\right]\bar{Q}=0 \tag{40}$$

In general, Eqs. (38) and (40) are hypergeometric and, hence, can be satisfied by combinations of power and logarithmic series. Finding solutions to the flow around a closed body, therefore, becomes dependent on piecing these types of series correctly. Employing such fundamental solutions to construct the overall solution is obviously preferable to using arbitrary series, since these fundamental solutions are "solid" in that they satisfy the equation of motion.

In order to transform Eqs. (38) and (40) into the familiar hypergeometric form, consider a reference q^* given by

$$\bar{c}^2=\frac{\gamma+1}{2}\bar{q}_*^2-\frac{\gamma-1}{2}\bar{q}^2 \tag{41}$$

and a change of independent variable given by

$$\bar{\tau}=\frac{\gamma-1}{\gamma+1}\left(\frac{\bar{q}}{\bar{q}^*}\right)^2 \tag{42}$$

Equation (42) transforms Eq. (40) to the following

$$\bar{\tau}(1-\bar{\tau})\bar{Q}_{\bar{\tau}\bar{\tau}} + \left[1 - \frac{(\gamma - 2 - k^2 J_0)}{\gamma - 1}\bar{\tau}\right]\bar{Q}_{\bar{\tau}} - \frac{m^2}{4\bar{\tau}}\left[1 - \frac{(\gamma + 1 - 2k^2 J_0)}{\gamma - 1}\right]\bar{Q} = 0 \tag{43}$$

An exact fundamental solution of Eq. (43) can be given by

$$\bar{Q} = B_m \bar{\tau}^{m/2} F_m(\bar{\tau}) \tag{44a}$$

where

$$\bar{\psi} = B_m \bar{\tau}^{m/2} F_m(\bar{\tau}) \cos(m\theta + \epsilon) \tag{44b}$$

where B_m are arbitrary constants to be determined by the boundary conditions of a particular flow problem, and $F_m(\bar{\tau})$ satisfy the following hypergeometric equations:

$$\bar{\tau}(1-\bar{\tau})\frac{\partial^2 F_m}{\partial \bar{\tau}^2} + \left[m + 1 - \left(m + 1 - \frac{1 + k^2 J_0}{\gamma - 1}\right)\bar{\tau}\right]\frac{\partial F_m}{\partial \bar{\tau}} + \frac{\beta}{2}(m+1)(m + k^2 J_0)F_m = 0 \tag{45}$$

where

$$\beta = \frac{1}{\gamma - 1}$$

An F_m satisfying Eq. (45) is a hypergeometric function given by

$$F_m(\bar{\tau}) = F(\bar{a}, \bar{b}; \bar{d}; \bar{\tau}) = 1 + \frac{\bar{a}\bar{b}}{1 \cdot \bar{d}}\bar{\tau} + \frac{\bar{a}(\bar{a}+1)\bar{b}(\bar{b}+1)}{1 \cdot 2 \cdot \bar{d}(\bar{d}+1)}\bar{\tau}^2 + \cdots\cdots \tag{46}$$

where

$$\bar{a} + \bar{b} = m - \beta(1 + k^2 J_0); \qquad \bar{a}\bar{b} = -\frac{\beta}{2}(m+1)(m + k^2 J_0), \qquad \bar{d} = m + 1 \tag{47}$$

In terms of the velocity potential, the fundamental solution is

$$\bar{\chi} = -B_m \bar{\tau}^{m/2}(1-\bar{\tau})^{-\beta}\left[F_m(\bar{\tau}) + \frac{2\bar{\tau}\,\partial F_m(\bar{\tau})}{m\,\partial \bar{\tau}}\right]\sin(m\theta + \epsilon) \tag{48}$$

Equations (44) and (48) represent some exact fundamental solutions for the stream function and velocity potential, respectively, in the hodograph plane. In the examples shown in this paper, the stream function solutions were used in constructing the flow solutions.

Computed Examples

The examples computed in this paper consist of the pressure variations with Mach numbers and Strouhal numbers (reduced frequencies) for some chosen points on a flat plate in a transonic flow and what may be considered as a preliminary attempt to compute the steady and unsteady transonic pressure distributions around a 70-10-13 supercritical wing section designed in the early seventies by Bauer, Garabedian, and Korn.[6] The procedure basically consists of trying to construct compressible (transonic) flows using incompressible flows around an elliptical cylinder resulting in a shape different from the cylinder with the help of the exact fundamental potential flow solutions above. This procedure has been thoroughly documented by Nieuwland[5] for the steady flow problem. Hence, no attempt has been made in this paper to redocument the basis of this approach. Therefore, readers are referred to Ref. 5. Suffice it to say that the approach involves a lot of "bookkeeping" and patience. Furthermore, it must be pointed out that this procedure can (and should) be better automated. This endeavor is currently in progress.

The flat plate results shown in Figs. 1–6 have basically two main features:

1) Dips in the pressure distributions when the Mach numbers are varied in the transonic regime seem to agree with the general trends in the behavior of transonic characteristics such as the lift coefficient, the so-called transonic dip, which is basically the loss of aeroelastic stability at transonic speeds.

2) The pressure distribution at a particular Mach number at a particular chord length seems to have an optimum reduced frequency (Strouhal number).

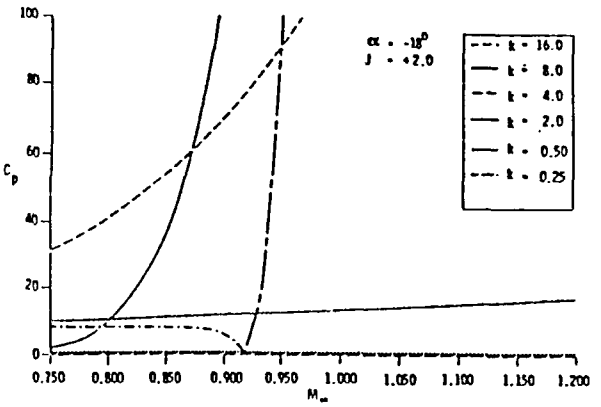

Fig. 1 Pressure coefficient vs Mach numbers for a flat plate.

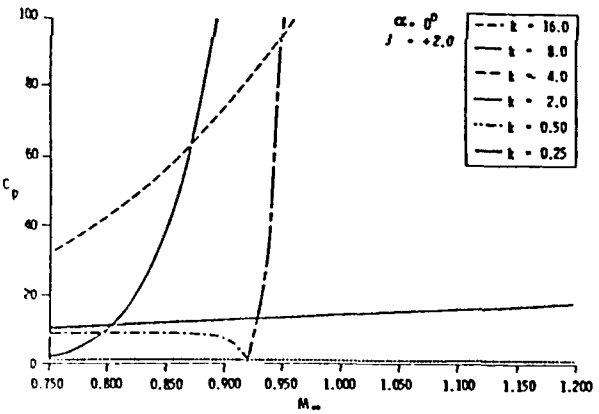

Fig. 2 Pressure coefficient vs Mach numbers for a flat plate.

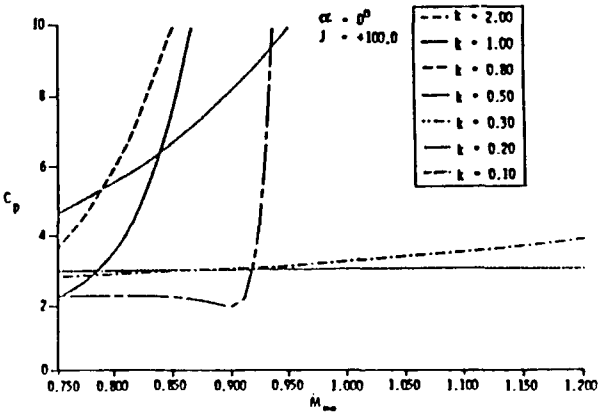

Fig. 3 Pressure coefficient vs Mach numbers for a flat plate.

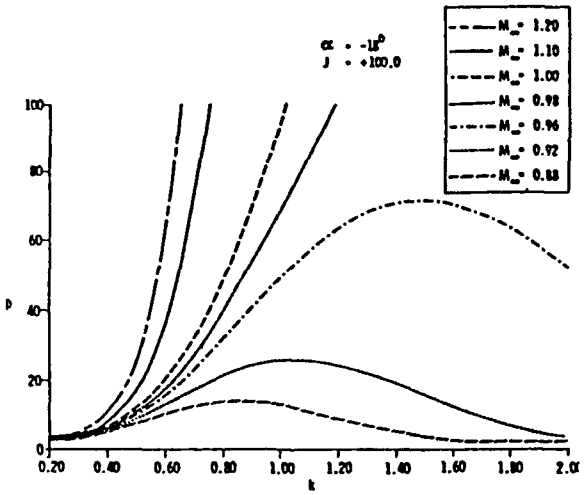

Fig. 4 Pressure coefficient vs reduced frequency for a flat plate.

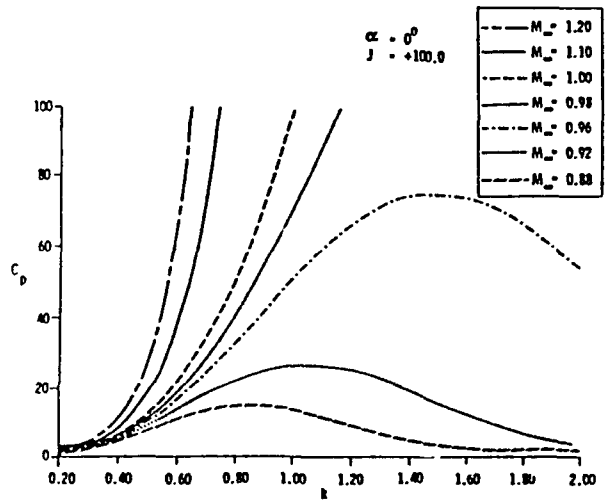

Fig. 5 Pressure coefficient vs reduced frequency for a flat plate.

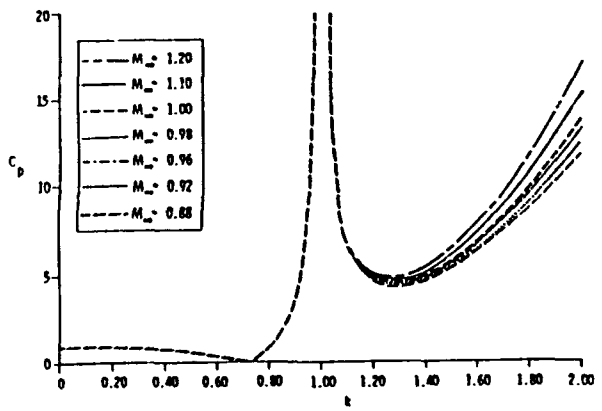

Fig. 6 Pressure coefficient vs reduced frequency for a flat plate.

Marble[26] has shown similar trends for a quasi-one-dimensional flow. The result shown in Fig. 7 for a 70-10-13 supercritical airfoil designed back in the early seventies,[6] which is preliminary in nature, seems to indicate the feasibility of using the approach outlined in this paper in designing unsteady aerodynamic characteristics for an airfoil. The pressure distribution for the supercritical airfoil, 70-10-13 shown in Fig. 7, is for a freestream Mach number of 0.7 and a lift coefficient

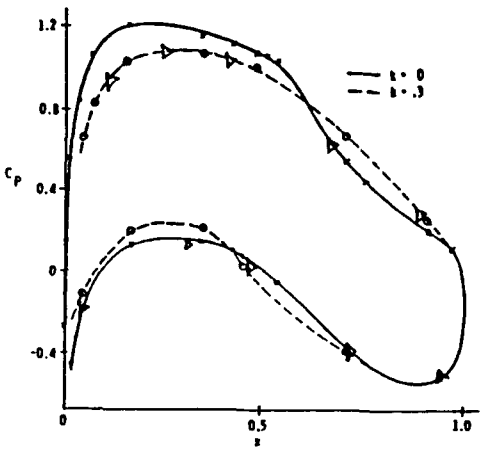

Fig. 7 Pressure distribution on a 70-10-13 supercritical airfoil.

$(C_L) = 0.98$, and the airfoil has a thickness ratio of 0.127. The angle of attack for the steady computation was 0 deg. For the unsteady computations it is assumed that $kt_0 = 0.1$, and that the airfoil is oscillating about the half-chord with a pitch amplitude of 1 deg. The main significance of Fig. 7 is that the approach outlined in this paper can be used to accurately compute the pressure distributions for supercritical airfoils, since these pressure distributions compare very well with the results obtained in Ref. 6 for the steady flow and also compare favorably with results of Ref. 15 for the unsteady flow. Because of the fact that the analysis in this paper is preliminary in nature, a more general set of conclusions would have to await more refined computations that are anticipated in the near future. Finally, it must be pointed out that the results presented in this paper are basically shockless inviscid results. Therefore, the plots shown for Mach numbers greater than unity can only be approximations to the weak shock solutions.

Concluding Remarks

This paper has attempted to establish the existence of exact closed-form fundamental solutions to the two-dimensional nonlinear unsteady potential aerodynamic equations. Evidence indicating why the traditional hodograph approach is not effective for solving the nonlinear unsteady two-dimensional flow equations is presented. Therefore, suitable mapping functions are employed to transform the nonlinear potential flow equations into the hodograph plane. An examination of the transformed flow equations in the hodograph plane reveals that if the Jacobian of the transformation is prescribed ab initio, the exact closed-form fundamental solutions for the velocity potential and stream functions can be obtained. It is seen that such Chaplygin solutions can be used in conjunction with the incompressible flow around elliptical cylinders to construct transonic flows over interesting shapes with the help of a methodology developed several decades ago by investigators such as Lighthill[3] and Nieuwland[5] for steady flows. Computations of the pressure distributions for certain points on the flat plates seem to indicate that dips exist in the pressure distributions as the freestream Mach numbers are varied in the transonic regime. The results also seem to show the existence of optimum reduced frequencies for the pressure distributions. A steady and an unsteady pressure distribution are also computed for a 70-10-13 supercritical airfoil designed back in the early seventies.[6] Although the approach needs more efficient automation, the results computed show that it is feasible to use this approach to solve the inverse problem of designing airfoils with desired unsteady aerodynamic characteristics. This, therefore, implies the possibility of designing airfoils that satisfy both the performance and stability criteria simultaneously.

Acknowledgments

This paper is dedicated to God for His inspiration. It is also dedicated to the memories of my father, S. Oyibo Obaje, and my uncle Ejima Alhaji who passed away on April 18, 1986, and May 31, 1975, respectively. The contributions of Professor P. Garabedian of the Courant Institute, New York University, New York, to this paper are acknowledged. The author also acknowledges helpful discussions with J. H. Berman and Dr. S. M. Scala, both of Fairchild Republic Company. The author is grateful to Drs. Anthony K. Amos and Arje Nochman who partially funded this work under AFOSR Contract F49620-87-C-0046 and AFOSR Grant 89-0055.

References

[1]Molenbrock, P., "Uber einige Bewegungen eines Gases bei Annahme eines Geschwindigkeits Potentials," *Archive of Mathematical Physics*, Vol. 9, 1890, pp. 157-195.

[2]Chaplygin, S. A., "On Gas Jets," *Scientific Memorandum, Moscow University, Mathematic Physics*, No. 21, 1904, pp. 1-21; NACA TM-1063, 1944.

[3]Lighthill, M. J., "The Hodograph Transformation in Transonic Flow. II. Auxiliary Theorems on the Hypergeometric Functions. III. Flow Round a Body," *Proceedings of the Royal Society of London*, Ser. A 191, 1947, pp. 341-369.

[4]Guderley, K. G., "On Transonic Simplifications of the Hodograph Equation," Wright Air Development Center, TR-53-183, Dayton, OH, 1953.

[5]Nieuwland, G. Y., "Transonic Potential Flow around a Family of Quasi-Elliptical Aerofoil Sections," National Luchten Ruimteuaartlaboratorium Rept. TR.T172, the Netherlands, 1967.

[6]Bauer, F., Garabedian, P., and Korn, D., *Supercritical Wing Sections: Lecture Notes in Economics and Mathematical Systems*, Vol. 66, Springer-Verlag, New York, 1972.

[7]Boersteel, J. W., "A Survey of Symmetrical Transonic Potential Flows around Quasi-Elliptical Aerofoil Sections," National Luchten Ruimteuaartlaboratorium Rept. TR.T.136, the Netherlands, 1967.

[8]Sobieczky, H., "Related Analytical, Analog, and Numerical Methods in Transonic Airfoil Design," AIAA Paper 79-1556, July 1979.

[9]Hassan, A., Sobieczky, H., and Seebass, A. R., "Subsonic Airfoils with a Given Pressure Distribution," *AIAA Journal*, Vol. 22, Sept. 1984, pp. 1185-1191.

[10]Garabedian, P., *Partial Differential Equations*, Wiley, New York, 1964.

[11]Courant, R. and Hilbert, D., *Methods of Mathematical Physics*, Vol. II, Interscience, New York, 1962.

[12]Bateman, H., *Partial Differential Equations of Mathematical Physics*, Dover Publications, New York, 1944.

[13]Guderley, K., *The Theory of Transonic Flow*, Pergamon, Oxford, 1962.

[14]Garrick, I. E. and Kaplan, C., "On the Flow of a Compressible Fluid by the Hodograph Method II—Fundamental Set of Particular Flow Solutions of the Chaplygin Differential Equation," NACA Rept. No. 790, 1944.

[15]Isogai, K., "Calculation of Unsteady Transonic Flow Over Oscillating Airfoils Using the Full Potential Equation," AIAA Paper 77-448, 1977.

[16]Ballhaus, W. F. and Goorjian, P. M., "Computation of Unsteady Transonic Flows by the Indicial Method," *AIAA Journal*, Vol. 16, Feb. 1978, pp. 117-124.

[17]Yang, T. Y., Guruswamy, P., and Stiriz, A. G., "Application of Transonic Codes to Flutter Analysis of Conventional and Supercritical Airfoils," *Proceedings of the 22nd AIAA/SDM Conference*, AIAA, New York, 1981.

[18]Dowell, E. H., Bland, S. R., and Williams, M. H., "Linear/Nonlinear Behavior in Unsteady Transonic Aerodynamics," *AIAA Journal*, Vol. 21, Jan. 1983, pp. 38-46.

[19]Edwards, J. W., Bennett, R. M., Whitlow, W. Jr., and Seidel, D. A., "Time-Marching Transonic Flutter Solutions Including Angle-of-Attack Effects," *Proceedings of the 23rd AIAA/SDM Conference*, AIAA, New York, May 1982.

[20]Magnus, R. J. and Yoshihara, H., "Calculations of Transonic Flow Over an Oscillating Airfoil," AIAA Paper 75-98, Jan. 1975.

[21]Tijdeman, H. and Seebass, R., "Transonic Flow Past Oscillating Airfoils," *Annual Review of Fluid Mechanics*, Vol. 12, 1980, pp. 181-222.

[22]Whitlow, W. and Harris, W. L., "An Analytical/Numerical Method to Solve Two-Dimensional Transonic Flow," MIT Fluid Dynamics Research Lab. Rept. No. 79-3, MIT, Cambridge, MA, Aug. 1979.

[23]Dowell, E. G., Curtiss, H. C., Scanlan, R. H., and Sisto, F., *A Modern Course in Aeroelasticity*, Sijhoff and Noordhoff International Publishing, the Netherlands, 1978.

[24]Zwaan, R., "Verification of Calculation Methods for Unsteady Airloads in the Prediction of Transonic Flutter," AIAA Paper 84-087-1/2, May 1984.

[25]Oyibo, G. A., "Unified Aeroelastic Flutter Theory for Very Low Aspect Ratio Panels," *AIAA Journal*, Vol. 21, Nov. 1983, pp. 1581-1587.

[26]Marble, F. E., "Response of a Nozzle to an Entropy Disturbance—Example of Thermodynamically Unsteady Aerodynamics," *Proceedings of the Unsteady Aerodynamics Symposium*, Vol. II, Univ. of Arizona, Tucson, AZ, March 1975, pp. 699-711.

[27]Morawetz, C. S., "On the Non-Existence of Continuous Transonic Flows Past Profiles, *I. Communications of Pure and Applied Mathematics*, Vol. 9, 1956, pp. 45-68.

[28]Sears, W. R., *General Theory of High Speed Aerodynamics*, Princeton Univ. Press, Princeton, NJ, 1954.

FORMULATION OF 3-D HODOGRAPH METHOD AND SEPARABLE SOLUTIONS FOR NONLINEAR TRANSONIC FLOWS †

Gabriel Oyibo*
Polytechnic University
Farmingdale, New York

Abstract

Formulation of a three dimensional hodograph technique for transforming the full nonlinear potential transonic flow equation from the physical space into an equivalent linear counterpart in the hodograph plane is presented. A very careful examination of the governing nonlinear equations in the physical space reveals that a mild constraint on the energy equation (which may even enhance the accuracy of this nonviscous formulation) would permit the separation of the nonlinear flow equations for an aircraft wing into a sectional component and spanwise component. This separation of variables normally believed to be possible only for linear equations seems to have been possible (for the non-linear equations) because of some inherent mathematical symmetry of the 3-D nonlinear flow equations. The consequential "three-dimensional" sectional equation is eventually transformed into the hodograph plane where it becomes linear. A further transformation of these linear hodograph equations into the characteristic hodograph plane provides the opportunity of obtaining the nonlinear flow field for a particular set of boundary conditions by just solving a set of first order characteristic equa-

*Associate Professor, Aerospace Engr. Dept., Associate Fellow AIAA

tions. The necessary computations can easily be carried out on a computer. Some preliminary computations show good agreement with previously computed data. This verification therefore provides confidence that the new tool can perhaps be used in an inverse manner to design a new family of 3-D lifting surfaces with great potential.

† Research sponsored by the Air Force Office of Scientific Research (AFSC), under Grant 89-0055. The United States Government is authorized to reproduce and distribute reprints for governmental purposes notwithstanding any copyright notation hereon.

Nomenclature

$\bar{a},\bar{b},\bar{d},f_o$	coefficients of hodograph equation
$B,\bar{B}$	complex constant and its conjugate, respectively
$c_p,\bar{y}$	pressure coefficient and fraction of wing half span (zero is wing root), respectively
C,C	speed of sound and 2-D component of 3-D speed of sound, respectively
C_i (i=1,2,...)	coefficients of separated physical equations
E,t	ellipse parameter and time, respectively
$\bar{x}$	fraction of chord length (zero is leading edge)
F	term in hodograph equation
M	Mach number
x,y,z	Cartesian coordinates (flow, spanwise, and vertical directions, respectively)
,v,w	flow velocity components
$\bar{u},\bar{w}$	2-D components of 3-D flow velocities
ϕ,ψ	velocity potential and stream function, respectively
χ	transformed potential
Φ,χ	section component velocity potential and transformed potential, respectively
Λ,α	spanwise component velocity potential and separation constant, respectively
f,h	functions in the hodograph plane
q,θ	flow speed, and flow angle, respectively
$r,\hat{q}$	ratio of specific heats and maximum speed, respectively
,,η	characteristic coordinates

ρ, k	air density and circulation parameter, respectively
X_i, Z_i	regular solutions in the complex characteristic hodograph plane
τ, λ	hodograph variable and characteristic roots, respectively
s, t	conjugate complex characteristics
$( )_\infty$	freestream quantities

INTRODUCTION

In the late 1800's, certain investigators[1,2] discovered that the hodograph transformation can be a very powerful tool for studying nonlinear inviscid fluid flow problems. Subsequently, later investigators[3-14] were able to reveal that this method could be used to design supercritical airfoils with superior transonic performance characteristics. These developments constituted a breakthrough in the study of transonic flow problems, which are characterized by equations which exhibit strong nonlinearities. The success of this method was due to the following two characteristics of solutions obtained from the hodograph equations as compared to solutions obtained from the equations in physical space. First, the hodograph equations are linear allowing solutions to be superimposed, which is not possible in physical space due to the nonlinearity of the governing equations. Second, the potential for formulating an inverse problem in hodograph space thereby allowing the desired fluid flow field to be specified as input and leading to the required geometry as the computed output.

Despite the success of this work, use of the hodograph technique has unnecessarily suffered from a major drawback: that is, that there is a general belief that the hodograph technique can only be applied to two-dimensional steady flow problems. This implies that neither unsteady two-dimensional flow nor steady three-dimensional problems can be studied using a hodograph approach and thus has limited the interest in, and application of, this powerful analysis tool.

However, recent research performed by Oyibo[15] has shown that the hodograph transformation is not limited to two-dimensional steady flows. The work reported in this paper is a direct cosequence of the discovery that, contrary to the aforementioned general belief, the hodograph technique can be employed to transform the nonlinear transonic flow problems with three independent variables into an equivalent linear set of equations in the hodograph plane.

The derivation of these transformed equations probably marks the first time in fluid mechanics that the hodograph technique has been extended beyond steady two-dimensional flow using full potential equations. It is important to note that a straight-forward

application of the usual hodograph (Legendre's) transformation for the case of three independent variables leads to an equation (cf. quation (4) below) which is even more nonlinear than its counterpart in physical space. While Equation 4 is consistent with the earlier research work published by Guderley[16] which was independently verified by Cole and Cook[17,21] using a different approach, small disturbance (not full potential) equations were used. The primary achievement of the new method was to find an alternate way of defining the transformation so as to result in a linear system of equations. The resulting equations have tremendous significance for the solution of both steady and unsteady fluid flow problems due to a number of features of the hodograph method in general and the new equations in particular.

First, since the transformed equations are linear, they allow superposition of solutions. This means that any complete solution can be constructed from a combination of fundamental solutions. This will enable an analytic determination of the influence of the input parameters on the solutions and hence will lead to a better understanding of the flow physics. This is not possible with the nonlinear equations in in physical space where, except for specialized cases, only purely numerical solutions are possible. These numerical solutions suffer from the drawback that they are both approximate and that it is difficult to understand the effect that the important physical parameters have on the solution to the problem, since these effects have to be deduced by studying the results from a number of different cases.

Second, as shown below in Section 1.1, the form of the newly derived hodograph equations for the both the unsteady 2-D case and the steady 3-D case are similar to the steady 2-D hodograph equations in that the highest order (second) derivative terms are identical for all three cases. The difference between the cases shows up in the inclusion of lower order terms which are not present in the steady two-dimensional hodograph equation. Since the computational solution techniques and the characteristics of partial differential equations are usually determined by the form of the highest derivative terms, and since that form is identical to the steady 2-D hodograph equations, then the solution techniques previously developed for steady two-dimensional

flow should be directly applicable to the 3-D steady case. This is particularly important in the case of transonic flow due to the non-uniqueness of the solutions as proven by Morawetz[20]. For the case of 2-D steady flow, Garabedian and Korn[6] have worked out a systematic and efficient procedure to enable "closed" bodies to be developed in a straightforward manner. Since the new equations are so similar to the ones solved in [6], this work is directly applicable to the current problem and forms the bases for excluding non-realistic solutions from the admissible set.

Finally, and perhaps the most important point, is that the transformed equations allow inverse solutions to be obtained, in which the pressure field is specified and the body geometry is calculated from closed form solutions. From the point of view of design, this is the desired situation rather than the usual trial and error method of picking the geometry and then examining the resulting calculated flow field. Thus solutions obtained from the new hodograph method could lead to the design of new families of wing shapes which should prove to have significantly reduced shock strengths and hence lower drag when shocks appear at off design conditions. The fuel savings for the commercial airline industry made possible by such an efficient wing design could approach hundreds of millions of dollars annually and thus the proposed technique as outlined in this paper could lead to immediate and substantial industrial value.

In reference 15, the two-dimensional unsteady nonlinear transonic flow case was treated using the new hodograph method and shown to lead to results in good agreement with previous computational solutions. The ease of obtaining solutions to the new equations was demonstrated by using a microcomputer to obtain these solutions. This should allow more room in big computers like the Cray for design optimation rather than just solving for the flow field.

Since that time, the derivation of the governing hodograph equations in three variables has been extended to the important case of steady 3-D flow. It is the purpose of this proposed paper to delineate the formulation of the 3-D hodograph equations and to carry out a preliminary study of their solutions for the case of steady flow around lifting surfaces of finite span.

THIS
PAGE
IS
MISSING
IN
ORIGINAL
DOCUMENT

THIS
PAGE
IS
MISSING
IN
ORIGINAL
DOCUMENT

Equations (7d) and (7e) probably are among the very few (perhaps the first set) of separable nonlinear equations. It can be seen that as a consequence of equations (7a) either of the following constraints on the energy (or Bernoulli) equation become necessary.

$$\left(\frac{u_\infty^2}{2} + \frac{c_\infty^2}{\gamma-1}\right) = 0 \text{ in three dimensions} \qquad (7f)$$

$$\text{or } (u_\infty, c_\infty) = (\bar{u}_\infty, \bar{c}_\infty)\Lambda(\alpha, y) \qquad (7h)$$

For the constraints in Equation (7f) to be enforced, γ must approach -1. This is either an interesting coincidence or something is being said about the realities of the isentropic assumptions in the potential flow formulations. This is because $\gamma = -1$ is the Karman-Tsien gas which has been shown to be so accurate that the results using this gas agrees very well with experimental results. This agreement which is really excellent, can be seen in Figure F,5b in reference 19. Figure F,5b further shows clearly that Karman-Tsien gas is very accurate even for truly transonic flows (flows with supersonic bubbles). The alternative constraint in Equation (7h) could be shown to work provided that U_∞, C_∞ represent the reference section free stream velocity and speed of sound respectively.

Therefore, for steady 3-D flows, the hodograph equation to be solved is:

$$(\overline{u}^2-\overline{c}^2)\overline{X}_{\overline{w}\overline{w}} + (\overline{w}^2-\overline{c}^2)\overline{X}_{\overline{u}\overline{u}} + 2\overline{u}\overline{w}\overline{X}_{\overline{u}\overline{w}} - \overline{J}_1\overline{X}_{\overline{u}} - \overline{J}_2\overline{X}_{\overline{w}} + \overline{J}_3\overline{X} = 0 \qquad (8)$$

$\alpha = 0$, Equation (8) reduces to the familiar 2-D hodograph equation.

Equation (8) is similar to the 2-D hodograph equation which has been studied for almost a century. Therefore any methods of solution for the 2-D hodograph equations are also applicable to this new equation. Due to the mathematical symmetry mentioned previously, the solution takes on the separated form given by Equation (4) and Equation (8) becomes the 2-D sectional analog of the 3-D flow problem. From Equation (7e) the following form are feasible solutions for the spanwise component:

$$A(\alpha,y) = \prod_{n=0}^{\infty} A_n e^{\alpha_n y} \qquad (9)$$

where α_n are constants determined by the boundary conditions of the flow and y is the spanwise coordinate.

The general solutions of the sectional component of Equation (8) are in terms of hypergeometric series. These solutions may be used along with the method of complex characteristics in which the flow is mapped into the unit circle in the characteristic hodograph plane in order to obtain solutions for Equation (8). The goal is then to obtain the body stream function that encloses the particular wing section (e.g. the root section). Thereafter the spanwise component is combined with this solution in accordance with Equation (4) to provide the flow field over the entire 3-D lifting surface.

1.2 Nonlinear Three-Dimensional Transonic Flow Investigation and Construction

The fundamental exact solutions to the new hodograph equations are hypergeometric series in the hodograph space. As mentioned above, the equation system in the hodograph plane closely resembles the two-dimensional steady hodograph case for which computational techniques are well established. It is expected that these solution techniques will therefore be directly transferable to the higher dimensional cases. The techniques that have been successfully applied in previous hodograph analyses fall generally into two categories, either solutions obtained by superposition of a series of fundamental solutions as in the manner of Nieuwland[5] and as was also done in Reference 15 or by converting the problem into an initial value problem (or a c. icteristic initial value problem) by using the method of complex characteristics developed by Garabedian.[10]

While either of the solution techniques can be used, the method of complex characteristics has more appeal since the location of sonic lines and limiting lines appear more naturally in characteristic coordinates and thus this method is expected to be more promising in this ongoing study. However, in the present study the series method way used for constructing the flows satisfying the necessary boundary conditions for 3-D wings and to study the fundamental solutions carefully to determine how to piece them together properly as was done in Reference 15 for the 2-D unsteady case. The details of this procedure are given in [15]. An alternate method, which follows the 2-D work of Garabedian, is expected to be the primary analysis tool the next stage of the study, and consists of: (i) reducing the linear hodograph equation into its canonical form, (ii) utilizing the method of complex characteristics to map the particular section flow onto the unit circle in the characteristic hodograph plane, (iii) examining the solutions to ensure that the body stream function encloses the particular wing section.

For that purpose, Equation (8) reduced to its canonical form, would lead to the following system of first order equations:

$$z_\xi + \lambda_+ x_\xi + \frac{F}{\bar{a}}\bar{w}_\xi = 0 \ , \ z_\eta + \lambda_- x_\eta + \frac{F}{\bar{a}}\bar{w}_\eta = 0 \qquad (10)$$

$$\bar{u}_\xi - \lambda_- \bar{w}_\xi = 0 \ , \ \bar{w}_\eta - \lambda_+ \bar{u}_\xi = 0 \qquad (11)$$

$$\chi_\xi - z\bar{w}_\xi - x\bar{u}_\xi = 0 \qquad (12)$$

where ξ and η are the complex characteristics and:

$$z = \chi_{\bar{w}} \ , \ x = \chi_{\bar{u}}$$

$$\lambda_\pm = \frac{\bar{b} \pm \sqrt{\bar{b}^2 - \bar{a}\bar{d}}}{\bar{a}} \qquad (13)$$

with:

$$\bar{a} = \bar{u}^2 - \bar{c}^2 \ , \ \bar{b} = \bar{u}\bar{w} \ , \ \bar{d} = \bar{w}^2 - \bar{c}^2 \qquad (14)$$

Notice that the canonical system of equations (10-14) are first order equations representing Equation (8) or (3). One way to solve these equations is to map the flow field in the physical space into the region inside a unit circle in the complex characteristic hodograph plane and then use the incompressible solution to provide initial data for solving the characteristic initial value problem resulting from the mapping. This approach (thoroughly documented in [5]) is efficiently automated for the steady 2-D case in a computer code which we have obtained from Prof. Garabedian. We have extensively exercised this code and are thoroughly familiar with it, and hence have a major part of the necessary code for the 3-D problem in hand due to the similarity between the 2-D and 3-D equations. A full run of this code takes only 30 to 45 seconds on a Cray X-MP when run with non-vectorized code. It is expected that vectorization of the code which is currently underway will enable a fully optimized (shock-free) 3-D wing solution to be obtained in about 10 minutes which appears to be significantly faster than the time current computational transonic 3-D codes would require to obtain an optimal flow.

1.2.1 Investigation of Fundamental Solution

In general either of the two methods outlined above can be examined and used. In that process, the fundamental solutions can be studied very carefully, particularly to ensure the proper handling of the singularities like the limiting lines, which are the zeros of the Jacobian of the transformation and the branch lines, where the Jacobian is infinite.

It is recognized that though the spanwise and sectional components of the flow are (in a sense) considered separately, the fundamental problem of shockless flow is basically to find smooth transonic solutions for Equation (1), describing a 3-D compressible flow about a lifting surface of finite span. However, it is also

recognized as shown by Morawetz[20], that smooth transonic solutions do not even exist for all sectional (2-D) shapes for the lifting surface (let alone for a 3-D lifting surface). The new hodograph transformation helps us to overcome this difficulty by making it possible to separate the 3-D flow into the two components mentioned above and solve them as an inverse problem instead. If the spanwise component is given by Equation (9), then the sectional component is to be determined from Equations (10-14). In this study therefore, we computed smooth transonic flow by piecing together the hypergeometric series solutions to equations 18 as in reference 15 from a desired flow field and find the finite span lifting surface which generates it. This procedure was used to find the necessary α and hence the spanwise variation of the flow field. In order to compute the sectional component of this smooth transonic flow by the method of complex characteristics, the variables in Equations (10-14) can be extended into the complex domain where a characteristic initial value problem along the complex characteristics may be solved. While this procedure can be done in a purely analytic manner, it can also be carried out conveniently on a computer. In the ture work, we propose to use the computational approach by modifying the existing code of Garabedian to include the additional terms appearing in the sectional equation (Equation 8)). When this is done as described below, the "3-D" section will be determined as well as α which provides the unknown in Equation (9) for the spanwise component of the flow.

Considering Equation (13), for real variables, for supersonic flow, λ_+ and λ_- are real and Equation (18) is hyperbolic. This means that the initial value problem, defined as specifying x and z on any non-characteristic curve as well as the characteristic initial value problem defined as one in which x or z is specified on one characteristic of each family are well posed. However, for subsonic flow, λ_+ and λ_- become complex conjugates and Equation (18) is elliptical. Here, both the initial and the characteristic initial value problem are no longer well posed in the real domain, and hence boundary values are generally needed for formulating a correctly set problem.

13 CREDIBILITY OF THE NEW HODOGRAPH METHOD

As has been mentioned earlier, the 2-D unsteady results have been shown, in [15] (which has been reviewed and accepted for publication in the AIAA Journal) to be accurate when compared with previously published purely computational results.

For the 3-D steady case, Figure 1 shows a comparison of preliminary results of the calculation of the flow from the new method with results obtained by Spreiter[18] using a local linearization technique for the case of $M=1$ flow around a rectangular wing with a parabolic arc section and an aspect ratio of 7.01. The results are shown to be in good agreement, with the differences attributable to the approximate nature of Spreiter's analysis.

Figure 2 shows comparisons between the results obtained using the new method and those computed using the FLO22 computer code of Jameson and Caughey[22]. This code uses a finite difference technique to solve the transonic full potential equations in non-conservative form. For the cases shown of a rectangular wing at $M_\infty = 0.7$, the results are seen to be in excellent agreement due to the more accurate model contained in the computer code than in the previous case. We thus feel that these preliminary solutions give credibility to the 3-D analysis and give confidence as to its potential.

1.4 RELEVANCE OF PROPOSED TECHNIQUE

Critics of the use, for design purposes, of the full potential equations (upon which the hodograph method is based) often say that numerical solutions of the either the three-dimensional Navier-Stokes equations or the Euler equations would provide a more accurate prediction of the flow field, particularly at lower Reynolds numbers or in cases involving strong shocks. However, accurate numerical predictions by themselves do not necessarily provide design solutions, nor do they provide guidance to designers as to what to do about poor aerodynamic performance nor any other adverse conditions resulting from the predicted aerodynamic characteristics. In contrast, the solutions from the hodograph space do provide these capabilities. In addition, it is important to keep in mind that strong shocks are highly undesirable from a design point of view and should be avoided. Thus the capability of predicting strong shocks in the flow field is not imperative for design point calculations. For the off-design condition, it is expected that for the aerodynamic shapes developed in this research, much weaker shocks are expected than for shapes designed based on two dimensional analysis. For this situation solutions to the full potential equation are still valid and the simulation of shocks developed as part of the proposed work should be adequate to predict off design aerodynamic performance.

Note that it is generally believed that the discovery of supercritical wing sections was made possible by the use of the hodograph transformation along with the full potential flow equations (although classified experimental work was evolving the same airfoil shapes independently). As a result, new characteristic families of airfoil shapes were defined and, in conjunction with wind tunnel tests, were proven to be the types of shapes that can postpone or eliminate local shocks at transonic speeds (a conceptual revolution!).

In retrospect, it was not necessary to use a more accurate theory like the Navier-Stokes equations in order to discover such an important, fundamental and revolutionary esult. In fact, it has been shown that the boundary layer correction effects can, in most cases, be satisfactorily incorporated empirically into the inviscid formulation (i.e., without necessarily using the Navier-Stokes equations). In addition, the difficulties of generating an appropriate grid and establishing the appropriate far field boundary conditions and their location for the computational solution of the equations still are problems that require considerable numerical experimentation.

In spite of the successful design of shock free airfoils using the hodograph method, true shock free wings did not evolve from this work. One of the drawbacks of trying to use supercritical airfoils to construct 3-D lifting surfaces is the inherent significant sensitivity of the transonic flow field to changes in its physical parameters due to the strong non-linearity of the equations. For example, small changes in a given set of transonic flow parameters can result in a significantly different flow field. This means, for instance, that a supercritical section designed to be shockless at a Mach number of 0.85 may end up having strong shocks at a Mach number of 0.8 or 0.9. This type of behavior is very typical of a nonlinear system (which is what the transonic flow problem is). The principle of superposition which is useful in linear systems does not apply to transonic flow. This, therefore, explains why a three-dimensional wing, designed with a set of two-dimensional sections along its span that are individually shockless, does not necessarily end up being a shockless wing. Unfortunately however, because the hodograph method (the principal tool for designing shockless sections) has been thought to be (up until now) a two-dimensional tool, designers have had no choice but to use the superposition idea to design a three-dimensional wing; this linearization practice (superposition) is fairly accurate in most flow regimes except the transonic. The penalty for such an inaccurate practice is the reappearance of strong shocks (and consequent deterioration of aerodynamic performance). Therefore, a three-dimensional hodograph approach should not only eliminate such an incorrect practice but should also provide the correct method for distributing the sectional properties (e.g., thickness) along the span (providing perhaps new characteristic families of wing shapes) that may provide truly shockless, three-dimensional transonic wings. It is

emphasized that the availability of a design procedure based on the three-dimensional hodograph space transformation would provide insight not available from any other approach.

The treatment of shocks is very important for transonic flow. When the hodograph approach is used as an inverse method, the shock is not treated, since the goal in such an approach is to produce "shockless" airfoils. Some investigators are skeptical about the existence of "shockless" airfoils, mainly because of the possibility of the appearance of shocks at the off-design points. This is a genuine concern since the "shockless" airfoils which have been designed using a two-dimensional theory have to operate frequently at off-design points e.g. operation in a three-dimensional or unsteady physical environment causing local off design conditions even at the design Mach number. The proposed work, which deals with application of the hodograph technique to the three-dimensional wing, should provide design points that are more practical and should alleviate such concerns.

Finally, this section may be concluded with a quotation from Sir M. J. Lighthill:[3] "It seems likely that *any general theory of compressible flow applicable to problems with regions both of sub- and supersonic flow* (such problems have been called 'trans-sonic') *must be based on the 'hodograph transformation'* (due originally to Molenbroek 1890 and Chaplygin 1904)."

1.5 CONCLUSIONS

In this paper the formulation of a new 3-D hodograph technique is presented. It is shown that a mild constraint on the energy/Bernoulli equation permits the separation of the nonlinear 3-D flow equations over an aircraft wing into the sectional component and spanwise component. These two component equations are solved in both physical space (spanwise component) and hodograph-plane (sectional component) and used for constructing flows over 3-D wings.

While the formulation of the complex characteristics method of solution for the sectional component is presented in this paper, the hypergeometric series solution method is utilized for constructing the flows whose results are shown in this preliminary computation work. A good agreement is seen when these results are compared

and FL022 code developed by Jameson and Caughey

to the previous work of Spreiter. That verification of the present work provides the confidence that this new technique which seems to have significant potential also seems to possess some credibility.

Acknowledgements: The author acknowledges the computational help provided by Prof. J. Bentson, Mr. John Nutakor and Mr. Robert Jesinowski all of the Aerospace Engineering Dept. (Polytechnic University). He also acknowledges several discussions with Profs. Paul Garabedian, Julian D. Cole, and William Sears of the Courant Institute of Mathematical Sciences (NYU), Rensselaer Polytechnic Institute and University of Arizona, respectively. The author is also grateful to Dr. T. C. Tai of David Taylor Naval Research Center (Washington) for his interest in and appreciation of the new method described in this paper. The author also thanks Mrs. B. Hein for patiently typing the manuscript.

1.6 REFERENCES

1. P. Molenbroek, "Uber einige Bewegungen eines Gases bei Annahme eines Geschwindigkeitspotentiales," Arch. Math. Phys., Vol. 9, pp. 157-195, 1890.

2. S. A. Chaplygin, "On Gas Jets," Sci. Mem. Moscow Un. Math. Phys. No. 21, pp. 1-21, 1904. Transl. NACA TM 1063, 1944.

3. M. J. Lighthill, "The Hodograph Transformation in Transonic Flow. I. Symmetric Channels. II. Auxiliary Theorems on the Hypergeometric Functions. III. Flow Round a Body," Proc. R. Soc. London, A191, pp. 341-369, 1947.

4. K. G. Guderley, "On Transonic Simplifications of the Hodograph Equation," Wright Air Development Center Tech., Report No. 53-183, 1953.

5. G. Y. Nieuwland, "Transonic Potential Flow Around a Family of Quasi-elliptical Aerofoil Sections," N.L.R. Report TR T172, 1967.

6. F. Bauer, P. Garabedian, and D. Korn, "Supercritical Wing Sections, Lecture Notes in Economics and Mathematical Systems," Vol. 66, Springer-Verlag, New York, 1972.

7. J. W. Boerstoel, "A Survey of Symmetrical Transonic Potential Flows Around Quasi-elliptical Aerofoil Sections," NLR TR T136, 1967.

8. H. Sobieczky, "Related Analytical, Analog, and Numerical Methods in Transonic Airfoil Design," AIAA Paper 79-1556, July 1979.

9. A. Hassan, H. Sobieczky, and A. H. Seebass, "Subsonic Airfoils with a Given Pressure Distribution," AIAA Journal, Vol. 22, No. 9, pp. 1185-1191, September 1984.

10. P. Garabedian, "Partial Differential Equations," John Wiley & Sons, New York, 1964.

11. R. Courant and D. Hilbert, "Methods of Mathematical Physics," Vol. II, Interscience, New York, 1962.

12. H. Bateman, "Partial Differential Equations of Mathematical Physics," Dover Publications, New York, 1944.

13. K. G. Guderley, "The Theory of Transonic Flow," Pergamon Press, Oxford, 1962.

14. I. E. Garrick and C. Kaplan, "On the Flow of a Compressible Fluid by the Hodograph Method II - Fundamental Set of Particular Flow Solutions of the Chaplygin Differential Equation," NACA Report No. 790, 1944.

15. G. A. Oyibo, "Exact Closed-Form Solutions for Nonlinear Unsteady Transonic Aerodynamics," DGLR Paper No. 85-22. Second Int'l Symposium on Aeroelasticity and Structural Dynamics, Technical University of Aachen, W. Germany, April 1-3, 1985. Accepted for publication in AIAA J.

16. Guderley, G., On Transonic Airfoil Theory, J. Aero. Sci., Oct. 1956, pp. 961-969.

17. Cole, J. D., Cook, L. P., Ziegler, F., Finite Span Wings at Sonic Speed, Mech. Rech. Comm., 1(4), 1980, pp. 253-260.

18. Spreiter, J. R., "The Local Linearization Method in Transonic Flow Theory", in "Symposium Trannssonicum" Aachen. Sept. 3-7, 1962

19. Sears, W. R., "General Theory of High-Speed Aerodynamics," Princeton University Press, Princeton, 1954.

20. C. S. Morawetz, "On the Non-existence of Continuous Transonic Flows Past Profiles, I," Comm. Pure Appl. Math., Vol. 9, pp. 45-68, 1956.

21. Cole, J. D., Cook, L. P., "Transonic Aerodynamics" North-Holland Series in Applied Mathematics and Mechanics, 1986.

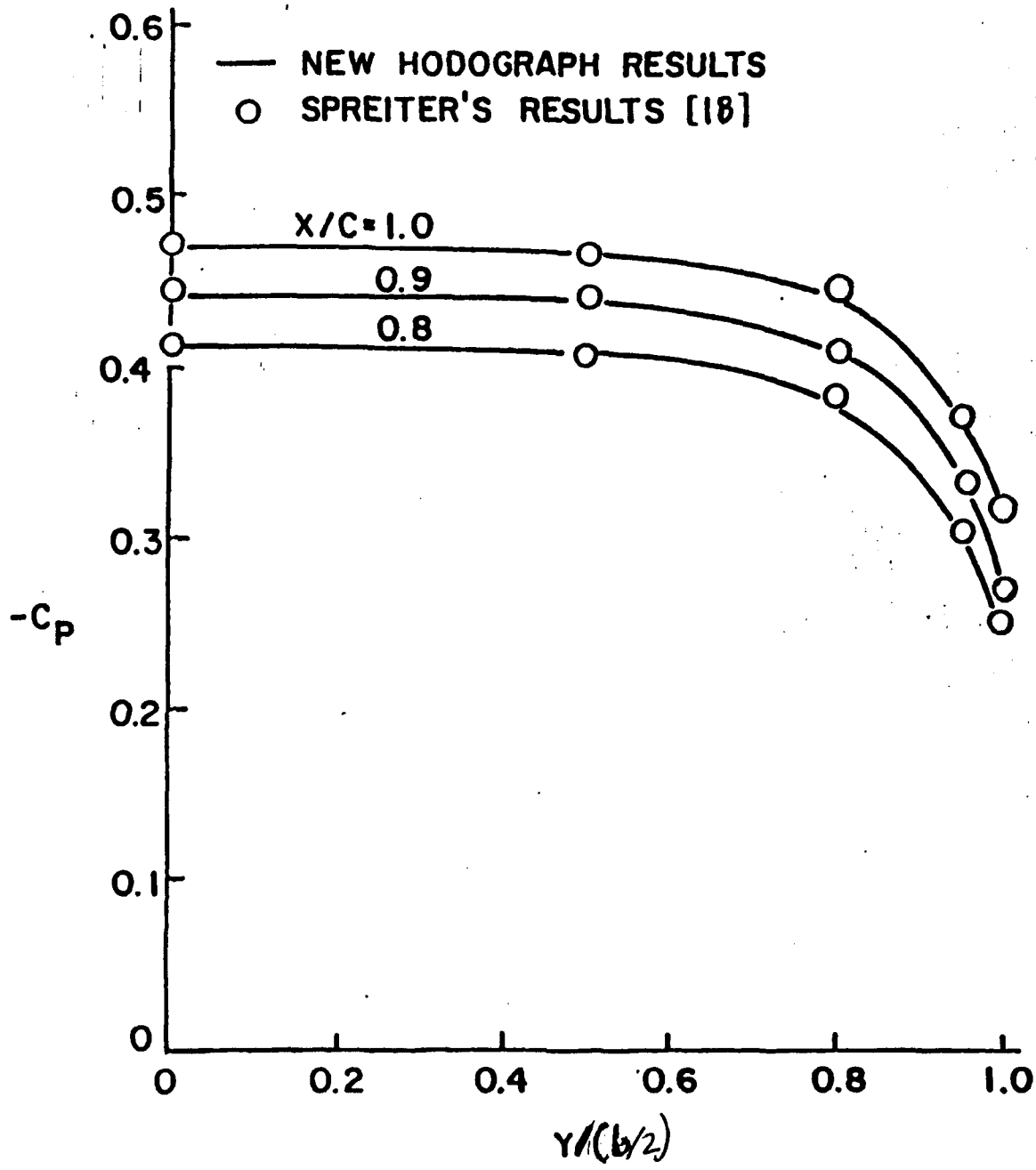

FIG. 1 PRESSURE COEFFICIENT VS SPANWISE STATION
M=1.0, α=7.7 DEGREES, RECTANGULAR WING
ASPECT RATIO=7.63, 6% PARABOLIC ARC SECTION

SUPERCRITICAL WING DESIGN, A THREE DIMENSIONAL HODOGRAPH APPROACH

presented at AIAA 10th Applied Aerodynamics Conference. California. Jan. 1992.

Gabriel a. Oyibo*
John Nucaker* and Kyung-soo Jang*
Polytechnic University
Farmingdale, New York

Significant contributions from various investigators have been responsible for the evolution of the hodograph methodology applicable to nonlinear potential flow. Works of Molenbrock[1] and Chaplygin[2] were complimented by later efforts of Lighthill[3], Guderley[4], Cole and Cook[5]. Recent works by Boraweta[6], Niewland[7], Bauer, Garabedian and Korn[8], Garabedian Hassan, Sobieczky and Seebass[9] established the applicability of the methodology to shockless supercritical section designs. Credibility of this methodology has since been clearly established experimentally by studies such as Whitcomb[10]. This marked a major breakthrough in transonic flow gas dynamics. However, due to the mathematical and perceptive constraints, this powerful methodology has been viewed as restricted to 2-D flow or gas dynamics. However Oyibo[12,13], in a recent finding was able to prove that 3-D hodograph methods exist and can be used to study 2-D unsteady and 3-D gas dynamic flows over 3-D wings of finite span. It was further shown in references 12 and 13 that it is possible to find smooth or shockless solutions to the 2-D unsteady and 3-D gas flow around wings sections and 3-D wings of finite span respectively. The smooth, shockfree solutions generated in 12 and 13 were generated using hypergeometric series (which are fundamental solutions) the singularities of which are forced inside the wing and out of the flow field. Reference 12 also showed the formulation of the basic 3-D hodograph equation in the characteristic hodograph variables in a manner similar to that formulated by Garabedian[8] for 2-D wing sections. This formulation along with the separability of the solution (into a "sectional" component and a wing spanwise component) as established in reference [13] makes it possible to modify and use the 2-D methods to solve the sectional problem and combine it with the spanwise solution to construct a smooth or shockfree solution around realistic closed 3-D finite wing shapes. This write up, therefore, uses this characteristic hodograph formulation from reference 13 as a basis for modifying the 2-D code from the Courant Institute of Mathematical Sciences for designing shockfree 3-D wings.

Figures 1-3 show the results obtained in this research. The preliminary conclusions (which confirm the findings of reference 13) seem to be that a shockfree 3-D finite rectangular wing is possible and feasible. In other words the research seems to suggest that sweep and/or twist may not be the only way to delay drag rise mach numbers or minimize shockwave effects.

* Associate Professor, Aerospace Engineering Department., Associate Fellow, AIAA

* Graduate Research Fellows, Aerospace Engineering Department

REFERENCES

1. Molenbrook, P., "Uber einige Bewegungen eines Gases bei Annahme eines Geschwindigkeitspotentiales," Arch. Math. Phys.. Vol.9, 1890, pp. 157-195.

2. Chaplygin, S.A., "On Gas Jets," Sci. Mem Moscow Un. Math.Phys., 1904 Transl. NACA TM 1063, No. 21, 1944, pp. 1-21.

3. Lighthill, M.J., "The Hodograph Transformation in Transonic Flow. I. Symmetric Channels. II Auxillary Theorems on the Hypergeometric Functions. III. Flow around a Body," Proc. R. Soc. London, A191, 1947, pp 341-369.

4. Guderly, K.G., " On Transonic Simplification of the Hodograph Equation," Wright Air Development Center Tech., Report No. 53-183, 1953.

5. Morawetz, C.S., "On the Non-Existence of Continuous Transonic Flow Past Profiles, I," Comm. Pure Appl. Math., Vol. (, 1956, pp 45-68.

6. Niewland, G.Y., "Transonic Potential Flow Around a Family of Quasi-elliptical Aerofoil Sections," N.L.R. Report TR T172, 1967.

7. Garabedian, P., "Partial Differential Equations," Wiley, New York, 1964.

8. Bauer, F., Garabedian, P., and Korn, D., "Supercritical Wing Sections, Lecture Notes in Economics and Mathematical Systems," Vol. 66, Springer-Verlag, New York, 1972.

9. Hassan, A., Sobiecczky, H., and Seebass, A.H., "Subsonic Airfoils with a Given Pressure Distribution," AIAA Journal, Vol.22, No. 9, 1984, pp 1185-1191.

10. Cole, J.D., and Cook, L.P., "Transonic Aerodynamics," North-Holland Series in Applied Mathematics and Mechanics, 1986.

11. Whitcomb, R.T., " A Study of the Zero-Lift Drag-Rise Characteristics of Wing Body Combinations near Speed of Sound," NACA TR 1273, 1956.

12 Oyibo, G.A., " Exact Closed-form Solutions for Nonlinear Unsteady Transonic Aerodynamics," AIAA Journal, Vol. 27, No. 11, 1989, pp 1572-1578.

13. Oyibo, G.A., " Formulation of Three Dimensional Hodograph Method and Separable Solutions for Nonlinear Transonic Flows," AIAA Journal, Vol. 28, No. 10, 1990, pp 1745-1750.

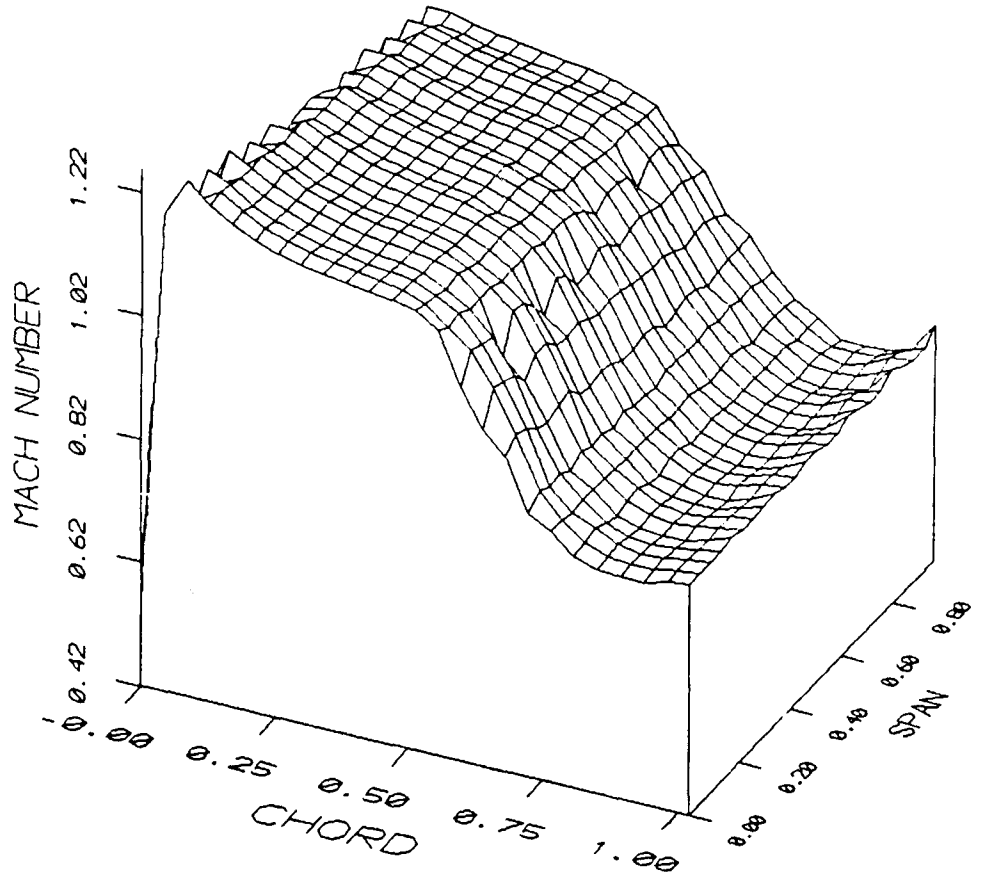

FIGURE1 DISTRIBUTION OF MACH NUMBER ON THE UPPER SURFACE OF A WING

FIGURE 2 DISTRIBUTION OF MACH NUMBER ON THE LOWER SURFACE OF A WING

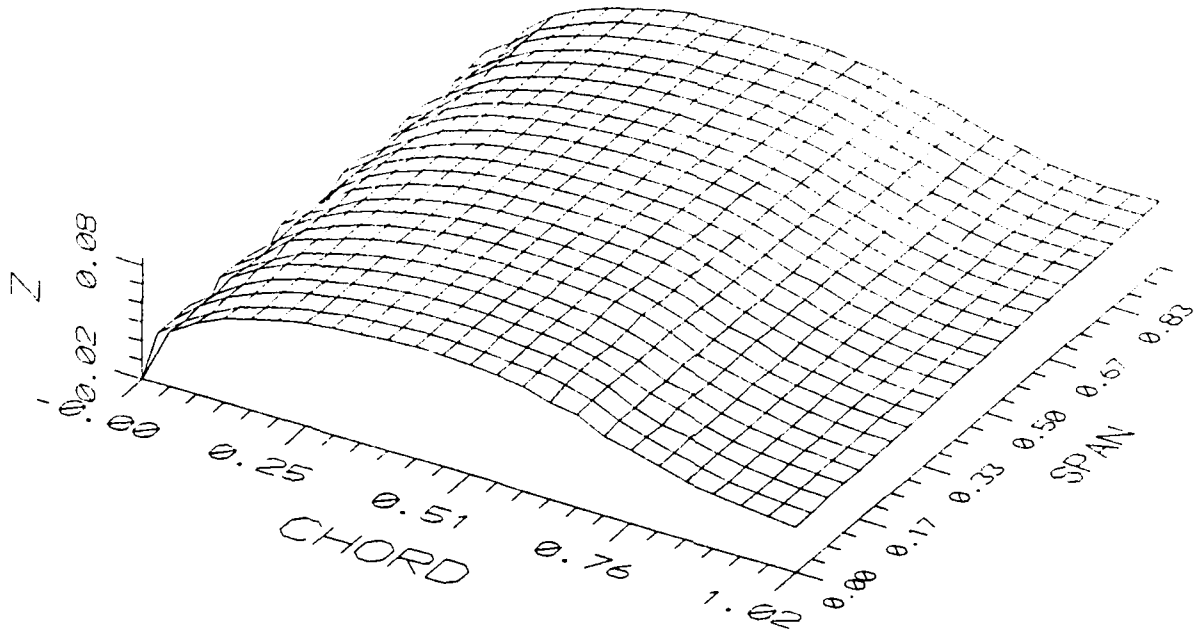

FIGURE 3 UPPER SURFACE OF WING

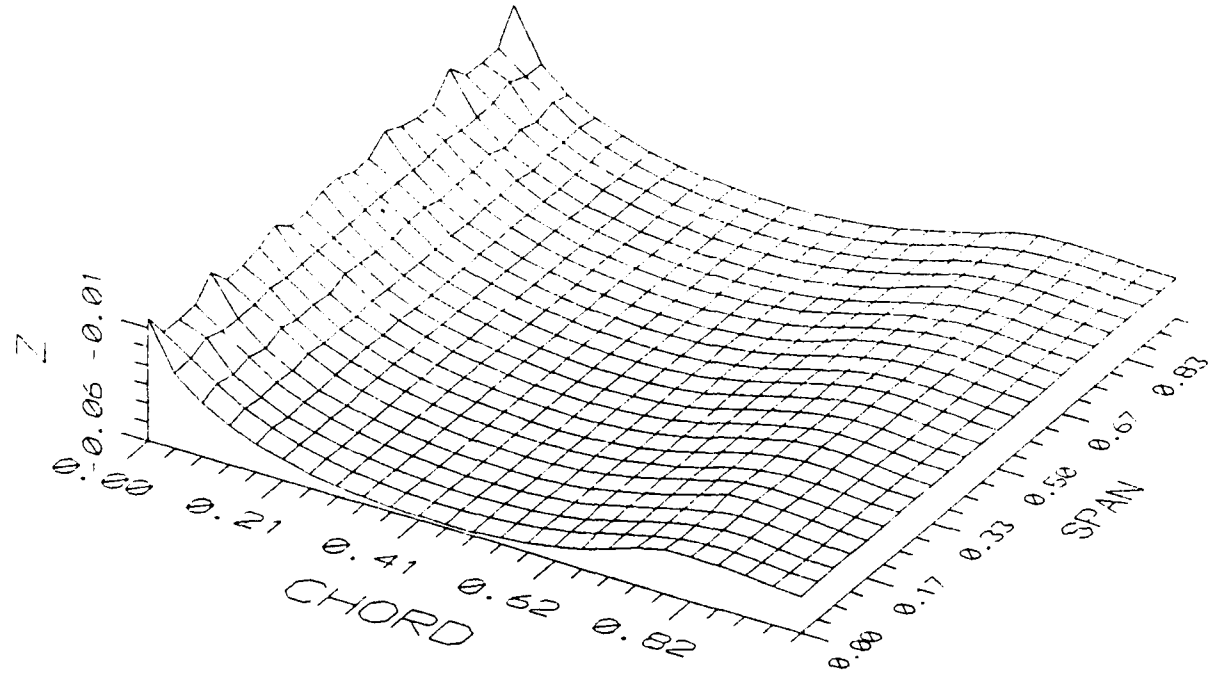

FIGURE 4 LOWER SURFACE OF WING

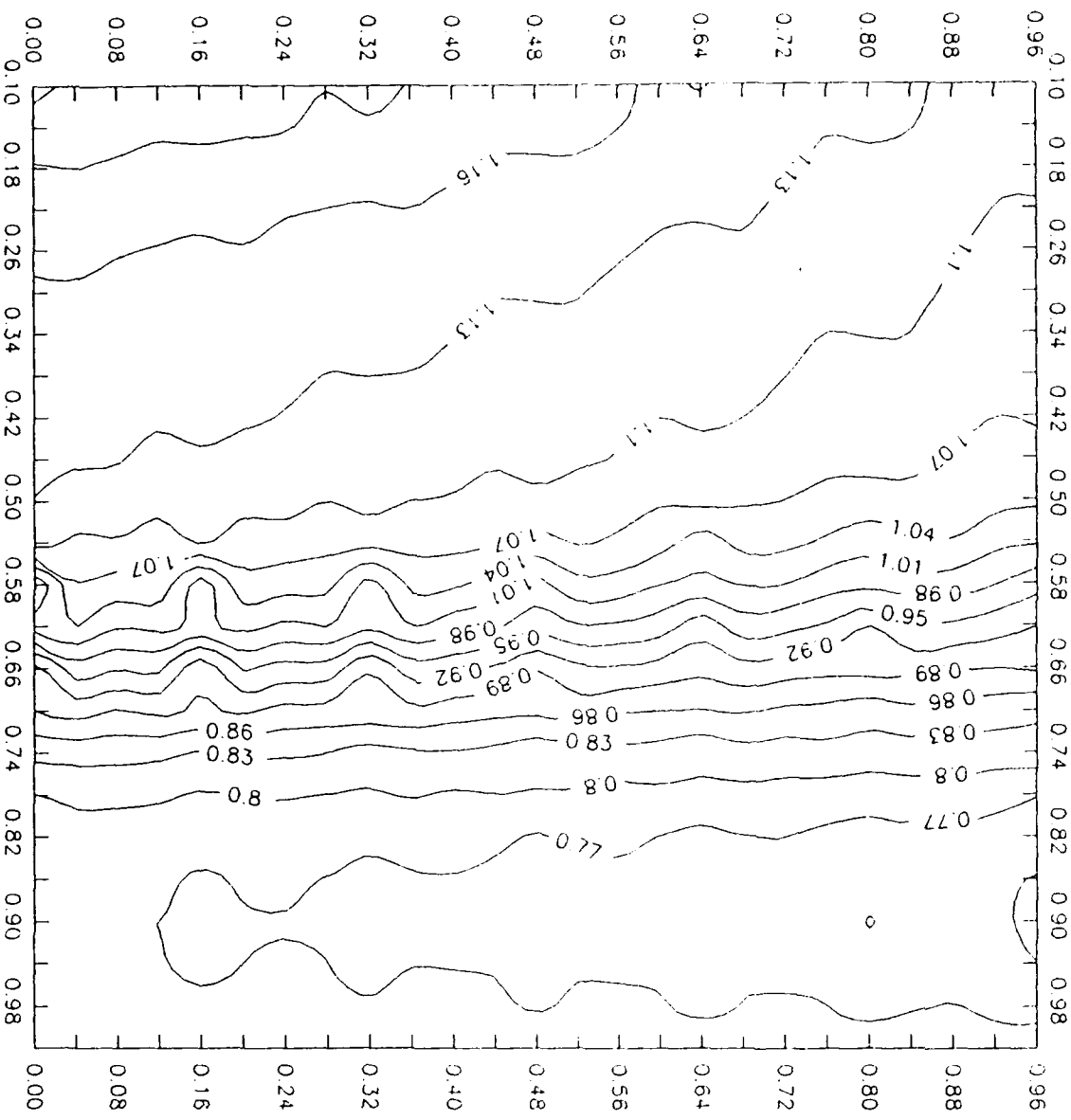

FIGURE 5 ISO-MACH ON THE UPPER SURFACE OF WING

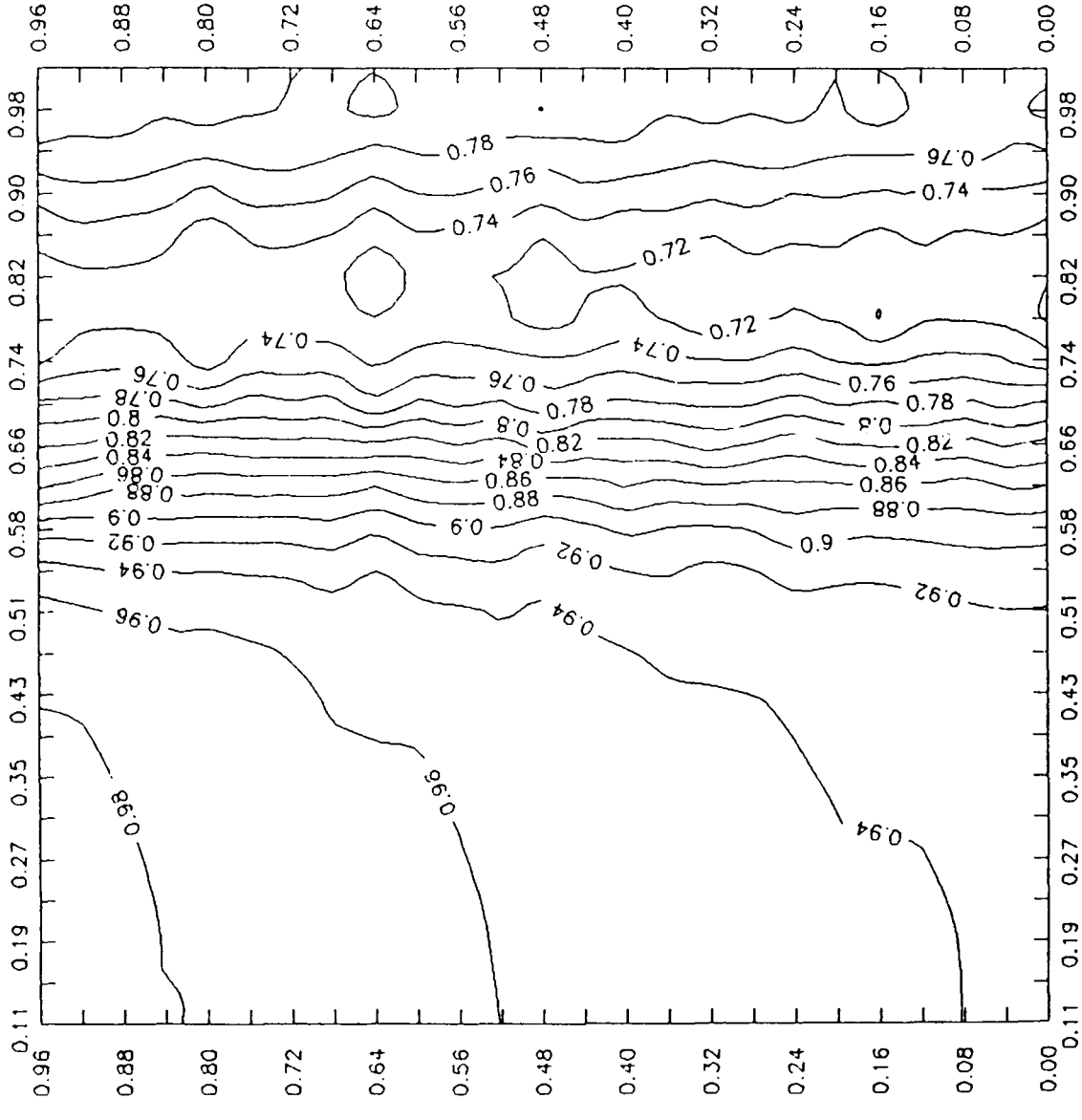

FIGURE 6 ISO-MACH ON THE LOWER SURFACE OF WING

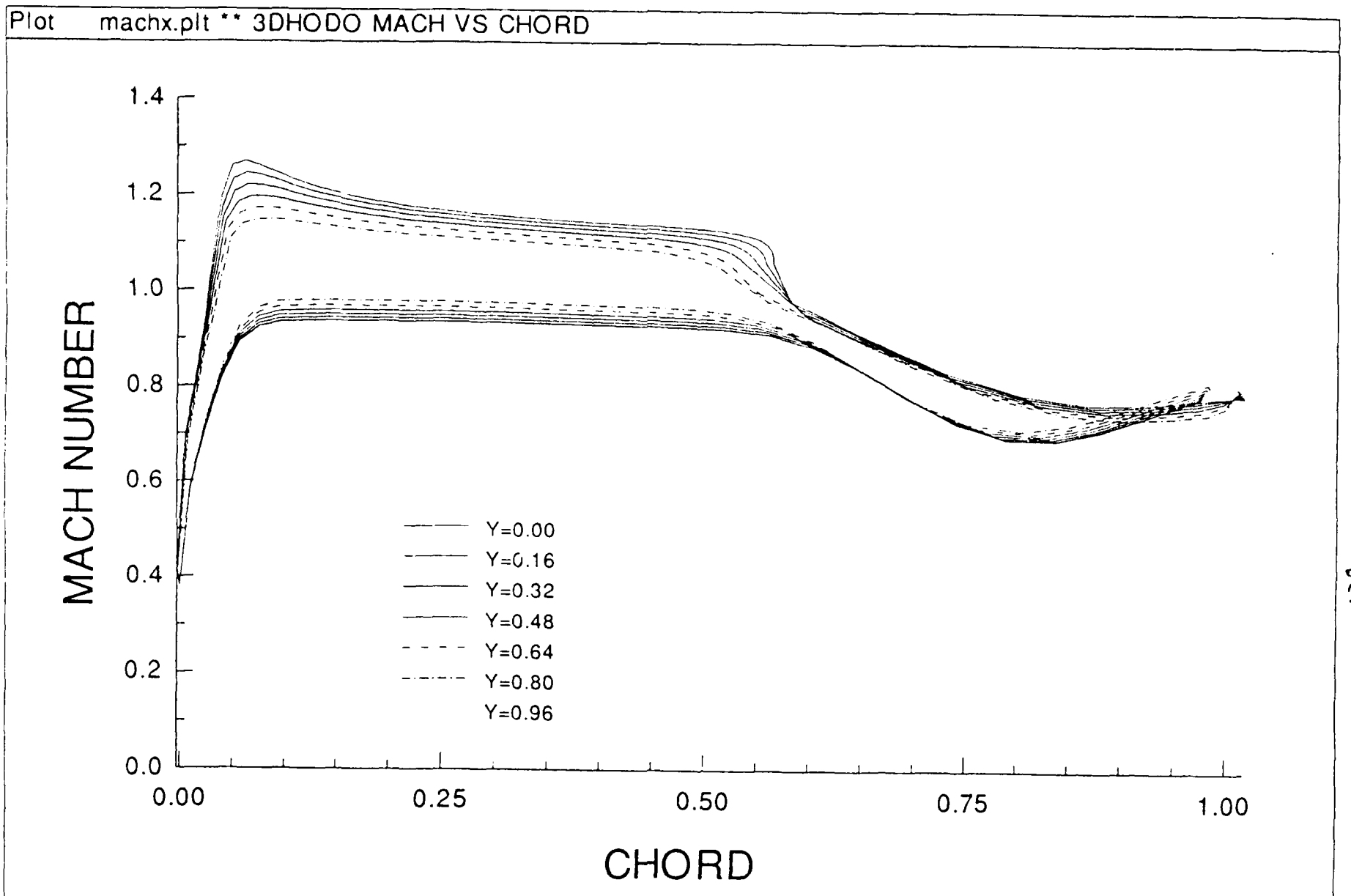

FIGURE 7 DISTRIBUTION OF MACH NUMBER ON THE UPPER AND LOWER WING

EXACT CLOSED FORM SOLUTIONS TO THE FULL NAVIER STOKES EQUATIONS AND NEW PERCEPTIONS FOR FLUID AND GAS DYNAMICS

Gabriel A. Oyibo*
Polytechnic University
Farmingdale, New York

The full Navier Stokes Equations are carefully investigated using the fundamental concepts of transformation group theory. This reveals that in some transformed spaces Navier Stokes equations can become very tractable mathematically and fairly transparent physically. The careful examination and exploitation of these findings permitted the formulation of rather general set of fundamental exact closed form solutions to these equations generally considered to be the most sophisticated mathematical description for continuum fluid and gas dynamics. These fundamental solutions are then used to construct the solution to the 2-D steady flow over a cylinder, a problem which apparently has never enjoyed exact closed form solutions using the full Navier Stokes Equations in the history of fluid or gas dynamics. For incompressible flow with constant viscosity the laminar separation points are predicted and are found to be in agreement with experimental data. Similarly the pressure distribution as well as the drag predicted by these new solutions are found to be in very good agreement with experimental data. This experimental data verification therefore provides the necessary basis for confidence in these new solutions and their legitimacy to be used to explore and evolve new perceptions in fluid and gas dynamics. In addition they should serve as benchmark solutions for validating the CFD codes.

* Associate Professor, Polytechnic University, Associate Fellow AIAA

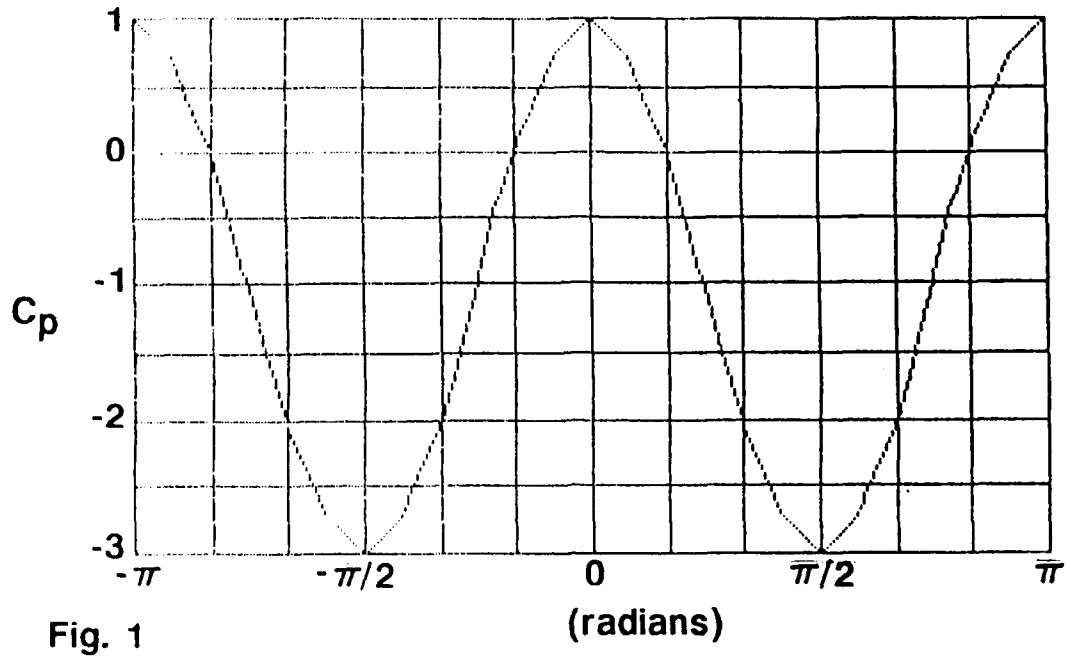

Fig. 1

FIG 1 Inviscid Potential Flow Pressure Distribution over a Cylinder

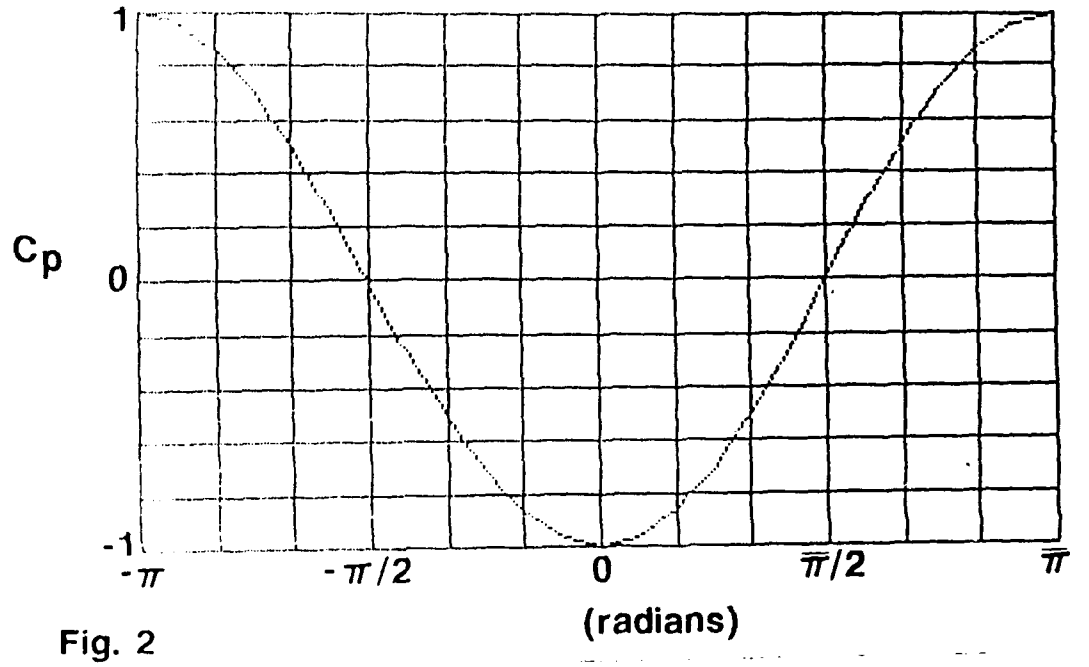

Fig. 2

FIG 2 Stokes Solution for Pressure Distribution of a Creeping Flow over Cylinder

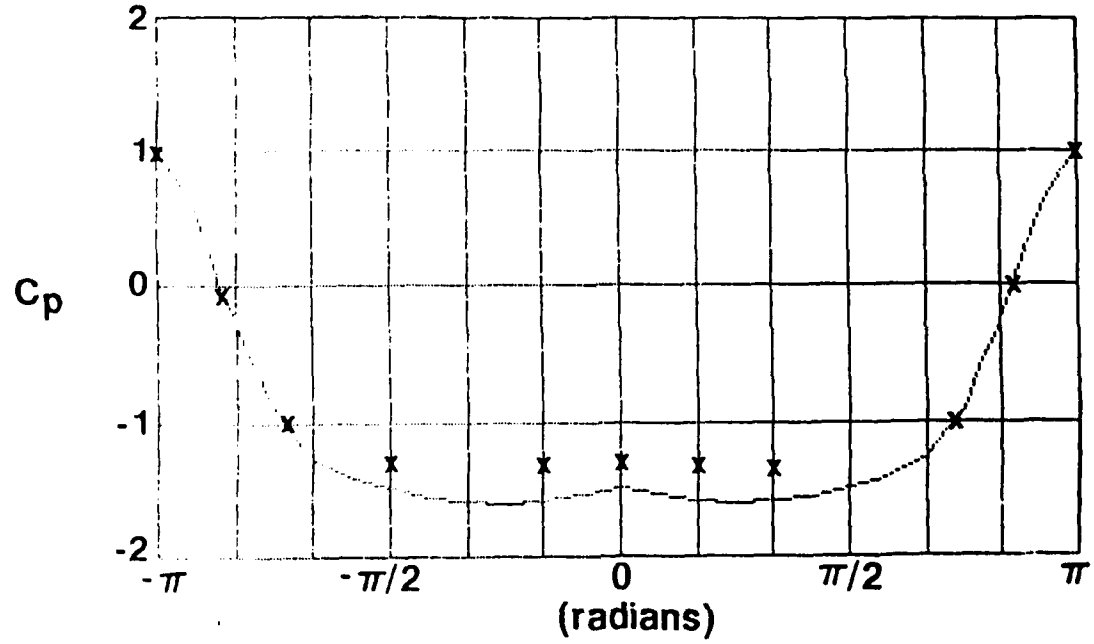

Fig. 4

FIG 4 Pressure Distribution due to a Viscous Flow Over a Cylinder

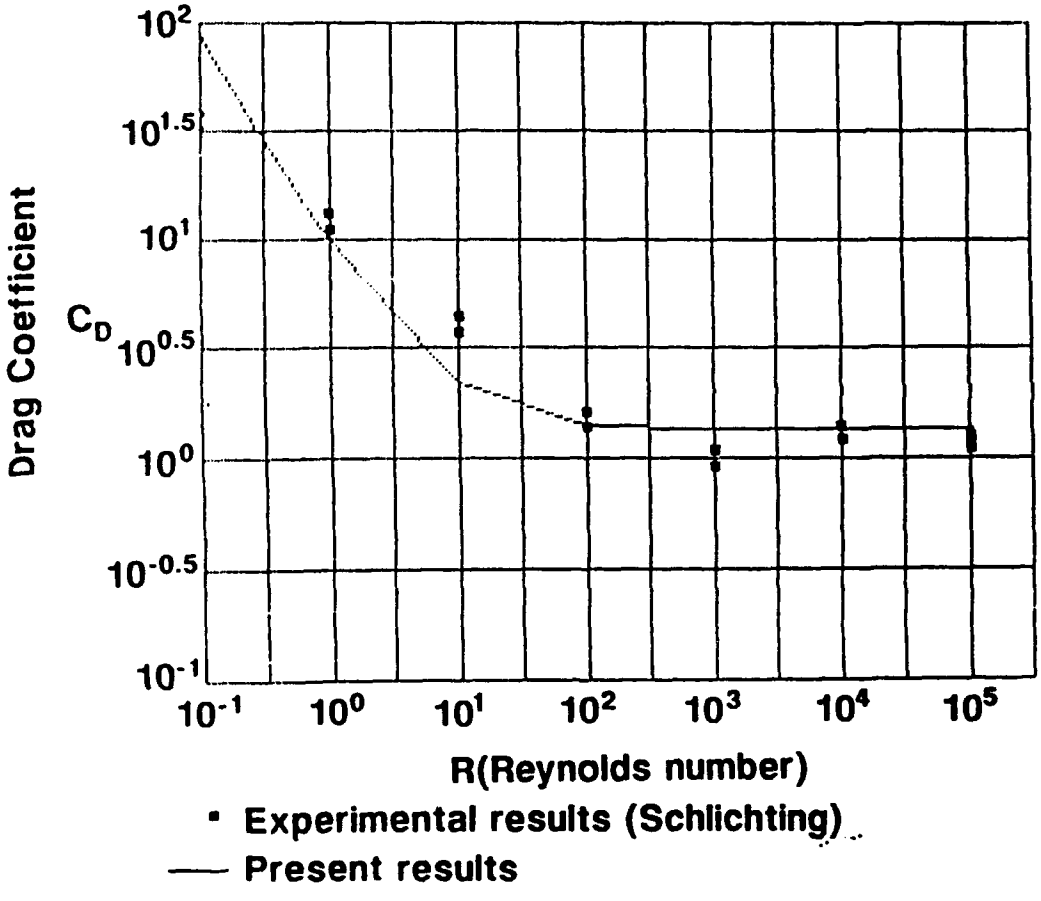

FIG 5 Drag Coefficient for a Cylinder versus Reynolds Number

6.0 STATUS OF PUBLICATIONS AND GRADUATE STUDIES

The significant results obtained thus far in this research program are being compiled and written up for publication in suitable technical journals. AIAA Paper No. 86-1006, a paper based on the first phase of research has been prepared and was presented at the AIAA/ASME/ASCE/AHS 27th Structures, Structural Dynamics and Materials Conference held in San Antonio, Texas May 19-21, 1986. A paper, "Exact Solutions to Aeroelastic Oscillations of Composite Aircraft Wings with Warping Constraint and Elastic Coupling" has been accepted for publication by the AIAA Journal. Another paper entitled "Some Implications of the Warping Restraint on the Behavior of Composite Anisotropic Beams" has been published by the AIAA Journal of Aircraft. In addition, a paper entitled "Exact Closed Form Solutions for Nonlinear Unsteady Aerodynamics", which provides the basis for the proposed next phase of the program, has been published by the AIAA Journal and included in this report. In the process of studying unsteady 2-D nonlinear transonic flows, what seems to be a major breakthrough was discovered: this breakthrough is the discovery that the #-D steady nonlinear transonic flow equations can be transformed into linear hodogragh equivalent. This discovery essentially reverses a hundred years state of thinking and belief in the scientific and mathematical community that the hodogragh method was limited to the 2-D flows. The results of this discovery have been written up and published in the AIAA Journal. In addition another paper AIAA 92-257 which presents practical shock free 3-D wing for transonic flight is to be presented in June, 1992 at the AIAA applied Aerodynamics Conference in Palo Alto, California. This research program seems to be seeing the beginning of what seems to be another breakthrough,

perhaps even more significant than what we have seen thus far. This is what seems to be a discovery that transformations methods can even be used to effectively study the ultimate set of equations in continuum gas dynamics known as the Navier Stokes set of equations. This new finding could be the key to effectively unlocking the secret of gas dynamics and aeroelastic phenomena for real gases with viscosity, which have been blurry at best thus far. This finding has resulted in a preliminary paper accepted to be presented at an international conference to be held in Colorado in August of 1992. It is being proposed that the investigation of these new findings be pursued in a proposed next phase of research. This is because if the findings are correct this could be the start of a new era of fluid or gas dynamics analysis.

Mr. John Calleja and Mr. George Papadopoulos have finished their Masters thesis' under this project. The support of AFOSR under Contract F 449620-87-C-0046 and Grant89-0050 of these thesis' are aknowledged in the thesis writeups.

7.0 NAME, ADDRESS AND TELEPHONE NUMBER OF PROFESSIONAL PERSONNEL:

1. Prof. Gabriel A. Oyibo
Principal Investigator, Program Manager
Department of Aerospace Engineering
Polytechnic University
Long Island Campus
Farmingdale, New York 11735

(516) 755-4251

2. Prof. Terrence A. Weisshaar, Investigator
Department of Aeronautics and Astronautics
Purdue University
West Lafayette, Indiana 47907

(317) 494-5975

3. Mr. John Nutakor, Graduate Student
Department of Aerospace Engineering
Polytechnic University
Long Island Campus
Farmingdale, New York 11735

(516) 755-4367

4. Mr. Kyung-Soo Jang, Graduate Student
Department of Aerospace Engineering
Polytechnic University
Long Island Campus
Farmingdale, New York 11735

(516) 755-4358